ORNL MASTER COPY

ornl

OAK RIDGE NATIONAL LABORATORY

MARTIN MARIETTA

Status Report on Accident Condition Fuel Performance Models

R. C. Martin

September 1990

See email from

STATUS REPORT ON ACCIDENT CONDITION FUEL PERFORMANCE MODELS

R. C. Martin
Oak Ridge National Laboratory

September 1990

<u>Distribution</u>

S. J. Brown, DOE/NP-60
P. J. Dirkmaat, DOE/NP-80
R. K. McCardell, INEL
J. D. Nulton, DOE/NP-60 (2)
D. K. Rhyne, DOE/ORO
G. Santos-Leon, DOE/NP-60
L. K. Seymour, DOE/NP-80
F. H. Southworth, INEL
H. Zeile, INEL
C. A. Baldwin
W. P. Barthold
G. L. Copeland
C. E. DeVore
W. A. Gabbard
F. J. Homan

H. Jones
M. J. Kania
J. C. Mailen
R. C. Martin (3)
D. L. Moses
B. F. Myers
N. H. Packan
P. L. Rittenhouse
O. M. Stansfield
J. O. Stiegler
J. C. Whitson
Laboratory Records (3)
Laboratory Records - RC
ORNL Patent Office

CONTENTS

TABLES

FIGURES

ABSTRACT

A simple diffusion model is used to analyze the release of fission products during accident condition testing of FRG fuel spheres. These spheres contain reference TRISO fuel particles for the High-Temperature Reactor program of the Federal Republic of Germany. Categorization of sphere release of cesium-137 based on fast neutron fluence permits predictions of release with accuracy comparable to that of the 1989 revision of the US/FRG accident condition fuel performance model, but with the potential for greater insight into the mechanisms of fission product release. Calculations are also performed for release of krypton-85, strontium-90, and silver-110m.

A brief chronological development of accident condition models for BISO and TRISO particles is presented, and the methodology of the predominant existing models compared to a model emphasizing diffusive release. Emphasis of existing models on the concept of fuel and coating failure is criticized for its ambiguity. A meaningful concept of non-mechanical failure should reflect fuel performance during repeated accident condition thermal cycling. Microstructural considerations which may play a role in future development of phenomenological models of fission product release are discussed in detail, with emphasis on neutron damage and thermal decomposition of silicon carbide. The radiation-induced segregation of silicon within the silicon carbide structure is postulated as a mechanism for enhanced fission product release during accident conditions. A near-term plan for efforts in accident condition modeling is described.

1. INTRODUCTION

This report represents continuation of the effort documented in the previous report, "Status Report on Reference Fuel Accident Condition Database and Modeling" [1], which briefly summarized existing accident condition (AC) fuel performance models and questioned some of the assumptions and modeling philosophy inherent in the reference AC models. A major question was raised regarding the existing assumption in AC modeling that diffusion of fission products (FP) across the silicon carbide layer can be neglected at accident-condition temperatures relative to a less-well-defined concept of SiC "failure" in FP release.

It appears that AC modeling over much of the last decade has fixated on this concept of SiC failure at the expense of a more mechanistic and microstructural explanation of SiC damage under irradiation and decomposition at high temperatures. A recent failure model concluded that the magnitude of fast neutron fluence has virtually no effect on FP release, which if true would make SiC perhaps the most remarkably neutron-resistant material known. Such a conclusion seems tenuous.

In order to relax the existing assumptions on AC modeling, a diffusion-based model very simple in concept has been applied to the FP AC release data for FRG spheres. This model is based on the simplest approach possible to diffusion through a SiC barrier layer: an analytical expression for diffusion through a thin spherical shell. Preliminary results from this model suggested the need to evaluate sphere release as a function of fast neutron fluence. By a judicious division of the sphere release data into groups based on fast fluence, followed by numerical averaging of the diffusion coefficients within each group, predictive capabilities for Cs-137 release statistically comparable to the recent US/FRG AC model revision [2] are possible, despite the US/FRG model's dismissal of diffusive release and fast fluence effects as dominant release mechanisms. Analysis of the FRG sphere release data is emphasized because of the minimal particle and coating variability from sphere to sphere relative to earlier U.S. and FRG irradiation tests.

This report does not claim that simple diffusive release will explain all aspects of FP release, and an oversimplified approach to FP release was purposely pursued as a first approximation. No

1

simple approach will adequately describe the intricacies of FP release under a variety of irradiation and heating conditions. However, a diffusive model can incorporate defect production under neutron irradiation and, with more difficulty, structural decomposition of the SiC layer at high temperatures can be included. The quality of a model is not simply in the numbers it provides, but also how much it can reveal or provide insight into the phenomena involved for a deeper understanding and greater predictive capabilities. Models that lean heavily on some aggregate concept of SiC failure may be limited in this regard. The dismissal of diffusion-related mechanisms of FP release without definitive evidence may be a tenuous assumption.

A general discussion of relevant microstructural phenomena which may play a role in FP release through SiC is presented, and some simple phenomenological models for radiation-enhanced FP release and SiC degradation are discussed. Considerable documentation on existing SiC data and models of neutron damage effects is included, to provide a compilation of source data and references for further work.

This work represents a multi-step approach to modeling: the first status report [1] represented an introduction to the FRG database and relevant modeling issues. This status report includes more fundamental investigation into relevant materials issues, the compilation of a introductory chronology into AC model development through the HTGR programs, and development of a simple alternate model of FP release based on diffusion. Upcoming work will feedback this information into evaluation of addition TRISO fuels database and the justification for models previously developed, as well as exploring further model development. Failure to include this intermediate step would limit critical and independent assessment of the fuel database and the models developed to describe that data.

2. HISTORICAL DEVELOPMENT OF ACCIDENT CONDITION MODELS

2.1 INTRODUCTION

A brief chronological development of accident condition models for BISO and TRISO fuels is presented for reference, with a cursory review of each model. Some of the discussion on model development within recent years is incorporated from the earlier status report. In addition, the mainstream modeling effort in the United States and Europe is briefly documented from the mid-1960's, and some alternate approaches to modeling are presented. Mainstream approaches refer to those models and governing assumptions which were developed and institutionally pursued over time. Non-mainstream models refer to those models whose assumptions have not been continuously pursued in time for model development. Chronological presentation of the models aids in understanding the origin and retention of certain assumptions which dominate the mainstream models today. Some comments on the development and present state of the AC modeling effort are then presented.

2.2 EARLY MAINSTREAM APPROACHES TO MODELING

2.2.1 Pressure Vessel Failure Model for Coated Particles (ca. 1966)

The potential for coated particles to undergo rupture has been a major concern since the earliest BISO particles. Mechanical failure of the coatings due to fission gas pressure and/or

radiation-induced dimensional changes of the coating layers can result in immediate loss of containment of the fission products within the particle. As sudden release of FP from the particle is the most serious form of containment failure, early modeling efforts were devoted to understanding this mechanical failure. An early analysis of stresses based on internal pressure and dimensional changes of the pyrolytic carbon (PyC) layers of BISO particles was performed by Prados and Scott [3]. The development of this model over time for BISO and TRISO particles can be traced through Kaae (1969) [4],[5], Stevens (1971) [6], Gulden et al. (1972) [7], and a model developed during the Dragon Project by Walther (ca. 1968) and described by Bongartz [8] which could calculate the stresses in particles with up to six coating layers. Kaae (1977) [9] follows the development of Stevens but incorporates a Weibull analysis to describe the stresses and strains generated in the outer layer of the BISO particle, while incorporating the current knowledge about the mechanical behavior of PyC. Bongartz (1977) [8] expands upon Walther's model by also incorporating the concept of the Weibull statistical distribution, and developed the brittle ring test [10] to obtain data on the strength and Young's modulus of SiC as input to these pressure vessel (PV) models. In 1981 Bongartz extended his work to develop a new model, which simplified the Walther model and accelerated computational speeds by assuming a quasi-rigid SiC layer in the calculations [11]. The PV approach to fuel performance modeling lead to development of the FRG code for TRISO particle failure, PANAMA-I [12], which incorporates the PV failure model plus a thermal decomposition mechanism for weakening of the SiC layer, as discussed in §2.3.2.

2.2.2 GA Models (ca. 1974)

By 1974 General Atomic Company was developing fuel performance models based on the concept of particle failure fractions for BISO and TRISO particles. C. L. Smith [13] emphasized a PV performance model to predict particle failure for TRISO UC_2 and BISO ThO_2 fuel particles, although kernel migration was also a contributor to failure. The internal fission gas pressure is the dominant factor influencing pressure vessel failure, and the fuel kernel diameter and buffer thickness were the design parameters with the predominant influence on particle survivability. Because of uncertainties in the model's formulation and in existing data, the model results were normalized to the irradiation test results available.

The results of a capsule test for TRISO UC_2 fuel particles lead to the conclusion that less than 1% of the fissile fuel particles in an HTGR would have calculated SiC layer stresses exceeding 200 MPa for irradiation at 1250°C to a fast neutron fluence of 8×10^{25} m^{-2} (neutron energy above 0.18 MeV) and burnup of 78% FIMA. Based on this, a maximum of 0.5% of particles undergoing PV failure during fuel lifetime was assumed, and relationships of particle failure as a function of fast fluence and burnup were developed. For specific irradiation parameters, the particle failure fractions resulting from fast fluence and from burnup were calculated independently, and the larger value used to predict fuel behavior. Figure 1 summarizes this approach, with isofailure lines plotted vs. burnup and fast fluence. Not enough data existed to predict the temperature-dependence of failure above 1250°C. Particle failures during thermal excursions were predicted by assuming 50% failure if the SiC layer stresses exceeded 30,000 psi, resulting in particle failures of 1 to 2% during excursions to temperatures of 1600 to 1800°C. Experimental results suggested failures could approach 10 to 20% at these temperatures.

Another GA approach for TRISO fuel performance modeling, as described in the Tokar report [14] and portrayed in Figure 2 [15], is to define an envelope of the irradiation and accident parameters below which no coating failures are assumed to occur, above which 100% failure is assumed, and within which the fraction of failures varies linearly across the envelope. In this case the parameters impacting failure are taken to be the irradiation time and fuel temperature. Figure

3

3 [16] shows an updated model of TRISO fuel performance in 1975. BISO particle failure fractions are treated similarly.

2.2.3 Tokar Report (1976)

Written in 1976 for licensing purposes, M. Tokar's "Evaluation of High Temperature Gas Cooled Reactor Fuel Particle Coating Failure Models and Data" may represent the most comprehensive and thoughtful evaluation of fuel performance models and philosophy of model development performed for the HTGR program. Although the models evaluated are outdated, Tokar's method of critically evaluating the existing models relative to the existing data and associated uncertainty, and his establishment of criteria which, if followed, could increase the faith in the reliability of the models, can still provide insight into model development today. Some relevant quotes from the Summary and Conclusions section are presented.

"... added conservatism was considered essential because the fundamental interrelationships of coating fabrication parameters, structure, and performance are not fully understood and are still the subject of considerable research and study ... The review of LHTGR fuel particle coating failure models and test data has shown that these particles can be expected to perform adequately ... A distinction must be made, however, between (generally) satisfactory performance and totally predictable performance. The LHTGR fuel particle qualification program has suffered from the fact that there are insufficient irradiation data on the reference fuel to permit development of failure models incorporating confidence intervals ... The LHTGR fuel particle coating performance models are, when modified according to our interim guidelines, acceptable for scoping studies ... It appears that the lack of an identifiable and unmistakable tie between fabrication parameters and performance models to a large degree results from the fact that the irradiation tests were conducted on a wide range of particles of varying design, fabricated under different conditions. The irradiation test results, therefore, are in most cases not directly applicable to the so called 'reference' design and are in almost all cases not easily traceable to particular fabrication methods and precursors. For future safety analysis reports used in licensing, fuel performance models should show a clear connection between fabrication, quality assurance, irradiation test results, and model predictions ... Moreover, future LHTGR fuel particle R&D should attempt to reduce the current uncertainty with respect to fuel particle failure detection ... Therefore, it is suggested that future fuel particle development programs should be designed keeping in mind the need to provide better quantified data with respect to fuel failure detection error."

If "LHTGR" were replaced by "MHTGR", the above statements could just as well have been written for the U.S. program in 1990 as in 1976. Of particular interest for modeling philosophy is the final statement of the report, which raises an issue rarely emphasized today although logically sound:

"For consistency, it is believed that there should ultimately be a single fuel failure model for the HTGR, that the model should accurately describe the relevant phenomena, and that this model should be applicable to all conditions; thus the same basic fuel failure model should be used for the accidents as well as for normal operation. It should only be necessary to change the input to the model; e.g., temperatures for different operating conditions ..."

2.2.4 COPAR (1977)

The GA code COPAR simulated FP release from particles by numerically simulating diffusion through multiple thin shells [17]. Fick's diffusion equation was analytically solved for each shell, and the equations coupled numerically using the interface boundary conditions. This code was

4
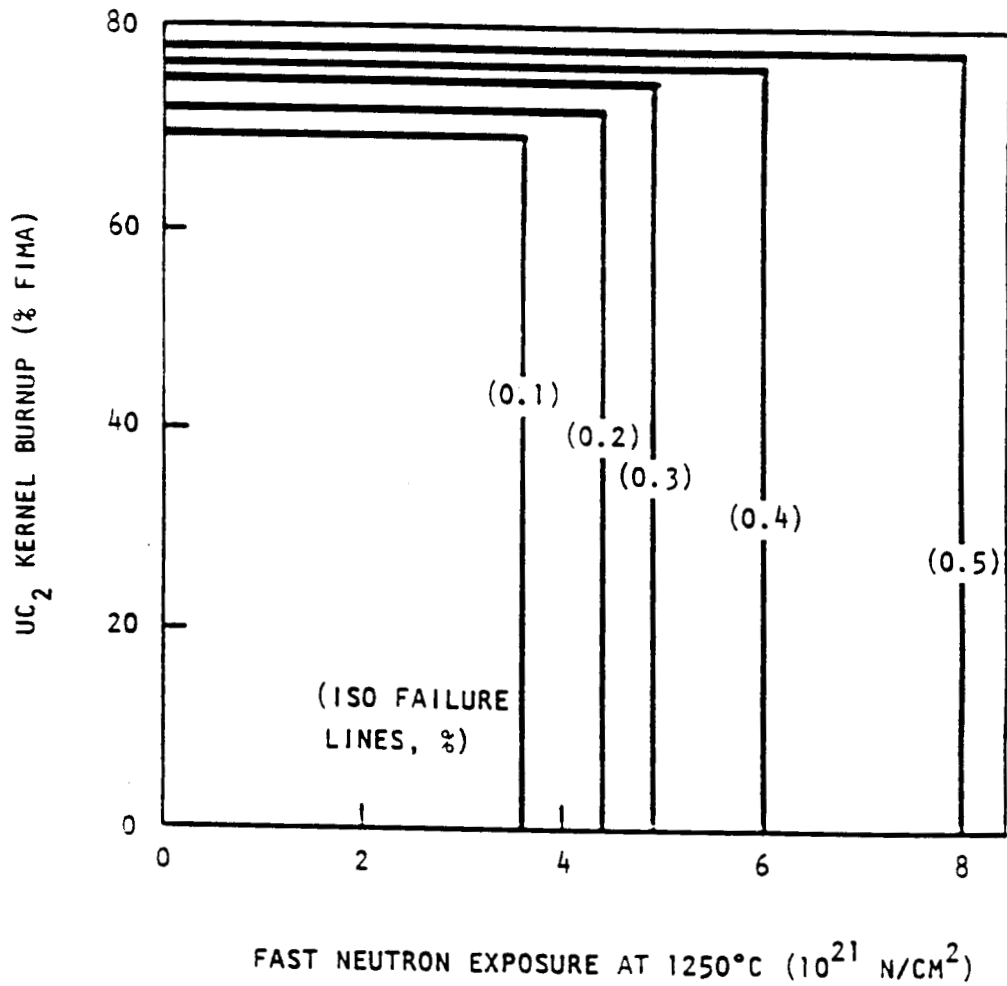
Fig. 1. Assumed TRISO UC_2 pressure vessel failure fractions (%) at 1250°C as a function of kernel burnup and fast neutron exposure, ca. 1974. (from [13])

5
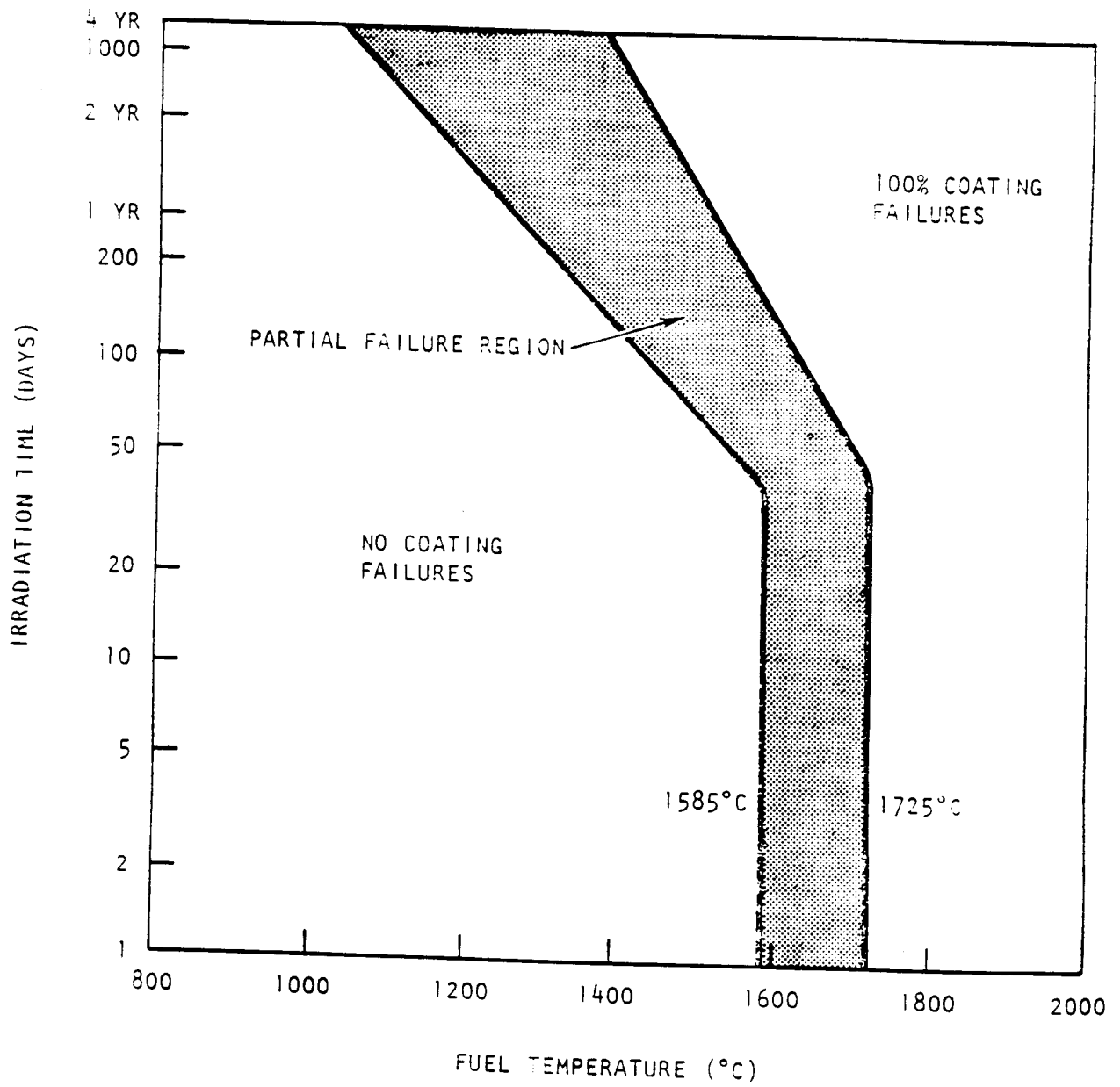
Fig. 2. TRISO fuel particle coating failure diagram, ca. 1974. (from [15])

6
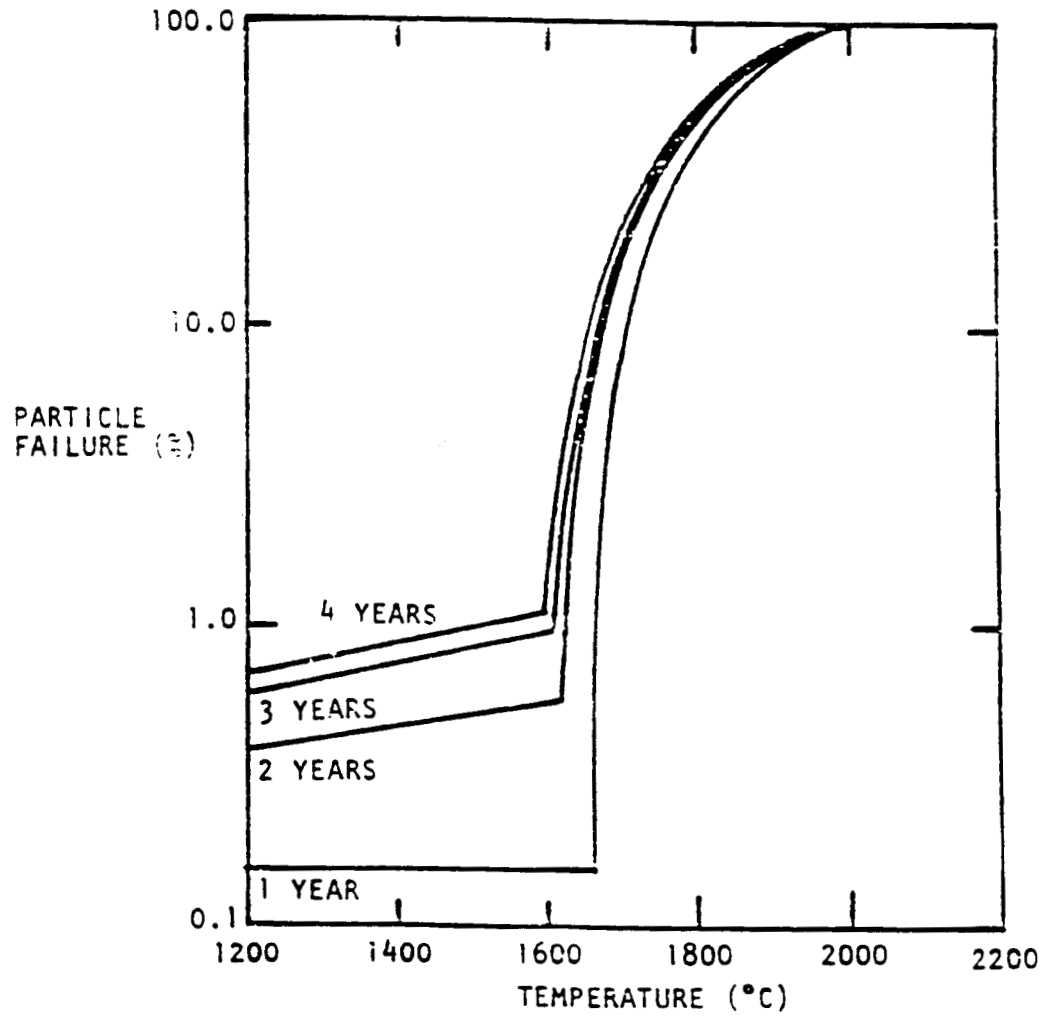
Fig. 3.   TRISO fuel particle coating failure diagram, ca. 1975. (from [16])

7

developed when computational capabilities were much more limited than today. Thus, an analytical solution for multi-layered diffusion was developed with sufficient approximations that results could be obtained within limited computer time. It was later realized that the calculated results may not be reliable when diffusion coefficients of the different layers were not similar, so modifications to the code were required [18]. The present status of the code is unknown.

2.2.5 GA Gas Release Models (early 1980's)

Several approaches to modeling fission gas release from HTGR fuel particles under accident conditions were pursued by General Atomic Company (later GA Technologies) in the early 1980's. The first is a simple analytical expression approximating krypton-85 release during AC heating ramp tests, in which Kr release is equated with the "total coating-failure fraction" (TCFF) [19]:

$$TCFF = 4.38 \times 10^{-6} \exp(0.0042\,T) \quad , \tag{1}$$

with the heating temperature T given in degrees Kelvin. This generic model is designed to approximate Kr release from all types of fuel particles: HEU UC_2, ThO_2, and LEU fuels (UC_2, UO_2, and UCO of varying stoichiometry). Evidence used to support this simple model includes Kr-85 release data from HEU and depleted UC_2 fuel particles, which did not suggest any dependence on burnup, irradiation temperature, fission density (i.e., number of fissions per cubic meter inside the SiC layer), fast fluence, or heating rate. This model assumes that ^{85}Kr release is directly related to total TRISO coating failure, and TCFF values determined by assuming the ^{85}Kr release fraction equals the TCFF. This assumption implies that all ^{85}Kr is immediately released from the particle upon failure of the coating.

The second approach derives governing equations to approximate release for two generic failure modes, and several parameters are incorporated into the governing equations which can be adjusted to approximate the fission product release data. This model is presented in the 1983 report by D. T. Goodin [20], and used parts of a model presented in 1980 by B. F. Myers and R. E. Morrissey [21]. The details of the model will not be described, but again the coating failure fraction of HTGR fuel is defined to be identical with ^{85}Kr release. Two coating failure mechanisms are postulated, although their separate contributions to failure are not quantified: fission product attack on the SiC (i.e., corrosion) and thermal decomposition of the SiC layer at high temperatures. Corrosive failure is assumed to occur linearly with time, and thermal decomposition is assumed to occur nonlinearly. A linear combination of these two contributions to failure comprises the governing equation, and variables within the governing equation are assumed to consist of various analytical forms whose parameters are then determined from existing data on ^{85}Kr release during GA's ramp and isothermal tests. Use of this model again concludes that fuel particle performance is not dependent on burnup, fast fluence, or kernel composition, but primarily on the thermal stability of the SiC coating layer. Although development of this model was apparently not pursued further, the concepts of dual failure mechanisms and numerical determination of the parameters within the assumed governing equation can be seen in the 1985 joint US/FRG accident condition fuel performance model [22].

A third approach to ^{85}Kr release involved work by W. J. Kovacs in collaboration with D. T. Goodin and K. Bongartz on a refined pressure vessel model [23]. Rather than only considering simultaneous failure of all coating layers (a "Category I failure"), they also postulated a "Category II failure" of a SiC layer with zero fracture strength, defective because of either manufacturing flaws or corrosion by FP or kernel attack. This Category II failure allows intact PyC layers to coexist with the

failed SiC layer. Failure fraction determinations for Category I failure are obtained by either metallographic or visual examinations, or by measurements of ^{85}Kr release. As intact PyC layers delay Kr release, a Category II failure can only be determined by measuring ^{137}Cs release or metallographic evaluation. Closed form stress solutions are obtained for both SiC and PyC layers, and calculations presented with respect to existing data. The irradiated ThO_2 fuel particles from which this Category II failure was postulated showed significant corrosion and kernel attack on the SiC layer [24].

2.2.6 GA Metallic Fission Product Release Model (1983)

Although fuel performance modeling efforts in the early 1980's focused on krypton release, sufficient metallic FP release data, especially for cesium, was accumulated to warrant development of a corresponding AC model for metallic FP release. A diffusive release model for volatile metallic FP was presented by D. T. Goodin in 1983 [25], based on a computational model developed by B. F. Myers [26]. Although a diffusive release mechanism for Cs was subsequently dismissed in 1985 in the US/FRG AC Fuel Performance Model, this diffusive model is nevertheless presented here for the sake of completeness.

Reference [25] presents calculations for both ^{137}Cs and ^{110m}Ag release. The primary assumption of this diffusive model is that retention of metallic FP is dominated by the effect of the SiC layer, and the kernel and PyC layers have only secondary effects on FP release. Likewise, the presence of Cs diffusing into the SiC layer during irradiation will be negligible compared to AC release. A reference diffusion coefficient for Cs in SiC was used for calculations. An arbitrary limit of 1600°C was used to differentiate normal operating condition models from this AC model, based on expected HTGR core temperature limits, observations of insignificant failure from an irradiation capsule test with cycling to 1600°C, and a suggestion that thermal dissociation of bare SiC will become significant above 1600°C.

2.3 RECENT MAINSTREAM APPROACHES TO MODELING: FRG MODELS

2.3.1 FRESCO

The FRG code FRESCO was developed in the early 1980's to obtain numerical solutions of the diffusion equation [27]. Two versions of FRESCO were developed: the "core" version [28] describes the complete HTGR core release of FP, and the "pebble" version [29] describes the FP release of individual spherical fuel elements containing large numbers of particles. This pebble version, FRESCO-II, simulates a two step release process for Cs in FRG fuel spheres as represented by effective diffusion coefficients, first through the SiC to the graphite grain boundaries, then by diffusion on the graphite grain boundaries and desorption into the coolant. As with the mainstream fuel performance codes, a particle failure function prior to release is required, which is either assumed based on the Kr release, or is obtained from the PANAMA-I code [27].

FRESCO results are in good agreement with release data from spheres, but careful selection of the two effective diffusion coefficients must often be employed to obtain such agreement. Effective diffusion coefficients reduced an order of magnitude or more from reference values for SiC and matrix graphite were commonly used. The effective diffusion coefficients used for SiC show some consistency, but those for matrix graphite vary by nearly two orders of magnitude.

9

2.3.2 PANAMA Codes

During the 1980's, a series of PANAMA codes were developed in Germany which emphasize pressure vessel failure mechanisms of the SiC layer. The PANAMA-I code [12] evaluates Kr release from the particles by assuming instantaneous failure of the SiC layer as a precursor to release. The failure function depends on both classical PV failure and on thermal decomposition of the SiC. Effects of the outer pyrocarbon layer on release are not considered. After SiC failure, Kr release is treated analytically as gas release from an exposed kernel (Booth model).

The PANAMA-II code [27] (ca. 1985) evaluates both Kr and Cs release. The immediate release of all Cs is assumed after the SiC layer fails, and this release is used as an indicator of SiC failure, analogous to the "Category II failure" of §2.2.5. The statistical failure rate of SiC incorporates two distributions which are coupled in a Weibull distribution: the SiC layer thickness and the SiC degradation rate. The degradation rate in turn depends on fission product corrosion and thermal decomposition mechanisms. An intact outer pyrocarbon (OPyC) layer delays the Kr release after failure.

PANAMA-III [27] (ca. 1988) returns to a PANAMA-I format, modifying some assumptions as to governing mechanisms and re-evaluating the relevant coefficients used in calculations. Both Kr and Cs release are modeled. Modifications from PANAMA-I assume thermal decomposition as the dominant failure mechanism and diffusion through the matrix graphite as relevant.

Comparisons of PANAMA results with release from several of the heating tests shows that PANAMA-I sometimes misrepresented Kr release by orders of magnitude, often overestimating release. The later versions of PANAMA gave better agreement, with PANAMA-III often approximating the magnitude of final fission product release. However, the PANAMA codes usually do not simulate the time-dependent release profiles with respect to initial release and the slope of the release curve as well as does FRESCO-II. With the assumptions of SiC failure prior to release, the PANAMA curves show a delayed release followed by a more rapid rise than do most of the samples [27]. The initial experimental release usually attributed to contamination is not considered by PANAMA. At present, PANAMA-I is still being used to predict Kr release from spheres, and Cs release predicted using FRESCO-II [30].

2.4   RECENT MAINSTREAM APPROACHES TO MODELING: US/FRG MODEL

2.4.1   US/FRG Accident Condition Fuel Performance Model (1985)

The basic assumptions of the joint US/FRG model [22] (also sometimes referred to as the Goodin-Nabielek model after D. T. Goodin and H. Nabielek) were: (1) SiC fails over time during postirradiation heating; (2) Cs does not diffuse through intact SiC; and (3) retention of Cs by the kernel and PyC layers is negligible after SiC failure. These assumptions parallel the "Category II failure" mechanism as described in §2.2.5. SiC failure is treated statistically using the Weibull parameter, similar to the PANAMA approach (although pressure vessel failure is not explicitly incorporated into the model), and Cs release is used as the indicator of failure. SiC failure was considered to result from two mechanisms: thermal decomposition and corrosion by FP. Few heating tests had been conducted on the modern German fuels at that point with which to derive parameters, so some of the results from earlier U.S. fuels were included in the model's database. Model predictions for Cs release were compared to release from six GA ramp tests, giving good agreement with release data near the end of the ramps, but poorer agreement early in the ramps. Predictions for sphere R2-K13/1 showed good agreement with experiment.

2.4.2 Revised US/FRG Model (1989)

With the additional data derived from the German heating tests, the US/FRG model was reevaluated [2]. The model was not significantly modified, but the model parameters were rederived using this new data. One revision assumes that thermal decomposition is the major SiC failure mechanism, thus downplaying corrosion. The new data indicated Cs retention in the matrix graphite of the FRG spheres was much greater than predicted. Thus, a correction factor called the Matrix Release Fraction (MRF) was considered for spheres showing FP release. This MRF is defined as the ratio of the Cs release from the sphere to the Cs release from the particles, and is assumed to be only a function of the fast neutron fluence. The MRF factor was used to estimate particle release from sphere release, and model calculations were then compared to this modified release data.

The revised US/FRG model rederived the model coefficients based on recent FRG heating tests, but did not include 7 out of 16 of the AVR sphere heating experiments and 3 out of 12 of the capsule tests in this calculation, because their release was either too small or too large with respect to the other samples. The derived expression for the frequency factor, used in Weibull parameter calculations, has exponential dependencies of $(\text{fission density})^{2.09}$, $(\text{fast fluence})^{0.041}$, and $(\text{irradiation temperature})^{4.14}$. The physical justification presented for these values is limited, thus these dependencies are not informative as to the governing phenomena involved in FP release.

Although results from the revised model for Cs release at end of heating typically give better comparisons with recent heating test results than does the earlier model, the agreement is not satisfactory for all samples. The shape of the calculated release curves are similar for all samples, i.e., delayed release followed by rapid rise after particle failure and then a slower rate of increase for the remainder of the heating time. The main difference between the calculated curves for different spheres is the initial value of Cs release. The experimental release curves show more variation in the rate of release than the US/FRG model. Simulation of initial experimental release values ("contamination") is not included in the model.

2.4.3 Martin-Goodin-Nabielek Model (1988)

The Martin-Goodin-Nabielek (MGN) model as implemented in the MACINTOSH code [31] represents a modification of the US/FRG model toward consideration of more fundamental physical mechanisms of FP transport and release. In evaluating experimental release data of cesium from TRISO particles, the authors conclude that neither a pure diffusive model nor a pure particle failure model (i.e., PV failure model) can reproduce the range of fractional release values observed within a single fuel sphere. In this model, the Weibull distribution for particle failure is coupled to a log-normal distribution of SiC grain-boundary corrosion rates and a normal distribution of grain boundary path lengths. Two failure models may be simulated: either the simultaneous PV failure of all coating layers within a particle, or failure of a single layer followed by diffusive release through the remaining intact layers [32]. The diffusion coefficient of cesium in SiC is assumed to be composed of two components, one representing bulk diffusion in the grain and one for grain boundary diffusion. The bulk diffusion coefficient is assumed to be negligible relative to grain boundary diffusion. Grain boundary diffusion is assumed to be negligible until damage occurs to the SiC, at a time determined by the Weibull parameter. After damage, the grain boundary diffusion coefficient is assumed to increase as a step function, followed by diffusion of Cs through the damaged SiC layer. MACINTOSH then simulates Cs transport through the fuel sphere as a one-dimensional diffusive process. Cesium transport across the matrix graphite is treated as a diffusive process with trapping, to simulate Cs uptake by the graphite and calculate Cs concentration profiles across the sphere. Temperature variation across the sphere is not incorporated into the model, and the particle

11

failure rate is assumed constant across the sphere. The calculated release from particles over each time step is spread uniformly across the sphere, thus enhancing the apparent release rate at shorter times and smaller releases. No fast fluence or burnup dependencies on particle failure are considered.

The MACINTOSH code was used to simulate ^{137}Cs release from spheres FRJ2-K13/4, HFR-K3/3, and AVR 76/18. With some model parameters estimated from the heating test for HFR-K3/3, the results of that test are well approximated by MACINTOSH. The release from spheres FRJ2-K13/4 and AVR 76/18 are overpredicted by a factor of three to four. The measured cesium profile across FRJ2-K13/4 is well approximated.

2.5 NON-MAINSTREAM APPROACHES TO MODELING

2.5.1 Introduction

During the development of AC fuel performance models over the last two decades, some models which would appear to be the most physically meaningful for atomistic FP transport have been relegated to non-mainstream areas of the modeling program. Diffusion modeling is the most obvious example of an approach largely rejected by the U.S. fuel performance modeling community over the past years, except for the model presented in §2.2.6 above. The FRG work has continued with the FRESCO diffusion code, although some particle failure function is also incorporated into this code prior to diffusive transport. In the early years of HTGR work some impressive effort was put into diffusive modeling which appears to be largely forgotten. This pre-1970 work will be briefly presented, along with counter-arguments and models presented in response to the 1985 US/FRG model.

2.5.2 Diffusion Modeling in the United States (1968)

R. W. Dunlap and T. D. Gulden [33] presented a parametric two-zone diffusion model appropriate for BISO particle release. Parametric results for R/B values as a function of the diffusion coefficients of kernel and coating, coating thickness, contamination fraction, decay constant of the FP, and partition coefficient at the kernel-coating interface. This partition coefficient represents the relative preference of a FP species for one of two neighboring materials, a factor rarely considered in mainstream fuel performance models (perhaps due to limited data and experimental uncertainties). The model was derived in spherical geometry, and assumed a zero concentration boundary condition at the particle surface. This model could approximate both steady-state release and transient times to reach steady-state release.

As an early model, this approach only saw limited comparison with experimental data, and further references to this work are few. The authors observed that experimental evidence existing at the time indicated that a diffusion mechanism for fission gas release from BISO particles appeared to be a good assumption. Although detailed parametric evaluations were presented of the effects of different coatings (e.g., SiC), coating thicknesses, levels of contamination, and partition coefficients, the authors concluded at the time that "the primary difficulty in applying such a model is the lack of available experimental information on the diffusion of the various nuclides during irradiation and, in many cases, on the levels of coating contamination." As they observed that the PV failure mechanism had been already extensively developed [3], this lack of experimental data for diffusion model development may have played a role in the pursuit of pressure vessel models relative to diffusion models.

12

2.5.3 Diffusion Modeling in Europe (1968)

H. Walther [34] presented an impressive piece of diffusion modeling which could simulate multilayered and TRISO particles with a more general boundary condition (i.e., evaporation) for the particle surface than that employed by Dunlap and Gulden. Fission product recoil from the kernel could also be incorporated. Included in the model are both bare kernel and intact particle release, a non-uniform contamination function, radioactive decay of the FP, and partition coefficients between the layers. Parametric studies were presented for variation of many of these parameters, and the effect of incorporating the SiC layer in TRISO particles was evaluated. The incorporation of the contamination factor with diffusive release generates fractional release curves which qualitatively approximate the shape of many of the FRG sphere release curves. Direct comparisons with experiment were again limited by the paucity of experimental data. The need for including a more complex transport process in graphite, such as diffusion with defect-trapping, was mentioned.

Although this diffusion model incorporated more physical mechanisms in FP transport than perhaps any other model to date, references to this work appear to be rare, and it is doubtful that this methodology was ever extended for comparison with or inclusion of experimental TRISO particle data. The methodology presented in this paper appears to merit serious consideration for any future development of a diffusion-based model of AC FP release.

2.5.4 Counter-Proposals to US/FRG Model (1986)

B. F. Myers [35] summarized the existing US/FRG collaborative fuel performance model and an existing alternate model of FP transport during accident conditions, while postulating a third model of FP release. The US/FRG model of 1985 states that particles with unfailed coatings do not release Cs or Kr, Cs release is an indicator of SiC failure, intact OPyC layers can delay Kr release after failure of the SiC layer, and SiC fails predominantly by SiC corrosion around 1600°C and by thermal decomposition at higher temperatures. Release of FP other than Kr or Cs is not considered by this model.

In contrast, the HRB model represented opinions expressed within the Hochtemperaturreaktorbau GmbH project of the FRG, and as described in Ref. [35] assumes that particles releasing Kr have failure of all coating layers, Kr release is an indicator of failure, and intact particles can release Cs by diffusion through intact coating layers. Evidence of diffusive release during particle and sphere heating tests is presented, and fast-fluence-dependent diffusion coefficients are presented as derived from results of sphere heating tests. A PV failure mechanism is included to account for [85]Kr release.

B. F. Myers then questions the dependence of these models on FP-induced corrosion of the SiC layer, and states "the effect of SiC-fission product reactions would appear in the view of the writer to be negligible under the irradiation and experimental heating conditions employed in evaluating metal and gas release from the fuel elements ...", a prophetic observation considering the 1989 revised US/FRG model revision's dismissal of the corrosion mechanism.

Myers then advanced a third model which relates FP release to the annealing of irradiation damage in SiC during heating, observing that electrical, thermal, and mechanical properties of SiC altered during irradiation are partially recovered by postirradiation annealing at higher temperatures. The transport across the SiC layer of fission gas and possibly metallic FP trapped in irradiation-induced voids and vacancies during the high-temperature annealing process is hypothesized. The importance of this release mechanism for Cs is downplayed by the inclusion of metallic FP diffusion across the SiC layer. The postulates of this "third model" are presented as:

1.   particles releasing Cs and Kr are predominantly intact,

13

2.   Cs release is governed by diffusion through the SiC layer,

3.   Kr release is governed by diffusion through the inner and outer pyrocarbon layers, and

4.   Kr transport across the SiC layer occurs during initial heating and annealing of the irradiation damage.

Thus, for this model Cs release is treated as in the HRB model, Kr release as in the US/FRG model, and the annealing transport mechanism is presented as an untested hypothesis. Among the other proposals presented in Ref. [35] is an interesting mechanism for silver release involving the trapping of silver atoms at neutron-induced defects within the SiC. The strength of the binding sites is postulated to restrict Ag release at normal operating temperatures, but the higher AC temperatures can release Ag from the sites and from the particles. Thus, the initial release of Ag from the particles during heating is postulated to result from release of all Ag trapped within the SiC. Analytical expressions are presented for the fast-fluence-dependent fractional inventory of Ag within the SiC layer which agree well with some experimental data. Comparable data for Cs release do not show such an explicit dependence on fast fluence.

In a subsequent report [36] which analyzes the Cs content of the SiC layer rather than the initial Cs release upon heating, B. F. Myers et al. expand upon this concept of SiC damage and trapping sites to propose a simple model for the uptake of Cs in SiC under irradiation: (1) the slowing down of fast neutrons causes structural damage in the form of trapping sites for Cs or pathways for Cs to enter the SiC layer, and (2) the Cs atoms move into the SiC to occupy these sites and perhaps along the paths generated by neutrons.

A significant hypothesis drawn from these assumptions is that the Cs content of the SiC is better described as a function of the number of neutrons passing through the SiC layer and of the reactor specific neutron flux spectrum than as a simple function of fast neutron fluence. Such a hypothesis might be applicable to other FP as well. By normalizing some experimental data with respect to a "damage probability" representative of the neutron energy spectrum, the Cs contents of the SiC layers were shown to approximate a linear relationship with respect to the fast neutron fluence. Such a hypothesis, if valid, would suggest a need to consider how hard the fast neutron spectrum is with respect to energy for different capsule irradiation tests, rather than simply tabulating all neutron fluence above a specific energy cutoff.

2.6   PRESENT STATUS AND EVALUATION OF MAINSTREAM MODELING EFFORTS

2.6.1   Additional Considerations Relevant to Accident Condition Modeling

Other experimental and modeling considerations which may be relevant for future efforts are briefly presented for completeness. A problem in simulating heating test results from AVR reactor spheres is that the irradiation temperature profiles are not well characterized. Temperature tests in the AVR discovered that maximum sphere surface temperatures can exceed 1300° C. Temperatures from sphere surface to center can also vary up to 200° C. Temperatures vary cyclically as the spheres are repeatedly passed through the core until peak burnup is achieved. Present models must assume an average irradiation temperature or make two calculations to span the temperature range.

As mentioned in §2.2.3, approaches which could avoid dichotomizing normal operating condition (NOC) and AC models would provide more self-consistency in modeling. As contamination and the initial FP release levels during heatup are more reflective of normal operating conditions than accident conditions, an approach that uses NOC FP distributions as initial conditions to AC release would be reasonable.

14

Although receiving much attention in the early 1980's, the corrosive effects of FP on SiC have been downplayed recently in favor of thermal decomposition of SiC. This change may partly reflect the reduced normal operating temperatures of the smaller HTGRs in current designs. Evidence of the reaction of palladium, silver, and other fission products has been presented [37]. This evidence could be reconsidered for its relevance to microstructural models. Thermal gradients were known to enhance corrosive attack, with the most severe corrosion mechanism involving kernel migration. The reduced thermal gradients in today's reference fuel designs may have reduced this problem, but thermal gradients do exist and their relation to FP transport may merit consideration for today's reference fuels [38],[39].

Many ceramographs are available from heated fuel particles which provide visual information on SiC degradation over time. Although the ceramographs from recent FRG heating tests clearly indicate nonuniform decomposition across the SiC layer, the existing AC models are limited to assumptions of uniform thinning of the SiC layer. As one FRG report states [40]: "The corrosive attack of fission products on the inner surface of the SiC layer can be seen ... One can see that the SiC layer is getting thinner from the outside ... During the heating test, grains have formed in the SiC, where decomposition has started at the grain boundaries." Relating these observations to a more detailed model of SiC decomposition could be informative.

The effects of repeated reheating of fuel particles have apparently not been considered in any detail in the literature, and no models have been presented to suggest reheating such as that expected from repeated AC scenarios would have any nonlinear effect on FP release. This question has great relevance for fuel integrity and reliability after exposure to AC heatup. Possible impact on refueling needs is discussed below. Although cycling during normal operating conditions is common, high-temperature AC cycling would generate more stress within particle coating layers.

Except possibly for the development of the pressure-vessel failure model, not much effort in incorporating relevant information from non-nuclear fields in the development of fuel performance models is apparent. As discussed in §5 below, SiC properties have been studied in great detail by the semiconductor industry, e.g., microstructure, decomposition, impurity diffusion, and radiation and neutron effects. More effort in incorporating the general scientific database into AC fuel performance modeling could prove rewarding.

2.6.2 Pressure-Vessel Failure vs. Diffusion

Most current models of FP release contain three assumptions: FP release is determined by failure of the coating layers, coating layer failure is experimentally described by FP release, and coating failure is theoretically described by some form of the Weibull distribution. Although other details are modified from model to model, these assumptions have rarely been seriously questioned in recent years. The dominance of the PV-failure approach to AC FP release is probably due to its continuing development from the 1960's onward.

The strongest point of the pressure-vessel failure model is its ability to introduce statistical uncertainty into particle failure and release rate through use of the Weibull parameter. Models which do not explicitly contain PV-failure mechanisms retain the Weibull approach to describing SiC decomposition or other phenomena. The real question is whether this statistical model correctly postulates the predominant phenomena involved in FP release, or permits the model to approximate other release mechanisms by deriving the model coefficients to obtain agreement with experimental results. Present modeling efforts apparently do not address a question of fundamental importance: are stress models directly applicable to FP release? Is mechanical performance of coating layers synonymous with microstructural performance? For example, a tiny pinhole-like imperfection or porosity of the SiC layer could generate significant release of FP without affecting the mechanical

15

performance of the particle; in fact, it could reduce the potential for PV-like failure through reduction of gas pressure. Likewise, neutron-induced disorder of the SiC crystal structure could enhance pathways for diffusive FP release, while only marginally affecting the strength of the SiC layer.

One experiment relevant to this issue involves FP release from particles with 35 μm and 51 μm SiC layers (i.e., FRG HFR-P4 spheres). An analysis in §3 does not indicate significant difference in the performance of these particles. Existing discussions of this experiment do not appear to have used these results to analyze the assumptions used in PV models. A recent report by O.M. Stansfield [41] contains the statement: "The KFA has lost some interest in SiC ring measurements as a means of strength determination since the failure of particles predicted with the ring strength results in overprediction of failure by 3 to 4 orders of magnitude." Considering the margin of error, could this observation relate to the relevance of stress models to FP release?

Recent models treat Cs diffusive release through SiC as insignificant. Recent reevaluations of the existing models see a need to incorporate a diffusive mechanism to improve predictive capabilities. Rather than instantaneous Cs release upon particle failure, a suggestion was made to incorporate a (surface) diffusion term for Cs along the SiC fault, to delay release and obtain better agreement with data [42]. A modification described as under way is the incorporation of a diffusion/trapping mechanism for Cs release from the sphere matrix [2], again to slow down the Cs release after failure. Both these suggestions perceive the need to provide a release mechanism somewhere between instantaneous release and classical diffusive release. The MACINTOSH code (§2.4.3) makes further efforts in this direction.

A limitation of existing PV models is their failure to incorporate microstructural phenomena. I have seen reference to enhanced stress concentration at voids, which could be significant in relating void growth during heating tests to PV models of failure. Extension of the existing PV methodology developed over the years to incorporate microstructural information and models could be useful.

2.6.3   What is "Failure"?

In 1982 a useful model for predicting fission gas release from particles was presented [19], as discussed in §2.2.5, which includes the observation that "the release of [85]Kr from HTGR fuel particles can be directly related to total TRISO coating failure. The total coating-failure fractions in this work were determined by assuming that the [85]Kr release fraction equals the total coating-failure fraction." The model was then developed with emphasis on this total coating-failure fraction (TCFF), although the [85]Kr release data was used synonymously with TCFF. As stated, the equivalence of the [85]Kr release fraction to the TCFF is an assumption. Other models employ similar analogies between particle failure and FP release.

Although nowhere explicitly stated, it appears likely that FP release was incorporated into the concept of particle failure in response to the criticism of the Tokar report [14] (§2.2.3): "... future LHTGR fuel particle R&D should attempt to reduce the current uncertainty with respect to fuel particle failure detection ... some methods of failure detection appear to be more accurate than others. Unfortunately, the visual methods upon which General Atomic has relied heavily, are among the most inaccurate, but the degree of error in each method has not yet been determined quantitatively ... it is suggested that future fuel particle development programs should be designed keeping in mind the need to provide better quantified data with respect to fuel failure detection error." Subsequently either visual examinations or FP release data were used to determine failure (see, e.g., Ref. [23]). At that point, it appears the modeling efforts lost sight of the independent nature of the supporting evidence (FP release) and confused that evidence with the primary hypothesis which the evidence was used to support. Productive modeling effort is devoted to

16

explaining physical evidence (i.e., FP release). Fixation on a failure hypothesis runs the danger of restricting objectivity in data analysis, with the potential for confusion as to dominant mechanisms of release. If the initial hypothesis is not correct or is limited in its validity, then subsequent modeling efforts may be limited in productivity.

If one is asked to describe particle failure, the standard response is the release of fission products through the coating layers. But if one asks why fission products are released from the particles, the current explanation emphasizes the failure of the particle coating layers by whatever mechanism, rather than the mechanisms themselves. Such circular reasoning avoids a precise definition of FP release, and can delay the incorporation of detailed microstructural information and mechanisms of FP transport.

Definition of particle failure as a digital state (either 0 or 1, either failed or unfailed) is only guaranteed success in modeling of PV failure. If FP release is instead an analog process, with either diffusion through or gradual loss of integrity of the SiC layer, then a failure hypothesis has limited meaning beyond a mechanical failure mechanism. Substantive evidence against a gradual decay and release mechanism has apparently not been presented, thus assumptions of failure prior to the onset of FP release may be unsupported despite their dominance within the mainstream AC fuel performance modeling effort. No fundamental distinction is made between a sphere fractional release of 10^{-4} and 1; the only difference is projected to be a failure of one particle vs. failure of one thousand particles. Fractional release of Cs from particles within the same sphere can show a wide range of values. Such evidence is more supportive of an analog than a digital release mechanism.

Failure models make no distinction of partial release of Cs (although Kr release can be delayed by the OPyC layer). At what point has a particle failed? Has a particle with less than 0.1% Cs release failed? If diffusive release is excluded, any particle releasing the smallest fraction of Cs (above contamination) must be considered failed. If FRG sphere fractional release exceeds approximately 10^{-4}, then particle failure is assumed to have been detected. But measured diffusion coefficients for Cs indicate diffusive release will occur during many of the FRG sphere heating tests [1]. At some time one must expect all particles to release, e.g., 0.1% of their Cs content. At that point do we consider 100% particle failure? In analogy with existing nuclear reactors, if a pressure release valve sticks open and a small amount of radioactive gas escapes, do we consider the nuclear reactor containment to have failed? Of course not, such a concept of failure is too simplistic. Then why incorporate a comparable methodology to FP release from particles, unless that approach has been demonstrated to be meaningful?

A better test of the failure hypothesis occurs during repeated high-temperature thermal cycling of the fuel particles. Conventional definitions of failure suggest an irreversible mechanism, i.e., if the particle has failed then it will have failed for all time into the future and will never again exhibit substantial containment under reheating. Thus, a reactor with conventionally failed fuel would probably require shutdown and refueling.

Now, instead of coating failure, consider a diffusive release mechanism during a depressurized core conduction cooldown event. We know all particles will release some FP if the heatup time is long enough, but this does not necessarily imply the SiC coating has lost its integrity. If the fuel then returns to normal operating conditions, the NOC release may be enhanced by escape of FP atoms already diffused into the SiC coating, but FP generated from continuing fissions may exhibit retention comparable to pre-heatup conditions. Thus, reactor shutdown and refueling would not be required. Only if SiC integrity is compromised during the thermal cycling of AC events will diffusive release and particle failure become synonymous.

Considering the above, the failure hypothesis of particle integrity could be better evaluated by release during thermal cycling rather than simple FP release. Simple FP release will not definitively favor a failure vs. diffusion hypothesis of release. However, if those heated particles

17

which show some FP release are reirradiated, heated, and monitored for continuing release, a "failed" particle would be expected to show substantially greater FP release than a particle exhibiting diffusive release. On this basis, a recommendation can be made to analyze the concept of failure based on the rate and magnitude of FP release during repeated thermal cycling and irradiation. Such a definition is relevant to the potential requirement of MHTGR refueling after undergoing depressurized core conduction cooldown events. A definition of particle failure based on the results of single heating tests is not sufficient to differentiate between analog and digital FP release, and thus does not distinguish coating failure from diffusive release through the coating.

2.6.4   Modeling of Sphere vs. Particle Release

The 1989 US/FRG model revision made a serious attempt at relating sphere release of Cs to particle release, using the concept of the matrix release fraction (MRF). As presented, the MRF is a useful concept, but is of questionable quantitative value. Only fast fluence dependency of MRF is hypothesized, although time and temperature of heating would be expected to play a major effect in values of MRF. The US/FRG model revision does not consider the MRF values for two low-fluence AVR spheres which deviate significantly from the hypothesized fast fluence dependency. One sphere shows little release, thus the MRF value is very high because release due to contamination is predominant. However, the other sphere is subjected to a high temperature ramp test and also shows a very high MRF value. From these results, the dependency of MRF on fluence as assumed in the US/FRG model has an inherent uncertainty of a factor of four or more. Also, the transition from contamination-dominated release (high MRF) to particle-dominated sphere release (lower MRF) is nowhere considered in the model. These observations are also made by others [27].

The use of the MRF in modeling is presently limited by the small number of deconsolidated spheres which can provide accurate MRF values, and this restricts the generality of the US/FRG model analysis. However, MRF based solely on fast fluence will likely never be quantitatively useful. A more accurate phenomenological interpretation of MRF related to heating conditions could prove useful in the future as a link between quantitative sphere and particle release. But without more information on deconsolidated spheres, direct comparisons between sphere and particle release must be approached cautiously.

2.6.5   Explanation of the IMGA Data for Sphere HFR-K3/3

Recent IMGA analyses [43] of particles from sphere HFR-K3/3, subjected to post-irradiation heating of 1800°C for 100 hours, showed a bimodal fractional release distribution for Cs with one component showing about 40% loss and the other about 80% loss. The higher-loss component appears to be centered in the outer portion of the sphere, suggesting a strong spatial dependence. Whether this loss is induced by irradiation temperature or gradients, by maximum neutron fluence at the outer surface, or by some other mechanism has not been determined. However, simulation of uniform irradiation conditions across the FRG spheres cannot account for these results. Apparently none of the present modeling approaches are designed to consider such spatial variations. As one example, the MACINTOSH code [31] as it presently exists cannot approximate this bimodal fractional release of Cs because of the assumed uniformity of temperature and particle failure rate across the sphere. The revised US/FRG model [2] and PANAMA-I [27] attempt to bracket FRG sphere release by making two calculations at either end of the expected temperature spectrum, but this approach cannot simulate the IMGA results.

A recent hypothesis advanced by K. Verfondern [44] to explain the bimodal Cs release distribution relates to the fact that sphere HFR-K3/3 was heated to 1800°C on two different

18

occasions, thus the effect of thermal cycling may play a role. Additional details on this hypothesis are not available at present.

An interesting area of speculation is the effect of fission neutrons generated within the spheres on the accumulated fast fluence of the SiC layers. These fast neutrons have initial average energies of about 2 MeV [45], much greater and potentially more damaging than the background reactor fast fluence in capsule tests. Due to self-shielding, the background fast fluence is a maximum at the outside of the sphere. The fission-induced neutrons enhance this maximum. By combining geometrical considerations and the mean free path within the sphere of these internally-generated neutrons, could a secondary maximum of accumulated fluence be located toward the interior of the sphere? If so, this could provide a useful hypothesis for explaining the IMGA results for sphere HFR-K3/3.

2.6.6   Philosophy of Modeling

Use of the MRF factor is a useful modeling concept, but incorporation into a quantitative modeling effort as in the 1989 US/FRG model introduces significant uncertainty. As mentioned in §2.6.4, the fast-fluence-dependent MRF may introduce a factor of four or more error in predicting the particle release from the sphere release data. The methodology of adjusting the experimental sphere release data to compare to the model predictions is questionable, as the model predictions could have been simply MRF-adjusted to compare to the actual sphere release data. Some may consider it a matter of semantics, but the uncertainty should be contained as much as possible within the model, otherwise one cannot be sure whether the benchmark data is even meaningful. Why introduce the uncertainty into the data?

A problem with the revised US/FRG model is that it provides us with little qualitative insight into release mechanisms beyond evaluation of coefficients which provide agreement between the model and the data. The expression for the frequency factor, used in Weibull parameter calculations, has exponential dependencies of (fission density)$^{2.09}$, (fast fluence)$^{0.041}$, and (irradiation temperature)$^{4.14}$. Without some physical justification presented for these values, such dependencies are not informative as to governing phenomena. One would conclude that Cs release depends extremely strongly on irradiation temperature but virtually not at all on fast fluence. Some explanation should be in order.

The synonymous use of either Kr or Cs release data as "failure" data is questionable. This concept of failure seems ill-defined at present. Fission product release is very specific and open to interpretation only within the limits of experimental uncertainty. To define FP release data as "failure" data seems to muddy the physical interpretation of FP release, with apparently nothing gained in the process. Why are the models not simply presented as an estimation of FP release, instead of the more nebulous concept of total failure (or partial failure, or any other type of failure)? Instead of being clear in modeling methodology, such an approach only provides a model of a model, instead of a model of FP release. As it presently exists, this concept of coating failure is apparently that, a model, a hypothesis, and one which has not been precisely defined based on existing experimental observations. At an earlier point in HTGR fuel development, fuel failure was probably a very convenient concept with which to evaluate overall reactor performance. However, as high-quality fuels were developed which frequently exhibited negligible release at high temperatures, fuel failure becomes less obvious and more ambiguous. This emphasis on failure is apparent in current mainstream modeling efforts, and the approach of the 1989 US/FRG model is identical to the 1982 work in this regard. Persistent efforts toward modeling a model rather than modeling precise experimental data and observations raises the danger of chasing one's tail.

The ultimate goal in FP modeling should reflect the fundamental importance and value of

models in general, as indicated by a statement in the previous status report [1]: "Models which are one step behind the data do not aid us in understanding the physics and chemistry of fuel dynamics unless predictive capability is demonstrated. A model which cannot predict behavior under new conditions is inherently limited in its usefulness and its verifiability. The most useful model is one which raises our level of understanding and teaches us something about the relevant phenomena involved through extrapolation to regimes in which data is not yet available. Hopefully existing fuel performance models can attain that goal, although much work remains to be done."

3. SIMPLE DIFFUSION MODEL FOR ANALYSIS OF FRG ACCIDENT CONDITION TESTS

3.1 INTRODUCTION

In the previous status report on AC modeling, evidence was presented which suggested a diffusive mechanism for Cs release through SiC cannot be summarily dismissed. If a diffusive mechanism is valid, then non-diffusive AC models may follow a wrong path with no guarantee of long-term predictive success despite the considerable time invested in them. To investigate the validity of a diffusion model for FP release, the simplest model of diffusive release feasible for a TRISO particle system is incorporated into a small computer code and used to evaluate and predict FRG sphere release data. Such a model must by necessity oversimplify the FP release process, but if the model provides meaningful results and insight into the existing release data, refinement of the model can be pursued. If not, it can be thrown onto the scrap heap of model development with no serious loss of time and effort.

3.2 HOLLOW SPHERE DIFFUSION MODEL

The simplest conceivable approach to diffusive release of FP through SiC is an analytical solution for diffusion through a thin spherical shell. The classic analytical solution is presented in Crank [46]:

$$\frac{Q_t}{4\pi ab(b-a)C_1} = \frac{Dt}{(b-a)^2} - \frac{1}{6} - \frac{2}{\pi^2}\sum_{n=1}^{\infty}\frac{(-1)^n}{n^2}\exp\left[\frac{-n^2\pi^2Dt}{(b-a)^2}\right] , \qquad (2)$$

with a and b the radii of the inner and outer surfaces of the shell, respectively, C_1 the concentration of diffusant at the inner surface, Q_t the quantity of diffusant escaping from the outer surface, D the diffusion coefficient, and t the time. By assuming a uniform internal concentration which is constant over time (i.e., neglecting kernel and inner layer effects on available diffusant concentration at the interior SiC surface), eqn. (2) can be cast in a form identical to that given in Appendix 1 of Ref. [47]:

$$FR = \frac{3b(b-a)}{a^2}\left\{\frac{Dt}{(b-a)^2} - \frac{1}{6} - \frac{2}{\pi^2}\sum_{n=1}^{\infty}\frac{(-1)^n}{n^2}\exp\left[\frac{-n^2\pi^2Dt}{(b-a)^2}\right]\right\} , \qquad (3)$$

with FR the fractional release. The assumption of a uniform internal concentration is acceptable as

long as the fractional release is not large; otherwise, approximations for a depleting source term should be incorporated to reduce the error and limit FR to values below one [48].

Equation (3) is valid for isothermal tests. For ramp tests, the following term for the temperature-dependent diffusion coefficient must be replaced in eqn. (3) by the summation [49]:

$$Dt \rightarrow \overline{Dt} = \sum_i D_i \cdot \Delta t_i \quad , \tag{4}$$

with Δt_i the time elapsed during interval i, and D_i the diffusion coefficient calculated from:

$$D_i = D_o \exp\left(-\frac{Q}{RT_i}\right) \quad , \tag{5}$$

with D_o the pre-exponential term for diffusivity, Q the activation energy for diffusion, R the ideal gas constant, and T_i the temperature during Δt_i. For continuous ramp tests, Δt_i can be chosen to be sufficiently small that the temperature and the diffusion coefficient can be approximated as constant during each interval i.

Equations (3), (4), and (5) are combined to give the governing equation for this analysis of diffusive release, with the knowledge that calculated values of FR which are very small or very large (near one) could have significant error. A reasonable approximation for diffusive release can be obtained for most of the FRG sphere heating tests, and the model can consider heating ramp tests and non-isothermal heating tests. The resulting computer code was named the SHELL code.

To evaluate the FRG sphere release data for each isothermal heating test, the effective diffusion coefficient was determined which, when used in eqn. (3), would reproduce the final experimental value for fractional FP release from the sphere. In effect, FP release was simulated as diffusion through the SiC layer of the individual particles with instantaneous release from the sphere upon release from the SiC, i.e., instantaneous release through the OPyC layer and matrix graphite, as approximated in some of the other AC models. Although an overapproximation, the effective diffusion coefficients so obtained reflect OPyC layer and matrix graphite effects in experimental release without explicitly incorporating them into the diffusive model. After compiling these effective diffusion coefficients for all relevant isothermal FRG sphere heating tests, the results were tabulated and compared. In plotting the log of the effective diffusion coefficients vs. the reciprocal of the temperature, an approximate linear relationship is the minimal requirement for the diffusive release mechanism to be valid, as in eqn. (5). These effective diffusion coefficients are not meant to exactly duplicate the diffusion coefficient of Cs in SiC; rather, their determination provides a means of normalizing the sphere release values with respect to heating time and temperature, to check the consistency of the results from different spheres.

All FRG sphere heating tests at 1500°C and above which show measurable release of fission products are listed in Table 1, along with relevant irradiation and heating parameters. In the following calculations, those spheres which were heated at multiple temperatures (1600° and 1800°C) were only analyzed for the 1800°C heating times, as diffusive release should be strongly dominated by the higher-temperature contribution.

3.3 CESIUM-137 RELEASE

The effective diffusion coefficients which match the SHELL release with the experimental

21

Table 1. FRG sphere irradiation and heating data.

sphere	T_{heat} (°C)	t_{heat} (h)	T_{irr} (°C)	t_{irr} (fpd)	burnup (%FIMA)	fast fluence (10^{25} m^{-2})	mixed oxide ?	reheat sphere ?
AVR 70/15	1500	140	AVR	910	7.1	1.7	yes	once
AVR 70/26	1600	304	AVR	1050	8.2	2.0	yes	
AVR 71/22	1600	500	AVR	481	3.5	0.9		
AVR 82/9	1600	500	AVR	1296	8.9	2.3		
AVR 82/20	1600	100	AVR	1253	8.6	2.2		
FRJ2-K13/2	1600	138	1000-1200	396	8.1	0.1		
HFR-K3/1	1600	500	1000-1200	359	7.7	3.9		
HFR-P4/1/8	1600	304	940	351	13.8	7.2		
HFR-P4/1/12	1600	304	940	351	11.1	5.5		once
HFR-P4/2/8	1600	304	945	351	13.8	7.2		
HFR-P4/3/7	1600	304	1075	351	13.9	7.5		
R2-K13/1	1600	1000	1000-1200	351	10.3	8.3	yes	
SL-P1/6	1600	304	800	330	10.7	6.7		
AVR 74/11	1700	185	AVR	853	6.2	1.6		
SL-P1/9	1700	304	800	330	10.7	6.3		
SL-P1/10	1700	304	800	330	10.3	6.0		
AVR 69/13	1800	92	AVR	1100	8.6	2.1	yes	thrice
AVR 70/33	1800	174.5	AVR	220	1.6	0.4		twice
AVR 74/10	1800	90	AVR	756	5.5	1.4		twice
AVR 76/18	1800	200	AVR	1034	7.1	1.9		
AVR 88/15	1600, 1800	50, 50	AVR	?	8.7	~2.25		
AVR 88/33	1600, 1800	50, 21	AVR	?	8.5	2.2		
AVR 88/41	1800	24	AVR	?	7.6	2.0		

sphere	T_{heat} (°C)	t_{heat} (h)	T_{irr} (°C)	t_{irr} (fpd)	burnup (%FIMA)	fast fluence (10^{25} m^{-2})	mixed oxide ?	reheat sphere ?
FRJ2-K13/4	1600, 1800	138, 100	1000-1200	396	7.6	0.1		
HFR-K3/3	1800	100	800-1000	359	10.2	6.0		once
HFR-P4/3/12	1800	279	1075	351	~12	5.5		once
AVR 73/12	1900	100	AVR	426	3.1	0.8		once
AVR 74/20	1900	50	AVR	1520	11.9	2.9	yes	
AVR 76/19	1900	30	AVR	1063	7.3	1.9		
AVR 80/22	1900	30	AVR	1325	9.1	2.4		
AVR 71/7	2000	100	AVR	248	1.8	0.5		once
AVR 80/16	2000	30	AVR	1136	7.8	2.0		
AVR 74/6	2100	30	AVR	770	5.6	1.4		
AVR 74/24	2100	30	AVR	1430	11.2	2.7	yes	
AVR 76/27	2100	30	AVR	1078	7.4	1.9		
AVR 76/28	2100	30	AVR	1005	6.9	1.8		

Ramp Tests

sphere	T_{max} (°C)	t_{heat} (h)	T_{irr} (°C)	t_{irr} (fpd)	burnup (%FIMA)	fast fluence (10^{25} m^{-2})	mixed oxide ?	reheat sphere ?
AVR 69/28	2250	56	AVR	870	6.8	1.7	yes	
AVR 70/18	2400	28	AVR	910	7.1	1.7	yes	
AVR 70/19	2400	27	AVR	303	2.2	0.6		
AVR 74/8	2500	27	AVR	399	2.9	1.4		
AVR 74/17	2500	27	AVR	1310	10.3	2.5	yes	
AVR 80/14	2500	27	AVR	1223	8.4	2.2		

fractional release of Cs from each sphere are listed in Table 2 and plotted in Figure 4 with the reference diffusion coefficient from Ref. [47]. B. F. Myers, in Ref. [47], provides two equations for diffusion coefficients for Cs in SiC, which are ascribed to laminar and columnar SiC structures. Although most experimental investigations indicate the preferred SiC structure is columnar, the columnar diffusion coefficient is too large to duplicate most Cs release experiments from FRG fuel, so the laminar diffusion coefficient is employed as the reference value. This coefficient is given by:

$$D_{Cs} = 6.68 \times 10^{-14} \exp\left(-\frac{12730}{T}\right) + 1.12 \times 10^{-4} \exp\left(-\frac{52560}{T}\right) \, , \tag{6}$$

in which the Q/R term in eqn. (5) has been combined into a single value. Figure 4 suggests the reference (laminar) value approximates the effective diffusion coefficients obtained from the SHELL code except at 1600°C (5.3 on the x-axis). Equation (6) is expressed as a linear combination of two terms, but the lower-temperature term is subject to greater uncertainty due to the very long experimental times required for accurate determination of the diffusion coefficient [50]. Because of this, a modified reference diffusion coefficient is also plotted in Figure 4 without the lower-temperature term, i.e., with the coefficient is expressed as:

$$D_{Cs} = 1.12 \times 10^{-4} \exp\left(-\frac{52560}{T}\right) \, . \tag{7}$$

Having been derived from data of several independent particle heating tests, the reference diffusion coefficient's approximation of the median value of the effective diffusion coefficients gives credence to this diffusive approximation of Cs release.

Following the approach used in the US/FRG model revision [2], some error measure related to the accuracy of model predictions relative to the experimental release can be obtained analogous to a standard deviation measure:

$$\sigma(\log FR) = \sqrt{\frac{1}{N-1} \sum_i (\log FR_{calc} - \log FR_{expt})^2} \, , \tag{8}$$

with FR_{expt} the experimental sphere release, FR_{calc} the calculated sphere release, and N the number of sphere tests predicted. By using the modified reference diffusion coefficient [eqn. (7)] in the SHELL code to predict FRG sphere release, and the results compared to the end-of-test experimental sphere release values using eqn. (8), a value of $\sigma(\log FR)$ of 0.97 was obtained. In comparison, the US/FRG model revision reports a value of 0.64 for MRF-adjusted release values [2]. Inspection of the results shows those samples heated at too low temperatures (especially at 1600°C) and too brief a time to expect diffusive release are greatly underpredicted by the SHELL code because of the initial release due to contamination. A diffusive release mechanism predicts no substantial release until a diffusive breakthrough time is exceeded [1], and thus cannot account for release due to contamination. To incorporate this initial release into the diffusion model, the fractional release values predicted by SHELL for each sphere were incremented to include the experimentally-determined release due to contamination, and the statistics recalculated to give $\sigma(\log FR)$ = 0.79, a significant improvement over the non-contamination-adjusted value. This contamination factor is included in all further predictions of Cs, Kr, and Sr release.

24

Table 2. FRG sphere release calculations for cesium-137.

sphere	T_{heat} (°C)	t_{heat} (h)	fast fluence (10^{25} m^{-2})	effective diffusion coeff.[a] (m^2 s^{-1})	FR_{expt}	FR_{calc}[a]	FR_{contam}	sample variance
AVR 70/26[b]	1600	304	2.0	4.70e-17	3.0e-5	1.52e-5	3.0e-5	3.17e-2
AVR 71/22	1600	500	0.9	2.78e-17	2.0e-5	1.30e-4	2.0e-5	0.766
AVR 82/9	1600	500	2.3	5.14e-17	7.6e-4	4.24e-4	4.0e-4	1.23e-3
AVR 82/20	1600	100	2.2	1.59e-16	6.2e-5	~0	2.0e-5	0.241
FRJ2-K13/2	1600	138	0.1	1.16e-16	3.9e-5	1.8e-11	1.3e-5	0.228
HFR-K3/1	1600	500	3.9	3.80e-17	1.1e-4	3.25e-4	9.0e-7	0.223
HFR-P4/1/8	1600	304	7.2	1.11e-16	1.9e-3	4.56e-3	2.5e-5	0.146
HFR-P4/1/12	1600	304	5.5	7.20e-17	2.6e-4	4.74e-4	2.0e-5	7.78e-2
HFR-P4/2/8	1600	304	7.2	1.88e-16	1.4e-3	3.50e-4	4.0e-4	7.34e-2
HFR-P4/3/7	1600	304	7.5	1.37e-16	4.0e-3	4.56e-3	2.4e-4	6.24e-3
R2-K13/1[b]	1600	1000	8.3	5.80e-17	0.015	7.85e-2	1.0e-6	0.517
SL-P1/6	1600	304	6.7	7.75e-17	3.8e-4	4.74e-4	3.0e-4	9.55e-2
AVR 74/11	1700	185	1.6	9.10e-17	7.6e-5	4.00e-3	4.0e-5	2.976
SL-P1/9	1700	304	6.3	5.80e-16	0.10	6.04e-2	N/A	4.80e-2
SL-P1/10	1700	304	6.0	4.27e-16	0.061	6.04e-2	9.0e-4	4.00e-6
AVR 69/13[b]	1800	92	2.1	6.50e-15	0.48	0.112	N/A	0.399
AVR 70/33	1800	174.5	0.4	4.20e-16	0.022	1.92e-2	N/A	3.48e-3
AVR 74/10	1800	90	1.4	1.60e-15	0.079	2.65e-2	N/A	0.226
AVR 76/18	1800	200	1.9	5.20e-16	0.045	0.107	5.0e-6	0.141
AVR 88/15	1800	50	~2.25	1.24e-15	0.014	1.05e-2	5.0e-6	1.56e-2
AVR 88/33	1800	21	2.2	1.16e-15	4.6e-4	4.26e-4	2.0e-5	1.96e-4
AVR 88/41	1800	24	2.0	7.90e-16	1.5e-4	2.97e-4	2.0e-5	0.106
FRJ2-K13/4	1800	100	0.1	5.58e-16	9.9e-3	3.41e-3	1.5e-6	0.214
HFR-K3/3	1800	100	6.0	1.24e-15	0.059	0.110	3.0e-6	7.29e-2

Table 2, continued

sphere	T_{heat} (°C)	t_{heat} (h)	fast fluence (10^{25} m^{-2})	effective diffusion coeff.[a] (m^2 s^{-1})	FR_{expt}	FR_{calc}[a]	FR_{contam}	sample variance
HFR-P4/3/12	1800	279	5.5	2.40e-15	0.52	0.398	5.0e-5	1.35e-2
AVR 73/12	1900	100	0.8	1.70e-15	0.10	4.99e-2	N/A	9.12e-2
AVR 74/20[b]	1900	50	2.9	1.07e-14	0.43	0.233	N/A	7.08e-2
AVR 76/19	1900	30	1.9	1.90e-14	0.46	3.94e-2	N/A	1.141
AVR 80/22	1900	30	2.4	3.70e-15	0.048	6.45e-2	N/A	1.66e-2
AVR 71/7	2000	100	0.5	1.60e-15	0.092	0.198	N/A	0.111
AVR 80/16	2000	30	2.0	1.04e-14	0.22	0.230	N/A	4.00e-4
AVR 74/6	2100	30	1.4	1.95-14	0.47	0.775	N/A	4.71e-2
AVR 74/24[b]	2100	30	2.7	2.05e-14	0.50	~1.0	N/A	9.06e-2
AVR 76/27	2100	30	1.9	2.73e-14	0.69	0.775	N/A	2.50e-3
AVR 76/28	2100	30	1.8	2.25e-14	0.55	0.775	N/A	2.22e-2

a   calculated from SHELL

b   mixed oxide sphere

N/A not available

Sample variance is calculated as:

$$s^2 = \left[\log\left(FR_{calc} + FR_{contam}\right) - \log FR_{expt}\right]^2$$
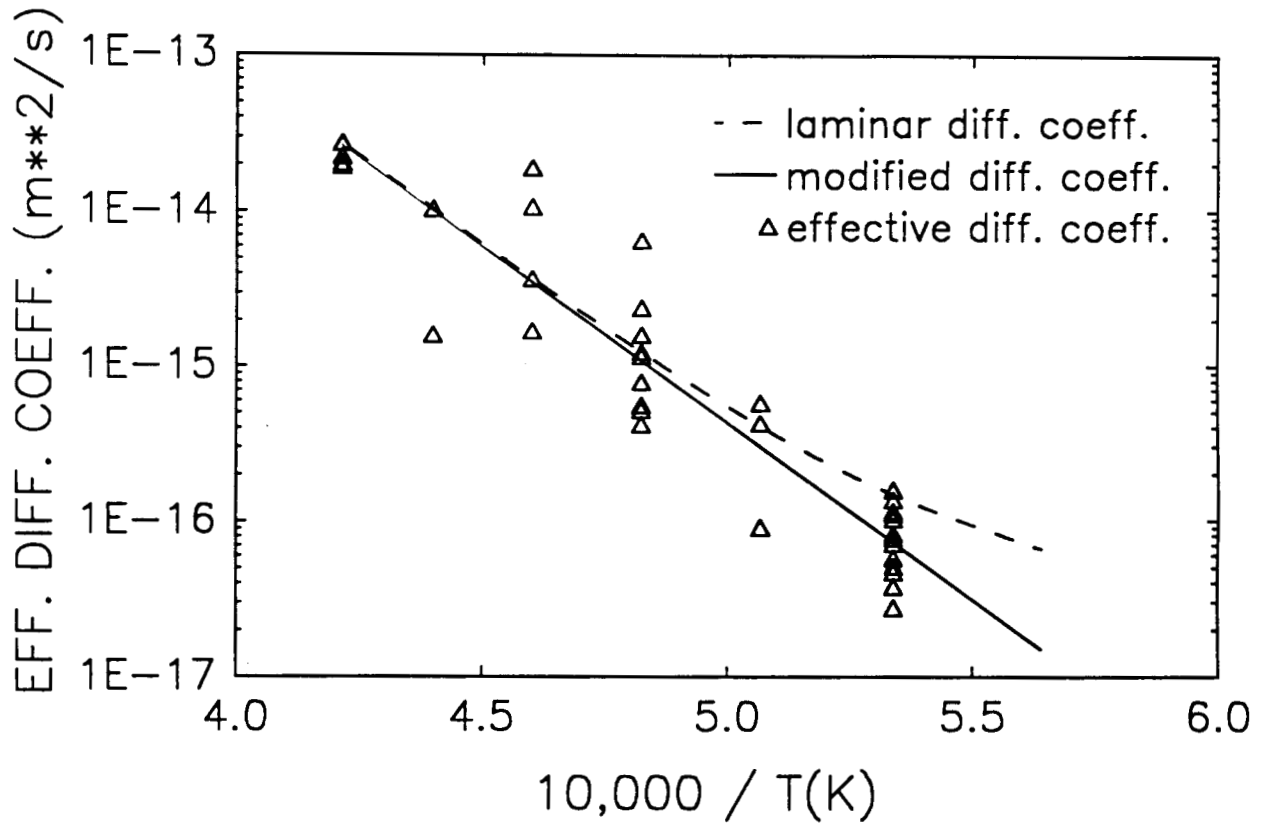
Fig. 4.   Effective diffusion coefficients for cesium-137 release from SiC, FRG spheres.

Figure 4 shows the logarithm of the effective diffusion coefficients varies linearly with the reciprocal of the temperature, which permits derivation of an average temperature-dependent effective diffusion coefficient as a modeling parameter analogous to eqn. (7). Inspection of the results in Figure 4 revealed a consistent trend: spheres exposed to low fast fluence (mostly AVR spheres) tend to fall below the reference value, and spheres subjected to large fast fluence in the material test reactor (MTR) tests tend to fall above the reference. Consistent with this, the MTR spheres FRJ2-K13/4 (fast fluence of 0.1×10^{25} m^{-2}) and HFR-K3/1 (3.9×10^{25} m^{-2}) fell closer to the AVR results than the higher-fluence MTR results. (The data point for sphere FRJ2-K13/2 is atypical, as discussed below.) Consistent with this observation, two average effective diffusion coefficients were derived from the SHELL data, one which includes all the low-fluence tests and one which includes the high-fluence MTR tests. Data for sphere HFR-K3/1, with fast fluence of 3.9×10^{25} m^{-2} intermediate between the two groups, was included in the low-fluence group based on its location in Figure 4. Only data from spheres AVR 71/22 and FRJ2-K13/2 were not used in deriving the diffusion coefficients, as their heating times of 100 and 138 hours respectively at 1600°C are too short to permit any expected diffusive release (as evidenced by their uncharacteristic locations in Figure 4) and thus are not appropriate to this model.

The data points in Figure 4 were also analyzed for trends with respect to other irradiation parameters, i.e., burnup, irradiation temperature, and effective full power days in the reactor. Although a trend based on fast fluence is apparent, the same can be said for a dependence on burnup. Most of the data in Figure 4 represent AVR spheres, which all have a nearly constant fast fluence to burnup ratio. A preferential dependence of FP release on either fast fluence or burnup is ambiguous.

Figure 5 shows the relation of the two average diffusion coefficients (labeled D_{AVR} and D_{MTR} for the low-and high-fast-fluence data, respectively) to the modified reference diffusion coefficient. Both average coefficients are approximately parallel to the reference value, with the higher fluence value shifted higher and the lower fluence value shifted slightly lower. If we speculate that the magnitude of fast fluence has some effect on SiC degradation and FP release, then the diffusive model gives results qualitatively consistent with expectations based on physical phenomena. The expressions for these diffusion coefficients, obtained by performing a least-squares fit to each group of data, are given by:

$$D_{AVR} = 1.08 \times 10^{-4} \exp\left(-\frac{52723}{T}\right) \quad , \tag{9}$$

$$D_{MTR} = 1.11 \times 10^{-3} \exp\left(-\frac{56262}{T}\right) \quad . \tag{10}$$

The D_0 values for both D_{AVR} and D_{MTR} and the adjusted activation energy (Q/R) are in good agreement with the reference values in eqn. (7).

These two derived diffusion coefficients were used to repredict the release from the FRG spheres listed in Table 2. Again combining the initial contamination values with the predicted diffusive release, the variation of these results from the experimental values is given by $\sigma(\log FR)$ = 0.73, nearing the reported US/FRG model value of 0.64.

Inspection of those data points which give the greatest error between prediction and experiment revealed additional interesting trends. For the AVR grouping (below 3.9×10^{25} m^{-2} fast fluence), those data points skewed toward unusually low effective diffusion coefficients consistently
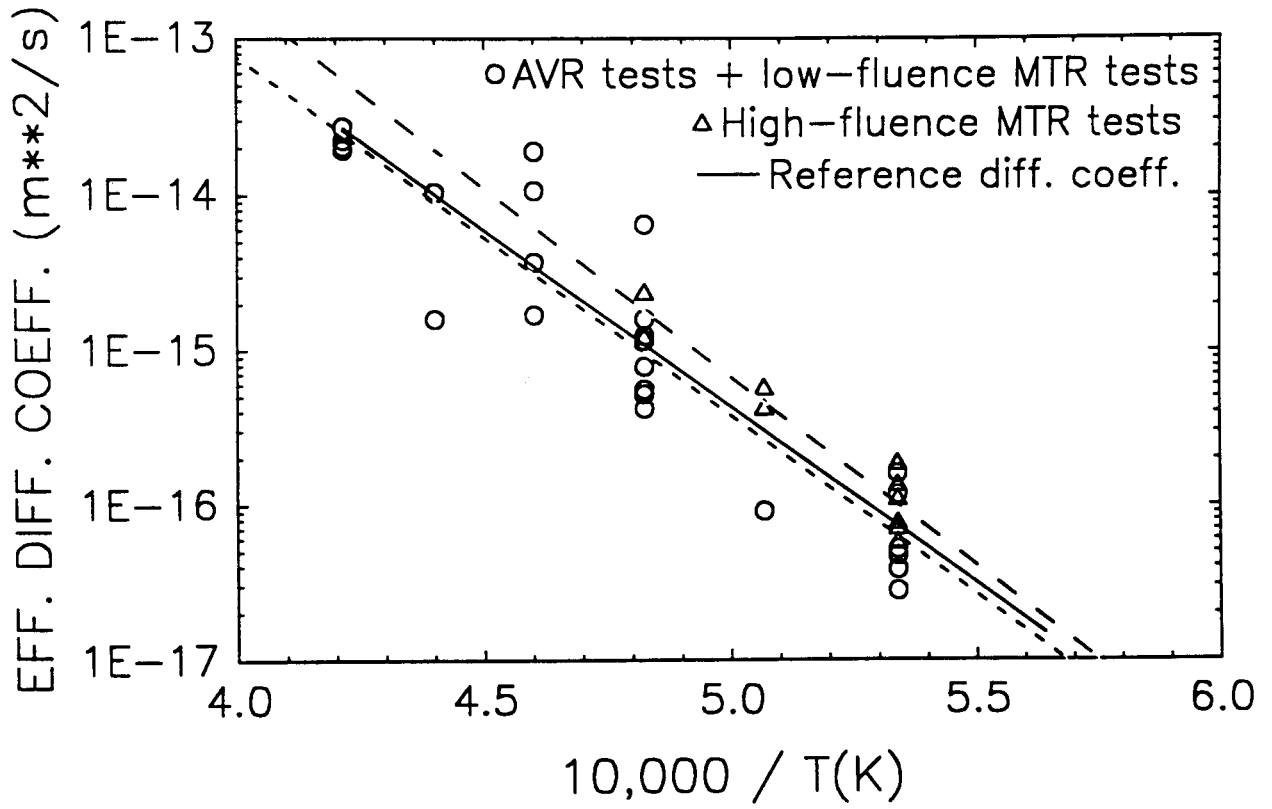
Fig. 5.   Effective diffusion coefficients for cesium-137 release from SiC, FRG spheres:
two-group model.

represented spheres which were exposed to the lowest levels of fast fluence (and burnup). Spheres exposed to fast fluences of 2.0×10^{25} m^{-2} and above tended toward higher effective diffusion coefficients, although a few spheres behaved unpredictably. Likewise, in the MTR group those spheres with the highest fast fluence (above 7.0×10^{25} m^{-2}) tended to have the highest effective diffusion coefficients (although these were only heated at a temperature of 1600°C). Based on this observation, the data points were again subdivided into five fast fluence groups (with fluences given here in units of 10^{25} m^{-2}): those spheres ≤ 0.9, those between 1.4 and 2.0, those between 2.2 and 3.9, those between 5.5 and 6.7, and those ≥ 7.5. Equations for effective diffusion coefficients for each group were derived. Again a distinct trend according to fast fluence is apparent. No temperature dependence could be determined for the fifth group, as heating was only conducted at 1600°C. The expressions for these diffusion coefficients were used to again predict sphere release, and the resulting error was expressed by $\sigma(\log FR) = 0.60$, comparable to the accuracy of the revised 1989 US/FRG model results.

A final analysis was performed on those remaining data points which were atypical with respect to the majority of the data points. Many of those points correspond to the five spheres containing the mixed oxide kernels, $(Th,U)O_2$. After heating for 1000 hours at 1600°C, sphere R2-K13/1 unexpectedly shows atypically low release despite being exposed to the highest fast fluence of any FRG sphere. This sphere is unique in having a relative fast fluence to burnup ratio of 0.81 (i.e., $8.3 \div 10.3$), compared to typical values of 0.25 for AVR spheres (including mixed oxides) and 0.50 for the high-fluence MTR spheres (UO_2). Perhaps the specifics of the neutron energy spectrum in this Studsvik R2 reactor relative to the other MTRs may play some role. Sphere AVR 70/26, heated at 1600°C for 304 hours, appears relatively normal in diffusive release. Sphere AVR 69/13, heated at 1800°C for 92 hours, represents by far the most skewed data point, with an effective diffusion coefficient several times greater than any other 1800°C test. However, this sphere was also heated to 1800°C on four different occasions, raising the possibility of adverse effects of reheating and thermal cycling on FP release. Sphere AVR 74/20, heated at 1900°C for 50 hours, appears a bit on the high side in release. In contrast, AVR 74/24 was heated at 2100°C for 30 hours, and shows release a bit lower than expected considering its fast fluence of 2.7×10^{25} m^{-2}, higher than the other 2100°C heating tests. Two other higher temperature ramp tests of mixed oxide spheres, not analyzed here, tended to show slower release than tests on UO_2 fuel spheres with comparable burnup [51].

Due to the lack of a consistent trend with these mixed oxide spheres, with at least 60% of these five spheres showing unexpected release patterns, these samples were split off into a sixth data group, and a separate diffusion coefficient derived for them. Reprediction of sphere release based on this six-group model reduced the statistical error to $\sigma(\log FR) = 0.49$. The average effective diffusion coefficients used in this six-group model are given in Figure 6, and these final computational results listed in Table 2.

A criticism could be made of the above method that breaking up the data into numerous groups and numerically fitting parameters to each group should certainly reduce the predictive error significantly. The fact that groupings were consistently applied according to one important physical parameter, the fast fluence, and that the information provided by the original diffusive model supported such groupings, lends some credence to the above approach. The groupings could have been based on burnup as easily as fast fluence, which suggests further investigation of fast fluence vs. burnup as the dominant mechanism related to AC FP release. Although details of the method can be questioned, the fact that the results point further investigation in a specific direction may be a truer test of the utility of an AC model than the exact numbers obtained.
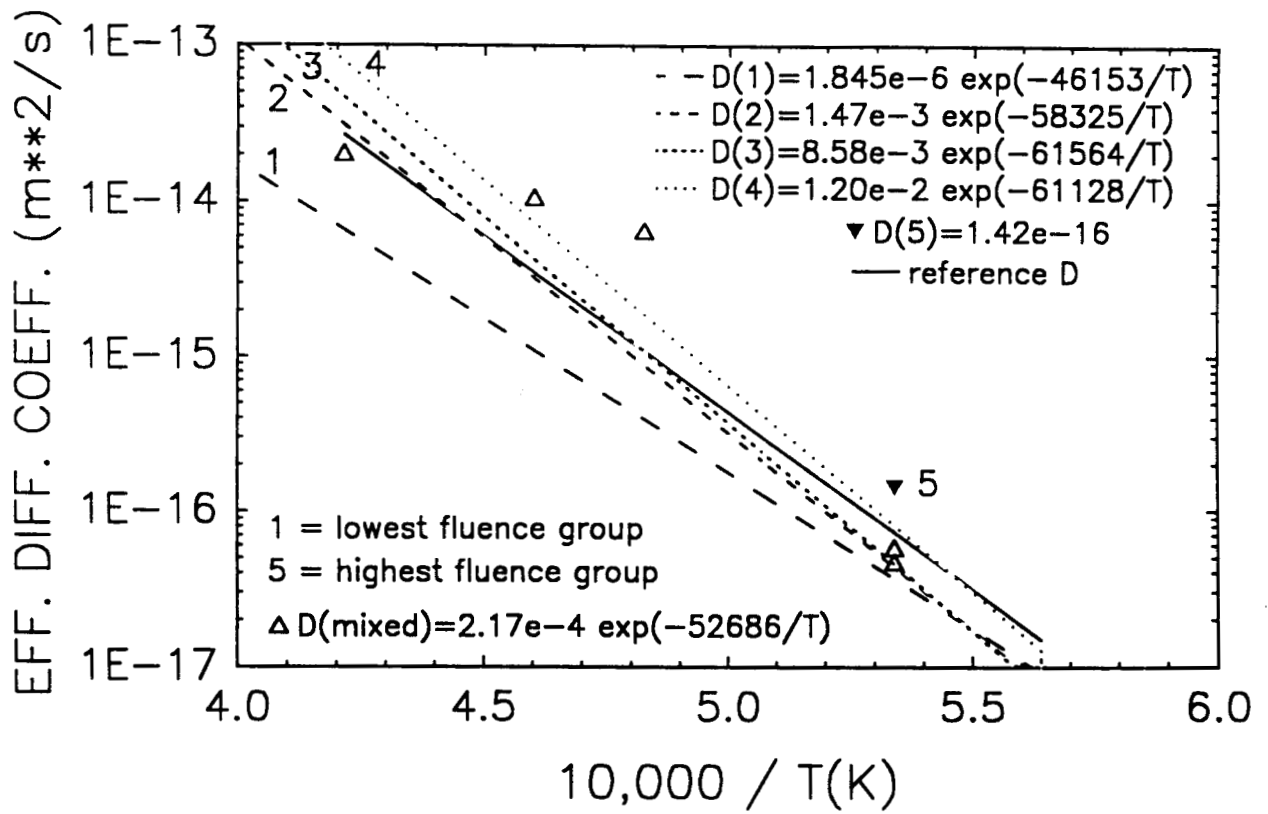
Fig. 6.   Effective diffusion coefficients for cesium-137 release from SiC, FRG spheres: six-group model.

3.4   KRYPTON-85 RELEASE

The methodology employed in deriving effective diffusion coefficients and predicting krypton release through SiC is similar to that employed for Cs above, and will be briefly discussed. Again, diffusion through a single layer of SiC is simulated, with the Opyc layer and matrix graphite ignored as a first approximation. With SiC the primary barrier to Kr release, transport through the SiC should be the rate-determining step over most of the AC simulation. In practice, calculations of effective diffusion coefficients based on diffusion in SiC would implicitly include effects of OPyC, etc. on release, although perhaps not as well quantified. Previous experience with noble gas release from nuclear fuels suggests release mechanisms more complicated than simple diffusion, e.g., trapped gas in voids and porosity which can be released in a burst when the porosity becomes interconnected to provide a direct pathway for release [52]. The motivation here is to simply test whether this simple diffusive release model can predict to some extent the experimental results for FRG sphere release of Kr. Detailed analysis of mechanisms of release and refinement of release models must await further study and modeling.

The SHELL code was again used to determine the effective diffusion coefficient for each FRG sphere which allowed SHELL to duplicate the experimental sphere release, and these values are tabulated in Table 3 and plotted in Figure 7. The average effective diffusion coefficient was calculated from all data points except the value at 1500°C and plotted in Figure 7, along with a diffusion coefficient used by K. Fukuda et al. [53] to calculate Kr release from TRISO particles. Obviously, use of Fukuda et al.'s diffusion coefficient would seriously underpredict the FRG sphere release, and was not used as a reference value.

Again the expected diffusion-like relationship is apparent between the effective diffusion coefficients and the reciprocal of the temperature. The average effective diffusion coefficient was then used for SHELL predictions of Kr release from each sphere, and the statistics calculated for comparison with the experimental values as was done for Cs. This single-group diffusion coefficient gave the value $\sigma(\log FR) = 1.62$, indicating well over an order of magnitude error in prediction for each sample. The next refinement calculated separate diffusion coefficients for the low-fluence spheres and the high-fluence MTR spheres. Four spheres which showed significant atypical release were not figured into the derivation of the diffusion coefficient for the low-fluence spheres (i.e., AVR 70/15, AVR 71/7, AVR 82/20, and FRJ2-K13/2), and in this case sphere HFR-K3/1 was figured into the high-fluence diffusion coefficient. The results are shown in Figure 8. Unlike the results for ^{137}Cs, the Q/R value for the high-fluence spheres is less than the low-fluence spheres because of the data at 1700° and 1800°C. Predictions of sphere release using these two diffusion coefficients gave an error measure of $\sigma(\log FR) = 1.45$. Next, the five-group diffusion coefficients were calculated as was done for ^{137}Cs, which significantly reduced the error measure to $\sigma(\log FR) = 1.17$. Finally, because of the atypical release from the mixed oxide spheres, those samples were split off into a sixth group and the statistics recalculated to give $\sigma(\log FR) = 0.97$, still about an order of magnitude variation between predictions and experiment. The average effective diffusion coefficients used in this six-group model are given in Figure 9. The final calculations are listed in Table 3, which shows most of the error is concentrated among about half a dozen spheres which show uncharacteristic Kr release.

Although the predictive errors resulting from this diffusive model are significant, they appear reasonable relative to the predictability of Kr release using, e.g., the PANAMA codes [27]. Inspection of the experimental Kr release data does show evidence of a PV-failure-type release mechanism in a significant number of spheres, i.e., sudden bursts of Kr release, which cannot be explained by diffusive transport. One could speculate on fission gas transport mechanisms analogous to those in the fuel, i.e., bulk diffusion and trapping in voids, followed by sudden release when the evolving porosity provides a direct path to the outer surface of the particle.

Table 3. FRG sphere release calculations for krypton-85.

sphere	T_{heat} (°C)	t_{heat} (h)	fast fluence (10^{25} m^{-2})	effective diffusion coeff.[a] (m^2 s^{-1})	FR_{expt}	FR_{calc}[a]	FR_{contam}	sample variance
AVR 70/15[b]	1500	140	1.7	1.23e-16	8.7e-5	~0	<7.0e-7	4.389
AVR 71/22	1600	500	0.9	1.80e-17	4.0e-7	2.46e-5	1.1e-7	3.208
AVR 82/9	1600	500	2.3	1.85e-17	5.3e-7	1.82e-6	1.1e-7	0.316
AVR 82/20	1600	100	2.2	8.20e-17	1.5e-7	~0	9.0e-8	0.0493
FRJ2-K13/2	1600	138	0.1	6.20e-17	6.4e-7	~0	≥5.3e-7	0.0067
HFR-K3/1	1600	500	3.9	2.20e-17	1.8e-6	1.07e-6	2.2e-7	0.0207
HFR-P4/1/8	1600	304	7.2	5.56e-17	5.0e-5	5.48e-4	6.3e-7	1.082
HFR-P4/1/12	1600	304	5.5	3.21e-17	5.0e-7	2.23e-7	5.2e-7	0.0296
HFR-P4/2/8	1600	304	7.2	1.11e-16	8.0e-5	9.16e-6	7.0e-7	0.826
HFR-P4/3/7	1600	304	7.5	9.38e-17	1.0e-3	5.48e-4	2.0e-7	0.0681
R2-K13/1[b]	1600	1000	8.3	1.97e-17	3.5e-4	1.55e-3	5.3e-7	0.417
SL-P1/6	1600	304	6.7	3.31e-17	7.0e-7	2.23e-7	5.0e-7	1.96e-4
AVR 74/11	1700	185	1.6	7.97e-17	3.0e-5	1.05e-5	2.0e-7	0.201
SL-P1/9	1700	304	6.3	5.30e-17	4.0e-5	2.05e-4	?	0.504
SL-P1/10	1700	304	6.0	5.99e-17	9.0e-5	2.05e-4	4.3e-7	0.129
AVR 69/13[b]	1800	92	2.1	5.59e-16	9.0e-3	2.21e-3	≤5.4e-7	0.372
AVR 70/33	1800	174.5	0.4	1.79e-16	1.7e-3	1.23e-4	1.0e-5	1.223
AVR 74/10	1800	90	1.4	3.50e-16	1.8e-3	1.84e-4	9.0e-7	0.976
AVR 76/18	1800	200	1.9	9.10e-17	1.2e-4	5.43e-3	1.5e-8	2.742
AVR 88/15	1800	50	2.2	4.25e-16	2.9e-4	1.15e-3	6.0e-8	0.359
AVR 88/33	1800	21	~2.25	9.30e-16	1.8e-4	5.89e-6	1.0e-7	2.184
AVR 88/41	1800	24	2.0	3.58e-16	2.4e-7	1.8e-10	2.3e-7	3.24e-4
FRJ2-K13/4	1800	100	0.1	1.66e-16	7.2e-5	1.06e-6	3.0e-7	2.969
HFR-K3/3	1800	100	6.0	2.62e-16	6.5e-4	2.16e-5	1.8e-6	2.088

Table 3, continued

sphere	T_{heat} (°C)	t_{heat} (h)	fast fluence (10^{25} m^{-2})	effective diffusion coeff.[a] (m^2 s^{-1})	FR_{expt}	FR_{calc}[a]	FR_{contam}	sample variance
HFR-P4/3/12	1800	279	5.5	1.03e-16	1.0e-3	3.93e-3	1.2e-7	0.353
AVR 73/12	1900	100	0.8	1.86e-16	1.4e-4	1.24e-4	1.3e-7	0.0027
AVR 74/20[b]	1900	50	2.9	1.44e-15	0.021	0.0110	4.0e-7	0.0790
AVR 76/19	1900	30	1.9	3.16e-16	6.9e-7	1.30e-4	2.2e-7	5.180
AVR 80/22	1900	30	2.4	2.02e-15	0.015	0.0201	2.7e-3	0.0331
AVR 71/7	2000	100	0.5	1.72e-16	8.6e-5	1.52e-3	1.0e-6	1.558
AVR 80/16	2000	30	2.0	2.20e-15	0.019	7.14e-3	1.2e-4	0.175
AVR 74/6	2100	30	1.4	2.54e-15	0.024	0.0521	2.0e-6	0.114
AVR 74/24[b]	2100	30	2.7	5.33e-15	0.092	0.155	2.0e-6	0.0511
AVR 76/27	2100	30	1.9	6.80e-15	0.14	0.0521	3.0e-5	0.184
AVR 76/28	2100	30	1.8	3.30e-15	0.048	0.0521	1.24e-4	0.00137

a   calculated from SHELL

b   mixed oxide sphere

?   unknown

Sample variance is calculated as:

$$ s^2 = \left[\log (FR_{calc} + FR_{contam}) - \log FR_{expt} \right]^2 $$
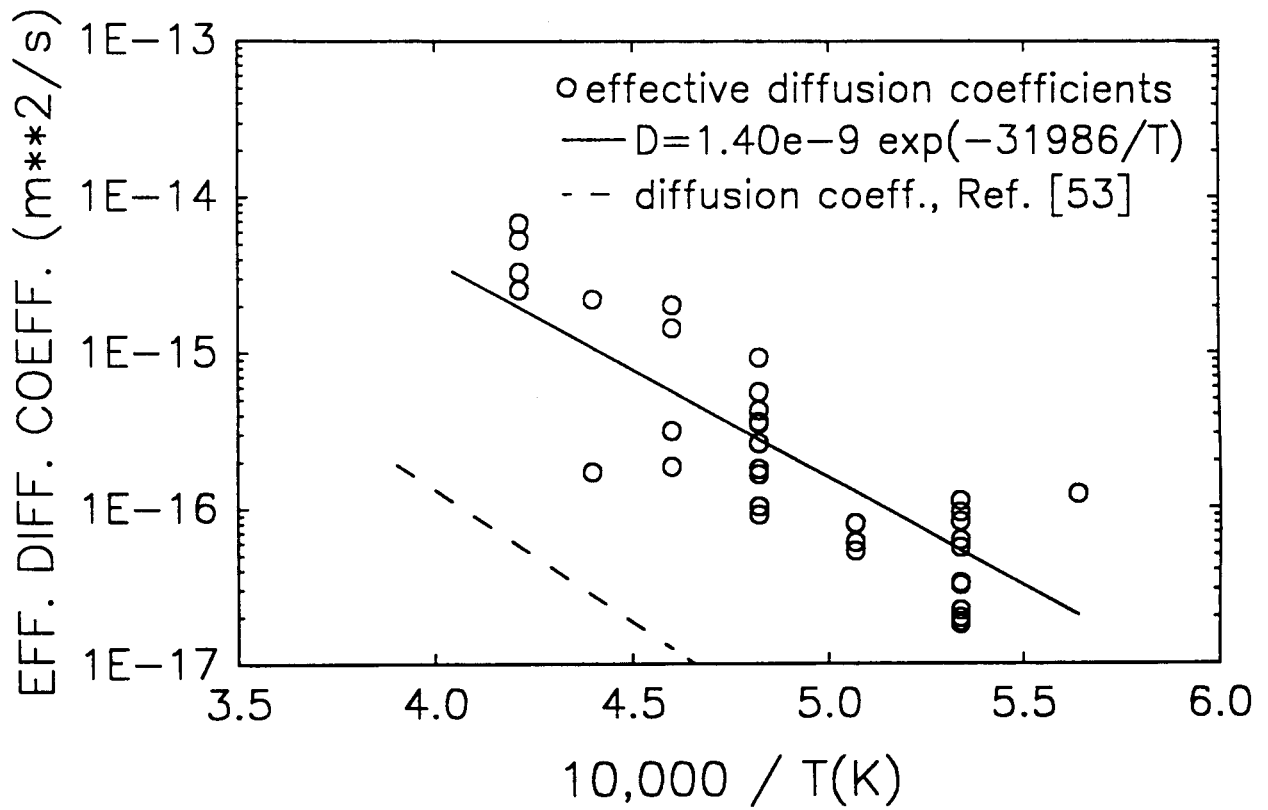
Fig. 7.   Effective diffusion coefficients for krypton-85 release from SiC, FRG spheres.
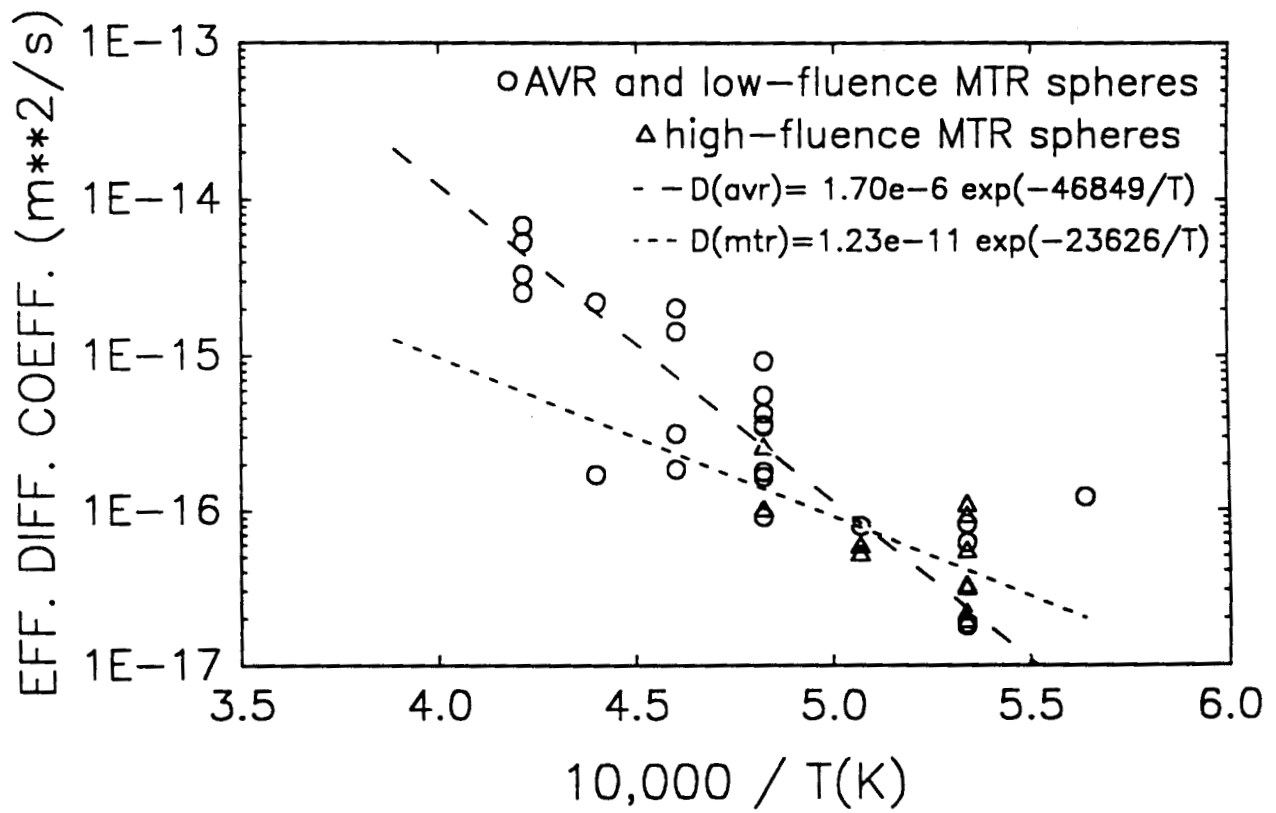
Fig. 8.   Effective diffusion coefficients for krypton-85 release from SiC, FRG spheres: two-group model.
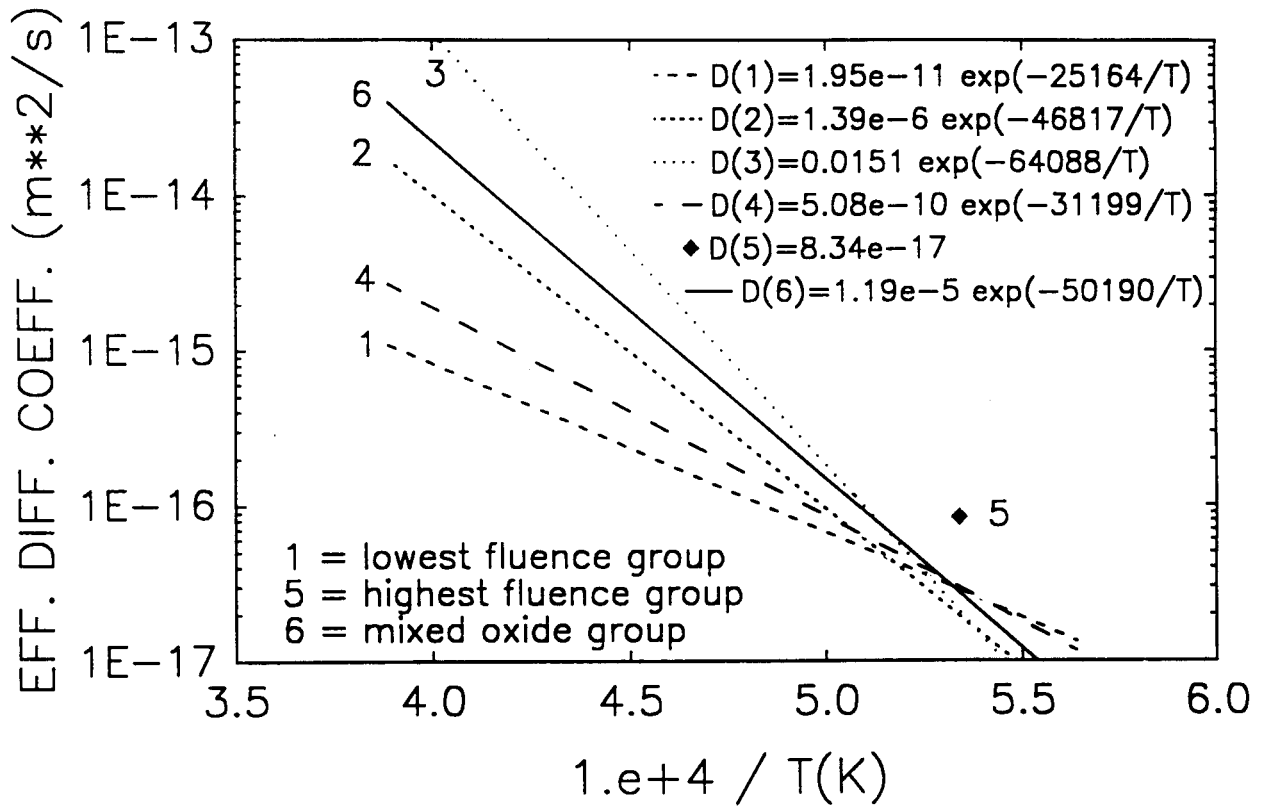
Fig. 9.　Effective diffusion coefficients for krypton-85 release from SiC, FRG spheres: six-group model.

3.5   SILVER-110m RELEASE

With the accelerated release of [110m]Ag relative to other FP and measurable release even during irradiation, a diffusive mechanism is commonly postulated for Ag release. As above, the SHELL code was used to obtain effective diffusion coefficients which could match SHELL predictions to experimental sphere release, and the results tabulated in Table 4 and Figure 10. Because of the large release values, contamination factors were not included in the calculations as with the other FP calculations. Only a dozen FRG spheres have been tested for Ag-110m release during AC heating experiments. An average effective diffusion coefficient was determined from the calculated diffusion coefficients using data for all the spheres, which was then used to predict the release from the spheres. The resulting measure of error gave $\sigma(\log FR) = 0.64$. Inspection of Figure 10 shows the data point for sphere AVR 71/22 at 1600°C is atypically low. By recalculating an average diffusion coefficient without this data point and re-doing the predictions, the error is reduced to $\sigma(\log FR) = 0.59$. The final calculations are listed in Table 4. Due to the limited number of data points, no effort was made to divide up the samples based on fast fluence. Fast fluence trends are not as obvious as for Cs and Kr, perhaps because the more rapid release of Ag reduces the effects of irradiation conditions.

An error measure of 0.59 without refinement represents a relatively good prediction of Ag release, and provides evidence supporting a diffusive model for Ag release. A reference diffusion coefficient for Ag in SiC [54] is also presented in Figure 10, and only shows reasonable agreement near 1800°C with the effective diffusion coefficients calculated here.

3.6   STRONTIUM-90 RELEASE

Fourteen FRG spheres were measured for ^{90}Sr release during AC heating tests. The experimental data and the effective diffusion coefficients calculated using SHELL are given in Table 5 and plotted in Figure 11. The average diffusion coefficient calculated from all data points in Figure 11 was used to predict sphere release, giving an error measure of $\sigma(\log FR) = 0.97$. As the values for spheres AVR 82/20 and FRJ2-K13/2 appear atypical at 1600°C, recalculation of the average diffusion coefficient without these two values and reprediction of sphere release gives $\sigma(\log FR) = 0.78$, a significant improvement. Calculations are listed in Table 5. Again, no division of the samples based on fast fluence was attempted due to the limited number of data points. A reference diffusion coefficient for Sr in SiC [54] is also plotted in Figure 11, which is significantly higher than the average effective diffusion coefficient calculated here. The large difference could relate to the observation that Sr is strongly retained by matrix graphite.

3.7   SUMMARY

The results obtained using the simple diffusion model appear to be reasonable, and the effective diffusion coefficients calculated for Cs release approximate the reference diffusion coefficient well. Hypothesis of a dependency of Cs and Kr release on fast fluence follows directly from the analysis, although an analogous dependency on burnup could have been postulated with comparable results. The diffusion model allows predictions of release of the common FP from FRG sphere tests to within an order of magnitude of the experimental results, and predictions of metallic FP release are considerably better than for Kr release. The accuracy of these predictions are comparable to existing models of FP release. The diffusion model permits modeling of the release

38

Table 4. FRG sphere release calculations for silver-110m.

sphere	T_{heat} (°C)	t_{heat} (h)	fast fluence (10^{25} m^{-2})	effective diffusion coeff.[a] (m^2 s^{-1})	FR_{expt}	FR_{calc}[a]	sample variance
AVR 71/22	1600	500	0.9	5.36e-17	9.0e-4	0.0171	1.636
AVR 82/9	1600	500	2.3	1.35e-16	0.019	0.0171	0.00212
FRJ2-K13/2	1600	138	0.1	2.71e-16	2.8e-3	8.73e-5	2.268
HFR-K3/1	1600	500	3.9	1.69e-16	0.027	0.0152	0.0620
R2-K13/1[b]	1600	1000	8.3	1.58e-16	0.103[c]	0.987	0.123
AVR 74/11	1700	185	1.6	5.87e-16	0.0483[c]	0.137	0.205
AVR 76/18	1800	200	1.9	3.80e-15	0.62	1.0	0.0433
AVR 88/15	1800	50	2.2	1.95e-14	0.81	0.305	0.180
AVR 88/33	1800	21	~2.25	1.53e-14	0.21	0.0994	0.106
AVR 88/41	1800	24	2.0	5.95e-15	0.077	0.120	0.0372
FRFJ2-K13/4	1800	100	0.1	6.50e-15	0.527[c]	0.635	0.0066
HFR-K3/3	1800	100	6.0	8.45e-15	0.67	0.635	5.3e-4

a   calculated from SHELL

b   mixed oxide sphere

c   A.E.R.E. data

Sample variance is calculated as:

$$s^2 = \left[\log FR_{calc} - \log FR_{expt}\right]^2$$
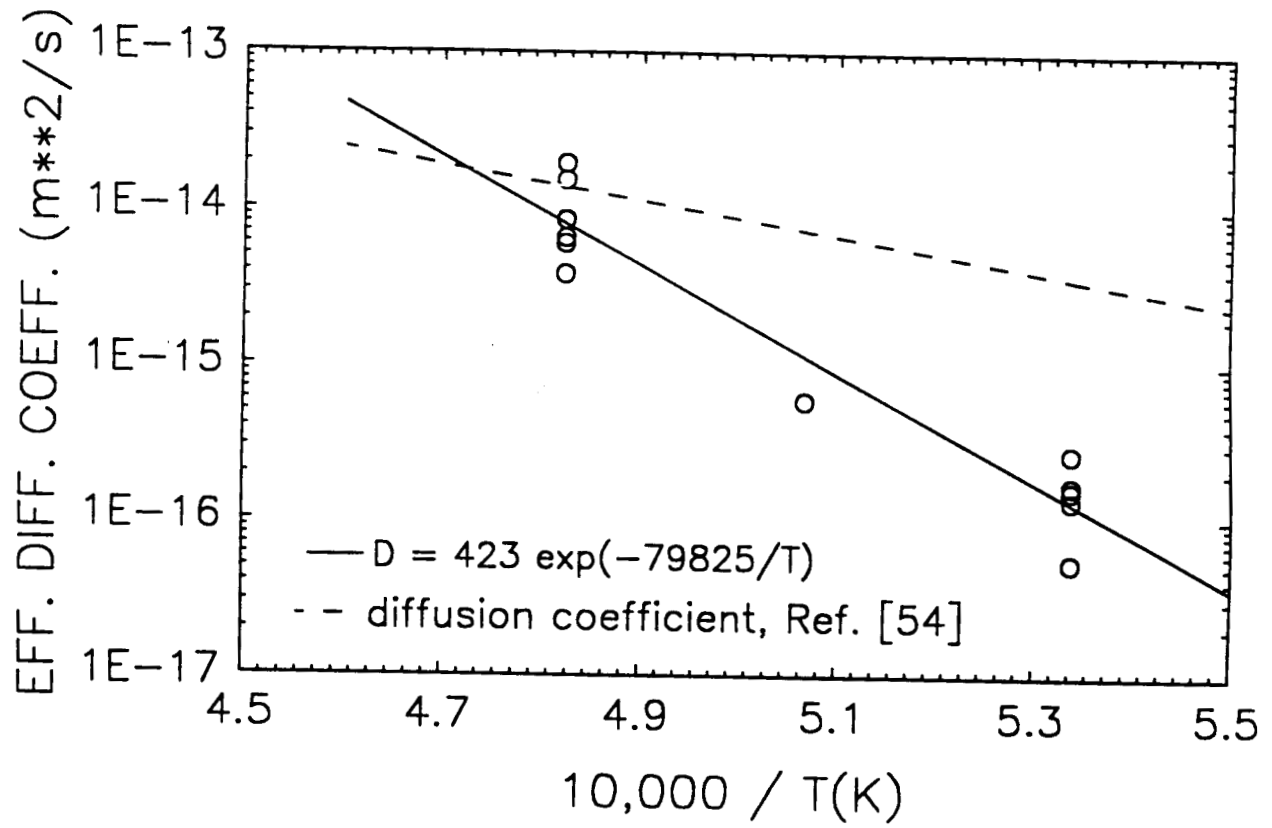
Fig. 10.   Effective diffusion coefficients for silver-110m release from SiC, FRG spheres.

Table 5. FRG sphere release calculations for strontium-90.

sphere	T_{heat} (°C)	t_{heat} (h)	fast fluence (10^{25} m^{-2})	effective diffusion coeff.[a] (m^2 s^{-1})	FR_{expt}	FR_{calc}[a]	FR_{contam}	sample variance
AVR 70/26[b]	1600	304	2.0	4.37e-17	1.8e-5	9.42e-6	2.0e-6	0.0342
AVR 71/22	1600	500	0.9	2.35e-17	5.3e-6	2.22e-4	3.0e-6	2.650
AVR 82/9	1600	500	2.3	3.41e-17	8.3e-5	2.22e-4	5.2e-5	0.269
AVR 82/20	1600	100	2.2	1.12e-16	3.8e-6	~0	9.0e-7	0.392
FRJ2-K13/2	1600	138	0.1	8.66e-17	3.8e-6	2.3e-10	3.0e-7	1.217
HFR-K3/1	1600	500	3.9	2.60e-17	8.3e-6	1.66e-4	4.4e-6	1.721
R2-K13/1[b]	1600	1000	8.3	2.60e-17	1.2e-3	6.00e-3	2.0e-6	0.489
AVR 74/11	1700	185	1.6	9.20e-17	8.3e-5	1.55e-3	2.0e-6	1.618
AVR 76/18	1800	200	1.9	6.50e-16	0.066	0.0555	3.0e-8	0.0058
AVR 88/15	1800	50	~2.25	1.10e-15	0.011	1.32e-3	N/A	0.846
AVR 88/33	1800	21	2.2	9.70e-16	2.3e-4	7.78e-6	9.0e-6	1.293
AVR 88/41	1800	24	2.0	7.60e-16	1.2e-4	2.21e-5	5.0e-6	0.417
FRJ2-K13/4	1800	100	0.1	3.10e-16	1.6e-3	0.0113	4.0e-9	0.721
HFR-K3/3	1800	100	6.0	3.30e-16	1.8e-3	0.0113	2.0e-6	0.637

a   calculated from SHELL

b   mixed oxide sphere

N/A   not available

Sample variance is calculated as:

$$s^2 = \left[\log\left(FR_{calc} + FR_{contam}\right) - \log FR_{expt}\right]^2$$
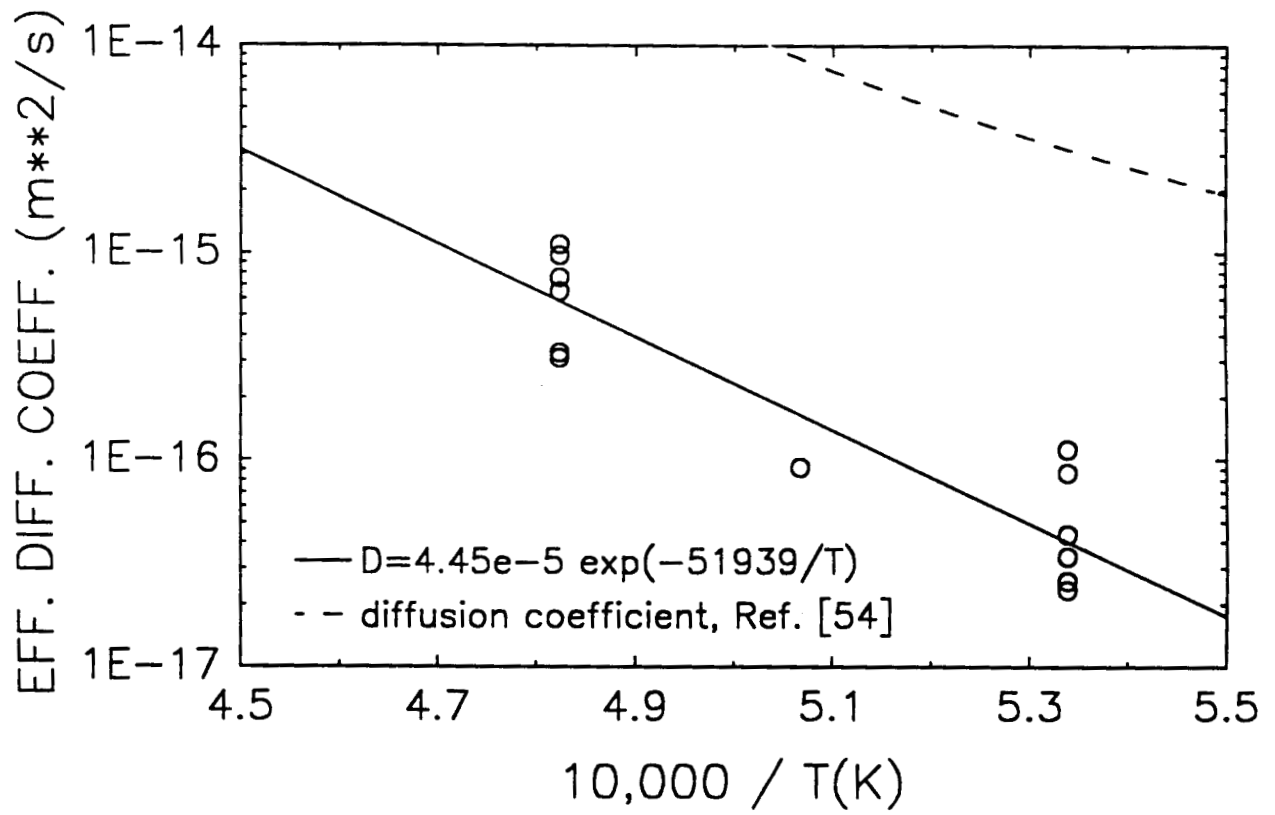
41

Fig. 11.   Effective diffusion coefficients for strontium-90 release from SiC, FRG spheres.

of all common FP, unlike current models which have not been extended to consider Ag and Sr release. A modeling approach based on diffusion is consistent, and does not depend on the postulation of different release mechanisms for the metallic fission products as do existing models. The dominant mechanism for Kr release is not as obvious. These results suggest further effort and refinement of a diffusive model of FP release could be promising.

Effective diffusion coefficients for Cs and Kr release calculated for sphere HFR-P4/2/8 (51 μm SiC layer) were not significantly different than those for HFR-P4/1 and HFR-P4/3 spheres (36 μm SiC layer). A diffusive release mechanism would not predict different diffusion coefficients for different layer thicknesses. However, one would expect models based on failure mechanisms (either pressure-vessel failure or uniform thermal decomposition) to predict measurable differences in release if the SiC thickness increases by 40%.

Analogous to the methodology of the US/FRG model [2] which uses a single governing equation to describe Cs release, this diffusive model could be used to derive one dominant parameter, the diffusion coefficient, based on fast fluence. The master equation would relate the two terms in the diffusion coefficient, D_0 and Q [eqn. (5)] to the fast fluence by numerical interpolation using the average effective diffusion coefficients derived for the different fast fluence groups, and such an approach could conceivably incorporate other irradiation parameters. Such an approach would unify the model but also increase the predictive $\sigma(\log FR)$ over that calculated above. However, continuation with this diffusive analysis would be more productive after evaluation of more refined models, such as those discussed in §5.4 below.

4. PREDICTIVE CAPABILITIES OF EXISTING MODELS

4.1 INTRODUCTION

Model development begins with the hypotheses upon which the model is based, followed by adaptation of the hypothetical model to existing data for derivation of numerical parameters. The true test of a model comes in the validation stage, in which the model is used to predict experimental results independently of those results. Existing AC models have not been subjected to adequate validation efforts to date, partly due to the limited number of FRG sphere release tests upon which they are based. With FRG sphere irradiations continuing, the opportunity exists to predict release prior to the AC performance experiments. These opportunities must be fully utilized to demonstrate some degree of confidence we can ascribe to these existing models. The FRG sphere tests provide a unique opportunity because of the relative uniformity of particle characteristics, which reduces the uncertainties in data interpretation from sphere to sphere. Earlier irradiation tests permit less predictability due to continuing variation of fuel design.

4.2 US/FRG MODEL AND AVR SPHERE 69/13

In the previous AC modeling status report [2], the heating test on AVR sphere 69/13 was mentioned as a test of the US/FRG model. This sphere was heated three separate times for a total of 42 hours at 1800°C. The measured Cs release was below detectable limits. Although this heating test did not show failure according to US/FRG model criteria, the model gave results in reasonable agreement with the limits of detection. Subsequently the sphere was heated for an additional 50 hours and showed significant Cs fractional release on the order of 50%. Using the MRF adjustment

for the US/FRG model, 100% Cs release from the particles would be expected. The US/FRG model predicts 3.8% Cs release after 92 hours at 1800°C, off by a factor of 25.

This result is not a fair comparison upon which to judge the predictability of the US/FRG model, as the Cs release from AVR 69/13 is atypically high. This experimental release also raises some question of reheating of FRG spheres and what effect this may play on subsequent release, as discussed elsewhere. This comparison is presented as an example of the types of predictions which are fundamentally important for model validation, but which have been underemphasized to date.

4.3 PREDICTIONS OF RELEASE FOR FRJ2-K15 FUEL SPHERES

The recent technical note from KFA Jülich by K. Verfondern and D. Müller [30] represents a significant step forward in efforts for model validation. This set of fuel spheres, presently under irradiation, has post-irradiation AC simulation experiments planned for heating at 1600°C for 300 hours, followed by heating at 1800°C for 182 hours. The irradiation conditions are given in Table 6. This irradiation test is unique in having both large values of burnup (16%) and very small values of fast fluence. In the technical note, predicted values of fractional release for Cs (obtained using the FRESCO-II code) and Kr (obtained using the PANAMA-I code) are presented at the end of each of the two isothermal tests, and listed in Table 7 below. The results at all temperatures except 900°C were taken from a figure and may not represent exact values. Also included in Table 7 are predictions of Cs release calculated using the latest US/FRG model revision, and predictions of Cs and Kr release obtained using the SHELL diffusive release code documented in §3. For the SHELL calculations diffusion coefficients for the lowest fast fluence group are used, appropriate for the irradiation conditions of this experiment.

Although the predicted magnitudes of FP release by all models are significant, the diffusion model suggests a lower release of FP. The SHELL predictions after 300 hours at 1600°C include approximate pre-AC levels of sphere contamination, which dominate the predicted Cs release and contribute half the predicted Kr release; at 1800°C contamination levels are insignificant compared to the calculated release. The US/FRG model does not predict Kr release. Comparisons with the existing FRG sphere release data (Table 3) show the PANAMA-I predictions of krypton release to be very large. Of the previously heated spheres, only those subjected to the highest fast fluence values (above 7×10^{25} m^{-2}) show comparable release after 300 hours at 1600°C, and the sphere subjected to the longest anneal at 1800°C (HFR-P4/3/12 at 279 hours) only gave a fractional krypton

Table 6. Irradiation conditions for experiment FRJ2-K15.

	Capsule 1 & 3	Capsule 2
Irradiation temperature (°C)	800 - 900	950 - 1050
Irradiation time (d)	550	550
Fast fluence (10^{25} m^{-2}, E>0.1 MeV)	0.2	0.2
Heavy metal burnup (% FIMA)	16.0	16.0

44

Table 7. Predictions of fission product release for experiment FRJ2-K15.

Code/model	T_{irrad} (°C)	Cesium		Krypton	
		1600°C, 300 h.	1800°C, 182 h.	1600°C, 300 h.	1800°C, 182 h.
FRESCO-II, PANAMA-I	800	2.0e-3	0.15	2.1e-4	1.0e-2
"	900	"	"	1.0e-3	7.9e-2
"	950	"	"	3.0e-3	0.26
"	1050	"	"	4.4e-2	0.51
US/FRG model	850	1.8e-3	9.9e-2	-	-
"	1000	5.1e-3	0.175	-	-
SHELL diffusion code	-	2e-5	2.9e-2	6e-7	1.0e-3

release of 10^{-3}, despite a relatively high irradiation temperature of approximately 1075°C. Although the burnup of the FRJ2-K15 spheres is very large, the accumulated fast fluence is very small. If fast fluence effects are the major determinant of FP release under accident condition temperatures below 2000°C, the PANAMA-I predictions would be expected to overpredict experimental Kr release because of the very low fluence of this irradiation. If burnup effects dominate FP release, PANAMA-I may more accurately predict Kr release because of the large burnup in this irradiation.

Comparison of predictions for Cs release with the FRG sphere data (Table 2) suggests that both FRESCO-II and the US/FRG model may overpredict Cs release after 300 hours at 1600°C. Only those spheres subjected to the highest fast fluence values (above 7×10^{25} m^{-2}) show fractional Cs release on the order of 10^{-3} under these conditions. This experiment should demonstrate the relative dominance of either fast fluence or burnup on release; the fast fluence is very low and the burnup is very high. As the diffusion model assumes a strong dependence of the diffusion coefficient on fast fluence, it predicts much lower Cs release than the other models. At 1800°C, Cs release in the percent range is typical, so the relative accuracy of the models cannot be predicted beforehand.

PANAMA-I suggests a strong dependence of Kr release on irradiation temperature. For Cs release, FRESCO-II suggests at most a weak dependence on irradiation temperature, while the US/FRG model suggests a stronger dependence. A dependence of FP release on irradiation temperature was not obvious during derivation of the diffusion model, so this dependence is not incorporated into the model. The variation in experimental Cs release for different irradiation temperatures will reflect on model validation.

4.4   SUMMARY OF PREDICTIONS FOR RELEASE FROM FRJ2-K15 SPHERES

The dominant mechanism for FP release will play an important role in which code or model

predicts Kr and Cs release most satisfactorily for the upcoming heating tests on the FRJ2-K15 spheres. Irradiation of these spheres provides an unusual combination of low fast fluence and high burnup. If fast fluence determines FP release, the SHELL diffusive model should prove superior. If burnup proves to be dominant, the diffusive model as presently derived may be inferior to the other models.

PANAMA-I predictions of Kr release from these future heating tests seem very high compared with existing sphere release data, and thus could be expected to overpredict release. Because of this, the SHELL model might be expected to offer better predictive ability for Kr release unless the high burnup dominates FP release. Burnup is believed to impact FP release by enhancing CO gas production and increasing the gas pressure inside the particle. The FRJ2-K15 experiment will provide a useful test of this pressure-vessel failure hypothesis.

For Cs release at 1600° C, both FRESCO-II and the US/FRG model predict release in the upper range of experimental values from previous heating tests (Table 2). After heating at 1800° C, all models predict Cs fractional release at 3% to 18%.

4.5   IMGA BIMODAL RELEASE RESULTS

As discussed in §2.6.5, no present model can explain IMGA data for sphere HFR-K3/3, which shows two distinct groupings of particles with significantly different maximum fractional releases of Cs. The largest fractional release occurs toward the outside of the sphere. The most obvious variables across the sphere are the irradiation temperature (maximum in the center), and fast fluence and burnup (expected to be highest toward the outside of the sphere due to self-shielding of the neutrons by the sphere). Other theories could include temperature gradient effects across the sphere (maximum toward the outside) and some effect of reheating the HFR-K3/3 sphere a second time on SiC integrity [44].

All models as presented could evaluate release for particles subjected to different assumed irradiation temperatures, fast fluence, burnup, etc. across the sphere, with more or less developmental effort. However, the ability of any of the existing models to approximate this bimodal distribution is uncertain. With questions still remaining on the validity of some of the basic assumptions used to develop existing models, it seems doubtful that a model would be able to explain these results without beginning with the correct assumptions for predominant phenomena involved in FP transport through and release from the SiC barrier layer. A credible explanation of these experimental results remains a critical test for any proposed or existing AC fuel performance model.

5. PHENOMENOLOGICAL CONSIDERATIONS FOR FUTURE MODELING

5.1   INTRODUCTION

This section consists of observations developed during background investigations into SiC structure and decomposition mechanisms, available literature on radiation effects on SiC, experimental investigations of SiC properties for both nuclear and non-nuclear applications, and modeling of neutron-induced defects and annealing as it has been applied to materials other than SiC. This section represents somewhat of a brainstorming approach to fuel performance modeling as it relates to SiC behavior, but some observations may be very relevant to future modeling efforts and are included for future reference, with plans to expand upon specific topics in the future.

5.2   PHENOMENOLOGICAL SiC DECOMPOSITION MODEL

5.2.1   US/FRG SiC Decomposition Model

The model for SiC thermal decomposition as used in the US/FRG model, based on the experimental work of R. Benz on the thinning of bare SiC layers [55], consists of an activation energy in an Arrhenius-type equation for overall thinning of the SiC layer linear which progresses linearly in time. Although ceramographs strongly suggest decomposition along preferential pathways into the SiC bulk, no attempt to model this behavior has been reported. The only model that suggests consideration of a related mechanism is the Martin-Goodin-Nabielek model (§2.4.3) which attempts to approximate SiC grain boundary damage using a Weibull-like dependence. As reported in Ref. [2], the activation energies determined by Benz and used in the US/FRG model approximate the activation energy for the predominant reaction in SiC thermal decomposition:

$$SiC\,(s) \;\rightarrow\; C\,(s) + Si\,(g) \quad , \tag{11}$$

where (s) refers to solid phase and (g) to gas phase.

Although the thinning rate is assumed to be linear in time, D. T. Goodin in one his reports comments that actual decomposition curves tend to be sigmoidal in shape, and that thinning is not uniform over the entire surface but predominates in localized regions of the SiC layer. Goodin's observation is correct in that decomposition of a solid consists of a combination of several kinetic processes, and the rate of decomposition can be enhanced at the beginning, middle, or end of the decomposition process depending on which mass transfer process is rate-limiting [56]. In no typical case would decomposition of a solid be expected to be linear over time.

5.2.2   More Realistic Decomposition Models

A non-pressure-vessel model of FP release would suggest that transport and release pathways would be differentially affected for a localized decomposition mechanism which penetrates into the SiC bulk vs. a uniform thinning mechanism over the entire surface. Significant work exists upon which a more realistic decomposition model for SiC could be based, which could avoid both assumptions of uniform thinning over time and over the SiC surface. Substantial work has been performed in the theory of solid reactions related to nucleation and growth of a second phase of material within the bulk of a solid material. Analytical equations describing phase transformations in space and time have been developed for a variety of geometries and conditions [57], some of which could be applicable to the transformation of high-integrity SiC into a porous graphitic layer during evaporation of Si at high temperatures. Some of these models consider the pressure dependence of the resulting gaseous chemical products, which should be relevant to our case of a SiC system sealed by PyC layers.

A factor which may play a role in accelerated SiC decomposition at higher temperatures is the melting point of free Si which will be exceeded at AC temperatures. The decomposition temperature of good integrity SiC is very high, but if for some reason significant quantities of free Si segregate within the SiC structure, the Si melting point of approximately 1400°C could be significant for structural modification and decomposition effects. The possibility of the segregation of free Si is discussed in more detail in §5.4.3 below. Chapter 10 of Reference [57] discusses the sigmoidal time dependence of the decomposition curve, resulting from either the pressure dependence of the decomposition products or the presence of partial liquefaction of the

47

decomposition products. During decomposition, if free Si can form and subsequently melt at AC temperatures, another mechanism for FP release becomes conceivable with thermal cycling of the fuel particles above and below the melting point of free Si. This "thawing and freezing" scenario would be expected to induce strain within the SiC structure which could impact its mechanical integrity and/or produce microcracks near regions of Si agglomeration (most likely near imperfections within the crystal structure such as grain boundaries).

Another source for detailed models of the decomposition process is provided by the general kinetic formalism of Searcy et al. [58], [59] for decomposition of a binary solid such as SiC, with its inclusion of all mass transfer processes which could be significant in the decomposition process. By approximating or postulating the relative significance of the various mass transfer mechanisms, Searcy's governing equations could be simplified to a model hypothetically relevant to SiC decomposition. Enough thermodynamic and kinetic data exist on SiC decomposition (see, e.g., [60], [61], [62], and others) that development of a more realistic model than simple linear thinning might be feasible.

5.2.3 Diffusion Through an Evaporating Medium

For purposes of evaluating high-temperature diffusion into silicon in conjunction with its significant vaporization at temperatures well above 1000°C, analytical expressions have been developed to describe diffusion into an evaporating medium [63]. These expressions approximate diffusion into a moving solid boundary. We might expect our SiC layer to preferentially evaporate at the exterior surface (i.e., at the OPyC layer) in agreement with ceramographic data and observations, rather than the inner surface where the FP are concentrated. However, the analytical approach used in these references might be adapted to our situation of diffusion into a thinning SiC layer, and numerical methods could certainly be developed for a more detailed analysis of this phenomenon [64],[65]. A more generalized approach to this problem would be the use of particle methods as described in Ref. [1] to treat diffusing FP atoms as individual entities in a Monte-Carlo-type transport routine, with much greater flexibility in specifying moving and irregular material boundaries. Treatment of non-uniform thinning would be very difficult analytically.

5.3   CONSIDERATIONS FOR DIFFUSION MODELING

5.3.1   "Columnar" vs. "Laminar" Diffusion of Cesium in SiC

In his 1984 analysis of Cs diffusion in SiC, B. F. Myers [47] compiled the existing data on the diffusion coefficients for Cs through SiC in HTGR fuel particles. In observing the range of data, he noted that those particles with SiC characterized as laminar in structure tended to have lower average diffusion coefficients than those with columnar SiC structure. In contrast, fuel fabrication methods are designed to promote deposition of SiC with columnar structure, as this tends to provide maximum theoretical SiC density, improve mechanical performance of the particles, and reduce SiC decomposition rates at high temperatures. No detailed explanation of the slower Cs diffusion in laminar SiC coatings has been advanced.

The only laminar diffusion coefficient data presented in Ref. [47] above 1500°C were derived from ramp heating tests up to 2050°C on GA particles. Because these ramp data are compared to isothermal heating test data, and because the total heating times are much smaller than for the isothermal tests, some uncertainty may exist in comparisons and thus this data will not be analyzed here. The data points for all other laminar samples were determined at or below 1500°C, and these

samples have lower average diffusion coefficients than the columnar samples. Mechanisms which might explain this differential release can be suggested from phenomenological models. It is commonly accepted that the higher-density columnar structures provide better mechanical performance and structural integrity at higher AC temperatures. Therefore, what mechanisms could account for reduced FP release at lower temperatures from SiC structures thought to be inferior? The major difference between the two structures is the relative orientation of the crystal layers and boundaries. Visual observation shows the columnar boundaries are oriented radially, while the laminar boundaries tend to be oriented concentrically around the kernel. Two transport mechanisms may conceivably be at work, one for the fission products themselves and one for escape of gaseous silicon generated by thermal decomposition of the SiC. At higher temperatures (above 1600°) stronger thermal effects may rapidly attack the weaker laminar structure, and thus the structural integrity would play the dominant role in retention of FP. However, at 1500°C and below, the experimental times required to measure diffusive release are very long, and some tests have been run for thousands of hours. Under these conditions, more subtle effects on release could come into play. Silicon vapor pressure is not insignificant at these temperatures, and transport of gaseous silicon out of the SiC structure could be expected to be enhanced by the radial structural features of the columnar structure. Likewise, grain boundary diffusion would tend to favor release from these columnar structures. A synergistic effect is conceivable whereby enhanced vaporization along the radial boundaries weakens the microstructure such that Cs diffusion could be enhanced over time.

An interesting feature of the derived diffusion curves is the change in slope at temperatures near 1500°C. It may be coincidental for this temperature to be near that of the melting point of free silicon (approximately 1410°C), but again the prospect of enhanced Si vapor transport from free molten Si along radial structures seems feasible. These suggested mechanisms are not supported by direct experimental observations, but they do provide more conceptual explanation of this apparent contradiction in columnar vs. laminar release than has previously been proposed.

5.3.2   Diffusion Through Semiconductors and Thin Films

Apparently nowhere in the AC modeling literature has it been noted that SiC is a semiconductor material, and thus diffusion of FP through SiC might exhibit characteristics unique to semiconductors. Nuclear engineers have traditionally been concerned with diffusion through metals. Consideration of diffusion through a semiconductor must take into account the possibility of unexpected nuances and phenomena richer in complexity than would be expected for diffusion in metals. An obvious example of such a phenomena is the charged character of microstructural defects and the potential for ionic trapping of impurities at those defects. Under neutron irradiation one must expect an abundance of such traps. Such charged traps are effectively neutralized in metals because of the large electrical conductivity, but ionic trapping of FP atoms at neutron-induced traps in SiC is not inconceivable.

A review article by R. W. Balluffi and J. M. Blakely on diffusion in thin film semiconductors [66] gives a good introduction into the richness of phenomena involved in this process, some of which could be relevant to AC modeling of FP release through SiC. Some of the issues raised in this article are listed below.

1.   The electronic surface states arising from defects or impurities may affect the rate of diffusion of ionized impurities near surfaces of thin films.

2.   Dislocations and grain boundaries can act as short-circuit diffusion paths relative to bulk diffusion.

3.   Large densities of dislocations which act as charged defects can modify bulk diffusion characteristics.

49

4.   Complex diffusion behavior can result from multiphase diffusion, which may be relevant to silicon segregation and vaporization during SiC decomposition.

Balluffi and Blakely discuss other phenomena, and refer to more detailed work [67], but they make some very interesting comments relating diffusion in thin films to a pressure-vessel-type scenario: "Relatively large biaxial stresses are often present in thin films ... [which] might be expected to exert significant effects upon thin film diffusion processes ... Local stress-motivated defect currents tend to exert a 'sweeping' effect on the solute atoms. Since there is generally a binding energy between defects and solute atoms, and since the defect jumping rates are generally altered in the vicinity of solute atoms, a defect current is expected to cause a redistribution of the solute atoms relative to the host atoms ... However, the problem is exceedingly complex ... biaxial stresses should also affect the diffusivities in grain boundaries and dislocations. Since the diffusion in these short-circuiting paths is often dominant in thin film diffusion zones, this effect must be considered ... Stresses may exert further effects on diffusion in thin films in cases where more than one phase is formed ... Finally, we mention the effect of biaxial stress on the production of fissures, pores, spalling, etc. in multiphase diffusion zones ... many intermediate phases formed in such zones are characterized by considerable hardness and brittleness and are particularly susceptible to fracture." Some of these comments could suggest means for unification of pressure vessel and diffusion modeling. Of particular relevance is the possibility of silicon segregation within the SiC and its effect on fracture strength.

5.3.3   Electrical Conductivity of Fission Products

SiC is known to have partially ionic character [68], with the Si atoms having a partial positive charge of about 12% that of a pure ion. I am not aware of any explanation offered to explain the relative rate of release of FP from TRISO particles, i.e., Ag > Cs > Sr > Kr, Xe, I, with Cs and Sr release sometimes comparable. Nor is it apparent why such a chemically dissimilar species as iodine would approximate the release kinetics of the noble gases from UO_2 fuels [69]. Analysis of the common elemental properties of these FP species (atomic and ionic radii, ionization potential, boiling point, heat of vaporization, electronegativity, electrical conductivity) only provides one apparent trend that approximates the above sequence of release: the room temperature electrical conductivity [70] (given in units of 10^6 Ω^{-1} cm^{-1}) for Ag is 0.63, Sr is 0.076, Cs is 0.049, I is 8×10^{-16}, and Kr and Xe are effectively zero. As Sr can form oxides within the kernel, such chemical trapping would inhibit its release relative to Cs. Although direct analogies to AC modeling would require consideration of high temperature electrical conductivities, and the validity of comparing bulk conductivities with the behavior of individual atoms is not certain, the fact that such a trend based on electrical properties exists raises some interesting possibilities for AC modeling. Consideration of the conductivities of other FP elements provides more food for thought: rhodium has a room-temperature conductivity (in corresponding units) of 0.21, molybdenum is 0.19, cadmium is 0.138, ruthenium is 0.137, palladium is 0.095, thorium is 0.07, uranium is 0.04, zirconium is 0.02, and the rare earths fall between 0.01 and 0.02. In contrast, the room-temperature electrical conductivity of high-purity β-SiC is negligibly small, although it could be significant at AC temperatures. If one does not consider those FP species which can form stable oxides at high temperatures, one is left with the following sequence of electrical conductivities: Ag > Rh > Ru > Pd > Cs ..., although it is known that rhodium, palladium, and ruthenium can form separate metallic inclusions within UO_2 fuel [71] (presumably favored at higher FP concentrations, i.e., at higher burnup). This sequence provides an interesting comparison with one study of FP corrosion of SiC in TRISO particles [37]: "Simulated Triso-coated UO_2, UC_2, and UO_2/UC_2 particles were mixed with varying amounts of Mo, Ru, Rh, Pd, Ag, and Cd were prepared ... Ruthenium, rhodium, palladium, and silver were shown to

50

interact with the SiC layer. The palladium-SiC interaction was the most severe." This analogy with the sequence of electrical conductivities may relate to mechanisms of FP release.

5.3.4 Atomic Size and Electronegativity Considerations in Fission Product Transport in SiC

Consider the following observation. Silicon and carbon atoms are dissimilar in both size and in electronegativity (i.e., an atom's relative attraction for a free electron). Because of the electronegativity difference, Si atoms in SiC have a partial positive charge of about 12% relative to a pure ion. Thus, if a neutron collision kicks out a Si atom, one would expect excess negative charge to remain near the resulting vacancy, which could act as a trap for any diffusing impurity atom (in this case, a FP atom). In particular, one would expect an atom similar to Si in size and electronegativity to be preferentially trapped at the vacancy. In terms of atomic radii, iodine and xenon are closest in size to silicon but their electronegativities are different by 40% and more [70]. Silver atom radii are 20% larger than Si, but the electronegativity is virtually the same, only a 2% difference. After that, palladium is 23% larger than Si with a 16% difference in electronegativity, followed by rhodium (25% difference in size, 20% in electronegativity), and ruthenium (29% difference in size, 16% in electronegativity). Other FP species show increasing differences; e.g., the Cs atomic radius is 129% larger than Si and electronegativity is 58% smaller. Comparing this sequence with the corrosion sequence of Ref. [37] again shows strong analogies. Of particular interest is the almost identical electronegativities and similar sizes of Si and Ag atoms. The data would suggest a silver atom might be quite satisfied sitting in a Si vacancy trap until heated to high temperatures. This observation would tend to strengthen the hypothesis advanced in Section 2.5.4 of Ag trapping in the SiC bulk followed by release during annealing.

5.4 MODELING OF NEUTRON-INDUCED DEFECTS, CLUSTERING, AND ANNEALING

5.4.1 Introduction

Analytical modeling of neutron-induced defects in SiC and their subsequent behavior has not been pursued, but such an approach appears sufficiently promising that further work is planned. A modeling philosophy which considers fast fluence effects to play a significant role in FP release must consider the microstructural effects of neutron bombardment. Although significant consideration of such effects has not extended beyond experimental results, sufficient modeling has been pursued for materials other than SiC and enough relevant data on SiC is available that simple analytical models could be developed within a reasonable period of time. The potential of SiC as a high-temperature semiconductor has lead to development of a significant database on the microstructural properties of SiC, including the effects of irradiation. This wealth of information has apparently not been considered in recent AC model development, and its relevance to the MHTGR program should be evaluated. The purpose of this discussion is to provide some flavor for the existing data and models available for incorporation into a microstructural model of SiC evolution and high-temperature decomposition under neutron irradiation.

5.4.2 The Relevance of Microstructural Phenomena

Common experimental methods employed for the characterization of the following SiC coating properties are discussed by Förthmann et al. [72]: crystallite size, lattice parameters, small-angle x-ray scattering intensity, sink-float density, grain-size distribution, optical anisotropy and light

reflectivity, and surface appearance by electron microscopy. Electron microprobe x-ray analysis has also been employed for FP concentrations across the particle [73], and gross excess Si concentrations in the percent range have been measured [74]. However, detailed microstructural evaluations of the effects of fast neutrons and high temperatures on SiC are not common. SiC coatings with a significant content of free Si are known to undergo more rapid thermal decomposition with reduced retention of FP. Naoumidis et al. [74] comment on the importance of microstructural properties on FP release: "Transport of solid fission products through SiC coatings at rates that are fast compared to those in the bulk material is evidently caused by β or (α + β) grain boundaries, and by impurities contained therein. One of the impurities occurring most frequently in these coatings is free silicon which can be regarded as being codeposited and intimately mixed with the SiC. This silicon is assumed to form, under some conditions, submicroscopic channels that lead to high rates of release of fission products. The proportion of silicon needed for this can be quite small ..." According to Yu. A. Vodakov et al. [75], excess Si exists mainly in the form of clusters or a subphase within the SiC structure. More et al. [76] report evidence of a silicon excess on the order of 2 at% in β-SiC. The use of Raman infrared spectroscopy to characterize SiC surface properties by Krautwasser et al. [77] provided interesting observations on surface modification under reactor and accident conditions: upon heating bare SiC coatings (no OPyC layer) to 1500°C for five hours, both Si-rich SiC (low deposition temperature) and C-rich SiC (high deposition temperature) showed formation of surface layers of graphitic carbon, which was attributed to the higher evaporation rate of Si at the surface. Surprisingly, after irradiation by fast neutrons amorphous Si is present on the surface for both Si-rich and C-rich samples, and C-rich samples irradiated at 900°C showed more amorphous Si than at 1250°C. Krautwasser et al. suggest the Si-rich surface layer is probably caused by faster transport of Si than C to the surface, and that neutron-induced lattice defects are recovered faster at 1250°C than at 900°C. Also, samples irradiated at 1250°C at twice the fluence of the 900°C sample showed comparable results as the 900°C sample.

5.4.3 Radiation-Induced Segregation of Silicon?

The question then arises: why does excess Si collect at the surface even for Si-deficient samples of SiC? Normal Si self-diffusion through β-SiC is know to be slower than C self-diffusion, although both species are believed to diffuse by a vacancy mechanism [78],[79]. (Future consideration must be given to the effects of radiation-enhanced diffusion such as those seen in uranium and mixed oxides [80] and in beryllium diffusion in neutron-irradiated BeO [81].) The logical explanation is either preferential neutron-induced displacement of Si from the SiC crystal lattice, or more rapid return of C atoms than Si atoms to the vacant lattice sites. Although the energy of formation of the Si vacancy might be 2 eV greater than that for the C vacancy in SiC [82], the displacement energies may show a different trend. Evidence for lower displacement energies of the heavier atom in polyatomic materials is available for Al_2O_3 [83] and for MgO [84] under electron irradiation. The displacement energy for Si atoms in SiC has been estimated to be 106 eV [85]. Yano et al. [86] report a fast fluence less than 2×10^{25} m^{-2} should correspond to one displacement per atom in SiC during irradiation. With the highly energetic neutrons, we might assume differences in energetics between Si and C atomic displacement to be insignificant as a first approximation.

Assuming an equal displacement of C and Si atoms, several factors favor preferential return of C to the vacant lattice sites with the concomitant generation of free Si within the SiC layer. First, C atoms diffuse faster in SiC and thus could fill the vacancies faster. The second reason arises from the fact that the C atomic radius is 0.91 Å and the Si atomic radius is 1.46 Å. This difference in size permits C atoms to occupy Si vacancies on the Si sublattice, but restricts Si atom occupation of the

smaller C lattice sites. This interpretation is supported by theoretical considerations [87] which suggest a C atom in a Si site is slightly more energetically favorable than the original SiC lattice (enthalpy change of -0.06 eV) while a Si atom in a C site is unfavorable (enthalpy change of +0.96 eV), giving a net preference of C atoms filling Si vacancies on the order of 1 eV. Also, because the larger displaced Si atoms generate more strain within the SiC lattice, they will be attracted to dislocation loops and grain boundaries. The disordered structure along grain boundary cores provides more relief for the lattice misfit of Si atoms, and energetic considerations would be expected to preferentially favor attraction of displaced Si atoms to grain boundaries relative to C atoms. Binding energies of interstitial atoms to grain boundaries are always much greater than binding energies of vacancies to grain boundaries [88].

All this information is supportive of the hypothesis of radiation-induced Si segregation from the SiC matrix and its clustering at defects such as grain boundaries. Segregation of impurities at grain boundaries can have significant effects on grain boundary diffusion. Evidence indicates enhanced diffusion in MgO with precipitation or segregation of solutes (e.g., Ca or Si) at the grain boundaries [89]. Unlike metallic systems, ceramic oxides with ionic character are known to exhibit electrostatic potential effects at the grain boundaries [90], with electrostatic potentials as much as a few tenths of a volt, which are strongly dependent on solute and impurity behavior, defect structure, and temperature. The 12% ionic character of the Si-C bond raises the question of the effects of these variables on diffusion of FP along grain boundaries under irradiation and heating. Any segregation of Si to the grain boundaries raises additional concerns at MHTGR accident condition temperatures above the melting point of free silicon (1412° C), as attack and decomposition of SiC samples at the grain boundaries by molten Si has been reported [79].

Obviously, information available in the scientific literature is rich in detail on SiC microstructural behavior and possible decomposition and impurity transport mechanisms. Incorporation of information which seems relevant to fuel performance models should provide more insight into SiC behavior and FP release than that presently available from models of uniform SiC thinning by thermal decomposition or pressure-induced structural failure.

5.4.4 Effects of Thermal Cycling?

Section 5.2.2 mentioned the possibility of stress effects on the SiC structure that any free Si could have during heating and cooling near its melting point of 1412° C, and the possible relation to stress-based models of fuel performance. An additional variable is the microstructural effect of thermal cycling and cooling. Evidence exists that solute segregation can be accelerated during cooling. One theory suggests the grain boundary acts as a vacancy sink [89]; if the interaction between vacancies and solute atoms is strong, the vacancies tend to drag along associated solute atoms to be concentrated at the boundary. This vacancy gradient and solute/vacancy interaction is then postulated to be the driving force for solute segregation at ceramic grain boundaries. The depletion of voids within a distance of 100 to 500 Å from SiC grain boundaries has been observed [91]. This vacancy mechanism suggests that the temperature dependence of radiation-induced segregation should approximate the temperature dependence of void swelling [92], as both depend on the concentration of mobile vacancies.

Another conceivable mechanism for enhanced release during thermal cycling is the formation of larger voids within the SiC structure during heating. If voids can act to enhance the localized stress within the SiC structure, the high temperatures encountered during accident conditions could act to impair the integrity of the SiC layer through this stress enhancement.

Effects on AC-like thermal cycling have apparently not been considered by existing fuel performance models. However, FP release results such as those for FRG sphere AVR 69/13, which

53

was heated on four separate occasions to 1800°C and exhibited abnormally high Cs release and high Kr release, raise the possibility of some enhanced release mechanism along the lines of this Si segregation hypothesis. The possibility was recently raised by K. Verfondern [44] that a thermal cycling effect on FP release may play some role in the bimodal FP release profiles of particles contained in sphere HFR-K3/3. Such a hypothesis is in line with speculation of both enhanced Si segregation during cooling and enhanced stress effects during solid to liquid Si phase transformations.

5.4.5 Modeling of Defect Formation, Void Growth, and Annealing

The review of SiC properties by R. J. Price [85] and the references contained therein contain much information on the microstructural evolution of SiC under neutron bombardment. SiC tends to undergo linear expansion of dimensional properties and of the lattice parameter up to about 1000°C, with the expansion saturating at smaller dimensional changes at higher temperatures. At higher fluences, the lattice parameter changes much less than the linear expansion. Annealing of these samples reduces the dimensional changes to their preirradiation values. Above 1000°C neutron irradiation also induces linear expansion, but the lattice parameter is only marginally affected. The linear expansion in this regime is attributed to void formation and growth. As irradiation temperatures increase toward 1500°C, the linear expansion is less than at 1250°C. Studies of void size and concentration as a function of fast fluence and irradiation and annealing temperatures have been reported; see, e.g., Refs. [86] and [91]. High-temperature annealing reduces the concentrations of the voids, but increases their size. An early study [93] of neutron damage to SiC reported two activation energies for annealing of defects, the predominant mechanism having values between 2.2 and 4.3 eV, with the maximum at 3.4 eV, and another mechanism with an activation energy about 1.6 eV. A more recent study [94] reported an activation energy for defect annealing at 3.0 eV, while T. Suzuki et al. [95] reported annealing activation energies of 1.6 eV for heavily-irradiated samples and 3.7 eV for lightly-irradiated samples.

Experiments related to the use of β-SiC as a semiconductor and its properties under neutron irradiation and annealing also provide information on defect structure. Electron spin resonance (ESR) measurements [96] on vacancy-type defects with unpaired electrons show similarities between the ESR signal intensity and the macroscopic length change during temperature ramps up to 1000°C. Application of deep level transient spectroscopy (DLTS) and electrical resistivity measurements [97] to low-temperature neutron irradiation of epitaxial β-SiC on a Si substrate indicate a two-stage recovery of lattice defects, around 150° and 300°C. The resistivity measurements show a linear change in resistivity up to a fluence of about 10^{18} m^{-2} (defined with respect to 1 MeV equivalent neutron fluence), and indicate that 90% of the neutron-induced traps for electrons are annealed out by 350 °C. However, the DLTS signal increases significantly with annealing temperature above 250°C. Without speculating on the nature of the electron traps, the authors conclude the defect represented by the DLTS peak is not a primary defect, but is formed after migration of some other species to form a new complex. This observation is not inconsistent with individual vacancies forming either vacancy complexes or a complex between a vacancy and another type of defect. This work also observes that the lattice mismatch during epitaxial growth of SiC on Si will vary the dislocation density across the 15 μm SiC layer. Such an observation could have relevance to the radial uniformity of the SiC microstructure of our TRISO particles, depending on the amount of lattice mismatch between SiC and the underlying pyrolytic carbon layer. Another detailed analysis of the annealing of radiation-induced damage in silicon and germanium [98] observed that, for silicon, the measured defect annealing activation energy of 1.2 eV corresponded to the activation energy for divacancy annealing; thus it was concluded that the divacancy defect in silicon determines the dose rate dependence of the crystalline to amorphous transition as well as the

low fluence annealing stage. This paper by Vook and Stein also provides an analysis of the relative damage of Si and Ge by neutrons and ions, and also presents an analytical model for the annealing of radiation-induced defects which has been employed in modeling by the nuclear industry [99],[100] and could be adapted for use in modeling radiation effects on SiC.

The above observations can be phenomenologically explained by the formation of point defects within the SiC structure during neutron irradiation. The displacement of atoms generates vacancies and interstitial atoms. The transport of vacancies is the dominant phenomenon related to the above observations. The transport of interstitial atoms is related to any radiation-induced segregation phenomena and amorphization of the crystal structure. At very low irradiation temperatures (e.g., near room temperature) thermal migration of the vacancies is largely nonexistent, and they will remain fixed in the lattice unless an interstitial atom available for recombination is in the immediate vicinity. Uniform generation of such isolated point defects throughout the lattice will take the form of expansion of the crystal lattice parameter and consequently as linear expansion of the bulk of the crystal. Bulk expansion results from these vacancy-interstitial pairs because the lattice dilation around an interstitial atom is greater than the contraction around the vacancy [101]. Raising the irradiation temperature will mobilize vacancy transport, allowing individual vacancies more opportunity to either recombine with interstitial atoms or to cluster with other vacancies. When the concentration and mobility of vacancies becomes large enough, significant clustering of vacancies will occur, which acts as the nucleus for void formation. As irradiation temperatures exceed 1000° C, vacancy mobilities are sufficiently large that individual vacancies will either recombine or encounter a vacancy cluster and be absorbed; at that point linear expansion does not depend on individual vacancies, but on growth of voids. At very high irradiation temperatures (1500° C) vacancies and interstitials are so mobile that thermal release of individual vacancies from voids becomes feasible, and the equilibrium begins shifting to smaller voids and reduced linear expansion. At high temperature anneals, the flow of individual vacancies from smaller to larger voids tends to reduce void concentration but increase void size. For those samples irradiated at lower temperatures without significant void formation, the ambient vacancy and interstitial concentrations are readily available for recombination, and the radiation damage anneals out more readily and at lower annealing temperatures. In general, at temperatures below the void nucleation and growth regime, property changes saturate when the thermally activated defect removal processes equal the fluence-fixed defect generation rate [101].

Models of defect generation, vacancy nucleation and recombination, void growth, and annealing have been presented for several ceramics and could be readily adapted to an analytical description of microstructural evolution of SiC under irradiation and accident conditions. A good review of some of this modeling effort is presented by Hj. Matzke [102]. N. Nakae and coworkers have presented a series of articles modeling these phenomena in uranium oxide [103],[104],[105]. Some of the earliest attempts at modeling defect generation and annealing as a function of temperature and dose rate, and linear expansion as a function of the change in lattice parameter, were applied to describe neutron effects on ceramic oxides such as BeO, Al_2O_3, and MgO [106],[107]. Adaptation of these existing models to defect generation and annealing in SiC will provide a framework for further analytical developments related to defect and microstructural evolution under accident conditions. Application of this methodology to a phenomenological interpretation of the bimodal Cs release data from the IMGA analysis of sphere HFR-K3/3 would be a useful test of the applicability of this approach. Non-microstructural approaches which can explain this IMGA data are not apparent.

55

6. NEAR-TERM PLAN FOR MODEL DEVELOPMENT

From the previous discussions, the author envisages a modeling effort emphasizing five areas.

1.   The analytical approach to defect formation and transport discussed in §5.4 should be pursued. Considerations such as fast fluence, neutron energy spectrum, diffusion coefficients, and annealing should be included. Effects of neutron-generated vacancy concentrations on FP diffusion coefficients could be considered. A practical goal of this effort is some understanding and explanation of the bimodal Cs release distribution in the IMGA data for sphere HFR-K3/3.

2.   Phenomena discussed in this status report emphasize SiC behavior, as transport through SiC is typically the rate-determining step for FP release. However, both PyC and matrix graphite are known to impact FP release from particles and spheres. The author requires more background on the effects of PyC and graphite on FP transport, for better understanding of non-SiC release mechanisms and for more thorough interpretation of release data.

3.   Analysis of the database on fuel performance should be expanded beyond the FP release data for reference FRG fuel spheres to include FP concentration and non-sphere data, and to include earlier data of heating tests on U.S. fuels. The FRG tests include data on FP concentration profiles across particles and spheres and FP release from bare kernels and individual particles, which can provide more detailed information on FP transport and release mechanisms from particles. Results from the heating tests performed at GA during the 1970's and early 1980's were extensively used to develop the earlier fuel performance models. The advantage in emphasizing the FRG results is the minimal batch-to-batch variability in SiC and particle properties within the FRG spheres, which simplifies data interpretation. Assessment and reevaluation of the earlier U.S. data with respect to the contents of this status report and conclusions drawn from FRG sphere results could be valuable.

4.   A diffusion model of FP release appears promising for further study. The SHELL code should be modified to incorporate the depleting source approximation for accurate simulation of high-temperature ramp release such as that from FRG spheres and GA particles. Specifically, the effective diffusion coefficients which can describe the ramp release from GA particles should be compared to those of modern FRG fuels. Silver release could also be simulated more accurately. The Booth model or some other approach to kernel release should be introduced into SHELL to simulate FP retention within the kernel and its effect on release from the SiC. Ultimately a diffusion model needs a two-layer or multi-layer model for TRISO particles. Such an approach could either explore the methodology developed by Walther (§2.5.3) or develop particle simulation methods for atomic transport across multiple regions.

5.   For future interplay between modeling and experiment, some compilation of the experimental methods that have been used and can be used to analyze fuel performance should be presented. Those methods previously applied for analysis of particles, coating layers, and FP release are widely documented. Other analytical methods exist which hold promise for fuel and FP analysis, including state-of-the-art methods not yet applied to fuel performance analysis. Of specific interest are methods which can be brought to bear on testing hypotheses of performance models, to either prove or refute existing assumptions in AC fuel performance modeling.

7. CONCLUSIONS

1.   Unifying conceptual threads can be traced through accident condition fuel performance models from the 1960's to the present. Specifically, the pressure-vessel failure model led to the incorporation of the Weibull parameter, and that coupled with the concept of particle failure remains dominant within current models.

2.   Although downplayed for years, a diffusion mechanism appears to hold promise as an alternative model for fission product release from TRISO particles. A simple analytical model for fission product diffusion through the SiC shell is presented, and determination of effective diffusion coefficients to describe FRG sphere release suggests a dependence of fission product release on fast fluence. The model as developed can predict fission product release from future FRG heating tests with reasonable confidence, especially for metallic fission products.

3.   The modeling concept of particle failure as commonly used contains ambiguities, and detailed mechanisms of fission product transport through the coating layers has been underemphasized. For a meaningful concept of failure, an alternative hypothesis is proposed based on repeated heatup to accident condition temperatures. If fission product release can be shown to correspond to significant lack of containment in future heatup, then the concept of failure is meaningful. If diffusive release occurs at high temperatures without loss of SiC integrity, and containment is demonstrated in future heatup, then the concept of failure is misleading. Observation of FP release does not necessarily imply structural or mechanical changes in the coatings.

4.   Existing fuel performance models largely neglect the microstructural behavior of SiC. The use of stress models to simulate fission product release is not convincing. Existing models cannot provide an explanation of the bimodal cesium release data obtained by the IMGA system for sphere HFR-K3/3.

5.   Much information is available on the microstructural behavior of SiC in the scientific literature, including radiation effects information, which hasn't been considered by fuel performance models. Analysis by the semiconductor industry is a notable example. Fuel performance models have apparently not investigated the use of previously-developed models of neutron damage effects on materials for use in modeling SiC behavior.

6.   As a microstructural hypothesis of fission product release, the radiation-induced segregation of silicon within the SiC layer is proposed, and existing evidence presented to support this hypothesis. Based on this hypothesis, the melting point of silicon at 1412°C might be relevant for fuel performance.

ACKNOWLEDGMENTS

REFERENCES

1.   R. C. Martin, "Status Report on Reference Fuel Accident Condition Database and Modeling," USDOE Report ORNL/NPR-90/13, May 1990.

2.   D. T. Goodin and H. Nabielek, "US/FRG Accident Condition Fuel Performance Models," USDOE Report DOE-HTGR-85107, Revision A, General Atomics, March 1989.

3.   J. W. Prados and J. L. Scott, "Mathematical Model for Predicting Coated-Particle Behavior," *Nucl. Appl.*, 2 (1966) 402.

4. J. L. Kaae, "A Mathematical Model for Calculating Stresses in a Pyrocarbon- and Silicon Carbide-Coated Fuel Particle," *J. Nucl. Mater.*, 29 (1969) 249.

5. J. L. Kaae, "A Mathematical Model for Calculating Stresses in a Four-Layer Carbon-Silicon Carbide-Coated Fuel Particle," *J. Nucl. Mater.*, 32 (1969) 322.

6. D. W. Stevens, "An Explicit Solution for Stresses in Pyrocarbon-Coated Fuel Particles," *Nucl. Technol.*, 10 (1971) 301.

7. T. D. Gulden, C. L. Smith, D. P. Harmon, and W. W. Hudritsch, "The Mechanical Design of TRISO-Coated Particle Fuels for the Large HTGR," *Nucl. Technol.*, 16 (1972) 100.

8. K. Bongartz, "Improvement of a Method for Predicting Failure Rates of Coated Particles During Irradiation," *Nucl. Technol.*, 35 (1977) 379.

9. J. L. Kaae, "The Mechanical Behavior of BISO-Coated Fuel Particles During Irradiation. Part I: Analysis of Stresses and Strains Generated in the Coating of a BISO Fuel Particle During Irradiation," *Nucl. Technol.*, 35 (1977) 359.

10. K. Bongartz, E. Gyarmati, H. Schuster, and K. Täuber, "The Brittle Ring Test: A Method for Measuring Strength and Young's Modulus on Coatings of HTR Fuel Particles," *J. Nucl. Mater.*, 62 (1976) 123.

11. K. Bongartz, "Status of the Fuel Stress and Failure Rate Calculations," Kernforschungsanlage Jülich Report Jül-1686, November 1980.

12. K. Verfondern and H. Nabielek, "PANAMA - Ein Rechenprogramm zur Vorhersage des Partikelbruchanteils von TRISO-Partikeln unter Störfallbedingungen," Kernforschungsanlage Jülich Report Jül-Spez-298, 1985.

13. C. L. Smith, "Fuel Particle Behavior Under Normal and Transient Conditions," General Atomic Company Report GA-A12971, October 1974.

14. M. Tokar, "Evaluation of High Temperature Gas Cooled Reactor Fuel Particle Coating Failure Models and Data," U. S. Nuclear Regulatory Commission Report NUREG-0111, November 1976.

15. M. H. Schwartz, D. B. Sedgley, and M. M. Mendonca, "SORS: Computer Programs for Analyzing Fission Product Release from HTGR Cores During Transient Temperature Excursions," GA Report GA-A12462, April 1974.

16. General Atomic Standard Safety Analysis Report (GASSAR) GA-A13200, 1975.

17. P. D. Smith and R. G. Steinke, "COPAR, A Program to Compute Release of Metallic Fission Products from Coated Particles," General Atomic Company Report GA-A14034, November 1977.

18. W. Hudritsch, "New COPAR Solutions," GA Technologies Document No. 907556, August 1984.

58

19. D. T. Goodin, "Accident Condition Performance of Fuels for High-Temperature Gas-Cooled Reactors," *J. Am. Ceram. Soc.*, 65 (1982) 238.

20. D. T. Goodin, "Accident Condition Performance of High-Temperature Gas-Cooled Reactor Fuels," GA Technologies Report GA-A16508, October 1983.

21. B. F. Myers and R. E. Morrissey, "Licensing Topical Report: The Measurement and Modelling of Time-dependent Fission Product Release from Failed HTGR Fuel Particles Under Accident Conditions," General Atomic Company Report GA-A15439, April 1980.

22. D. T. Goodin and H. Nabielek, "US/FRG Accident Condition Fuel Performance Models," USDOE Report HTGR-85-107, Rev. 1, GA Technologies Inc., December 1985.

23. W. J. Kovacs, K. Bongartz, and D. T. Goodin, "High-Temperature Gas-Cooled Reactor Fuel Pressure Vessel Performance Models," *Nucl. Technol.*, 68 (1985) 344.

24. C. A. Young and C. S. Jones, "Pre- and Postirradiation Evaluation of TRISO ThO_2 Particles Irradiated in Capsule HT-34," General Atomic Company Report GA-A15612, October 1980.

25. D. T. Goodin, "Metallic Fission Product Release Models for Accident Conditions," GA Technologies Document No. 906957, July 1983.

26. B. F. Myers, "Models and Codes for Calculating Fission Product Release," GA Technologies Document No. 906965/1, July 1983.

27. K. Verfondern and D. Müller, "Code Development for Fission Product Behavior in HTR Fuel for Safety Assessments," Kernforschungsanlage Jülich Report KFA-ISF-IB-10/89, October 1989.

28. H. Krohn, "Freisetzung von Spaltprodukten aus dem Core eines Kugelhaufenreaktors bei Störfällen mit Core-Aufheizung," Kernforschungsanlage Jülich Report Jül-1791, August 1982.

29. H. Krohn and R. Finken, "FRESCO-II: Ein Rechenprogramm zur Berechnung der Spaltproduktfreisetzung aus kugelförmigen HTR-Brennelementen in Bestrahlungs- und Ausheizexperimenten," Kernforschungsanlage Jülich Report Jül-Spez-212, 1983.

30. K. Verfondern and D. Müller, "Prediction of Cesium and Krypton Release from Fuel Elements Irradiated in the Experiment FRJ2-K15 under Heating Conditions," Kernforschungsanlage Jülich Technical Note 28/90 ISR-1/11, June 1990.

31. J. L. Martin and H. Nabielek, "Modelling of Fuel Element Heating Tests," KFA Jülich Report HBK-TN-4/88, December 1988.

32. J. L. Martin and H. Nabielek, "Fission Product Transport Modelling in Fuel Spheres," KFA Jülich Report HBK-TN-2/88, July 1988.

33. R. W. Dunlap and T. D. Gulden, "Diffusion Model for Release of Fission Products from Coated Particle Fuels," *Nucl. Sci. Eng.*, 32 (1968) 407.

34. H. Walther, "Calculation of the Release of Fission Products from Coated Fuel Particles," *Nukleonik*, 11 (1968) 171.

35. B. F. Myers, "Update of Accident Condition Models," GA Technologies Document No. 908776, May 1986.

36. B. F. Myers, F. C. Montgomery, and K. E. Partain, "The Transport of Fission Products in SiC," GA Technologies Document No. 909055, September 1986.

37. R. L. Pearson, T. B. Lindemer, and E. C. Beahm, "Simulated Fission Product-SiC Interaction in Triso-Coated LEU or MEU HTGR Fuel Particles," Oak Ridge National Laboratory Report ORNL/TM-6991, November 1980.

38. O. M. Stansfield, F. J. Homan, W. A. Simon, and R. F. Turner, "Interaction of Fission Products and SiC in TRISO Fuel Particles: A Limiting HTGR Design Parameter," GA Technologies Report GA-A17183, September 1983.

39. S. S. McElmury and O. M. Stansfield, "An Analysis of the Effect of Buffer-IPyC Coating Separation on the Temperature Distribution in TRISO UC_2 Fuel Particles," General Atomic Company Report GA-A13500, December 1975.

40. W. Schenk, D. Pitzer, and H. Nabielek, "Fission Product Release Profiles from Spherical HTR Fuel Elements at Accident Temperatures," Kernforschungsanlage Jülich Report Jül-2234, September 1988.

41. O. M. Stansfield, "Report of Foreign Travel of O. M. Stansfield, Metals and Ceramics Division, to Federal Republic of Germany and France," Oak Ridge National Laboratory Report ORNL/FTR-3687, July 1990.

42. D. Goodin, "Status of US/FRG Fuel Performance Model," GA Technologies Document No. 909606, December 1987.

43. C. A. Baldwin and M. J. Kania, "IMGA Examination of Set #4 Fuel Under Project Work Statement FD-20," USDOE Report DOE-HTGR-88381, Oak Ridge National Laboratory, 1989.

44. O. M. Stansfield, personal communication, August 1990.

45. J. R. Lamarsh, *Introduction to Nuclear Engineering*, 2d edn., Addison-Wesley, Reading, Mass., 1983, p. 75.

46. J. Crank, The Mathematics of Diffusion, 2d edn., Clarendon Press, Oxford, 1975, p. 100.

47. B. F. Myers, "Cesium Diffusion in Silicon Carbide During Post Irradiation Anneals," Kernforschungsanlage Jülich Report HBK-TN-01/84, January 1984.

48. M. T. Morgan and A. P. Malinauskas, "Cesium Release and Transport in Biso-Coated Fuel Particles," *Nucl. Technol.*, 35 (1977) 457.

49.   P. G. Shewmon, Diffusion in Solids, McGraw-Hill, New York, 1963, p. 31.

50.   B. F. Myers, personal communication, August 1990.

51.   H. Nabielek, W. Schenk, W. Heit, A.-W. Mehner, and D. T. Goodin, "The Performance of High-Temperature Reactor Fuel Particles at Extreme Temperatures," *Nucl. Technol.*, **84** (1989) 62.

52.   D. R. Olander, *Fundamental Aspects of Nuclear Reactor Fuel Elements*, National Technical Information Service, Springfield, Va., 1976, p. 318.

53.   K. Fukuda, T. Ogawa, S. Kashimura, K. Ikawa, K. Iwamoto, K. Yamamoto, T. Itoh, and H. Matsushima, "Release Behavior of Fission Gas from Coated Fuel Particles under Irradiation," *J. Nucl. Sci. Technol. [Tokyo]*, **19** (1982) 889.

54.   R. Moorman and K. Verfondern, "Methodik umfassender probabilistischer Sicherheitsanalysen für zukünftige HTR-Anlagenkonzepte Ein Statusbericht (Stand 1986). Band 3: Spaltproduktfreisetzung," Kernforschungsanlage Jülich Report Jül-Spez-388, March 1987.

55.   R. Benz, "Kinetics of Decomposition of CVD SiC in Modified TRISO-coated Fuel Particles at Temperatures of 1600 to 2200°C," Kernforschungsanlage Jülich Technical Note IRW-TN-124/82, October 1982.

56.   A. K. Galwey, *Chemistry of Solids*, Chapman and Hall Ltd., London, 1967, p. 168.

57.   W. E. Garner, ed., *Chemistry of the Solid State*, Academic Press, New York, 1955, chapter 7.

58.   A. W. Searcy and D. Beruto, "Kinetics of Endothermic Decomposition Reactions. 1. Steady-State Chemical Steps," *J. Phys. Chem.*, **80** (1976) 425.

59.   A. W. Searcy and D. Beruto, "Kinetics of Endothermic Decomposition Reactions. 2. Effects of the Solid and Gaseous Products," *J. Phys. Chem.*, **82** (1978) 163.

60.   S. G. Davis, D. F. Anthrop, and A. W. Searcy, "Vapor Pressure of Silicon and the Dissociation Pressure of Silicon Carbide," *J. Chem. Phys.*, **34** (1961) 659.

61.   S. V. Baranov, A. G. Vodop'yanov, G. K. Moiseev, and G. N. Kozhevnikov, "Thermodynamic Analysis and Kinetics of Dissociation of SiC," *Inorg. Mat.*, **18** (1982) 1097.

62.   G. G. Gnesin and A. V. Kurdyumov, "The Importance of the State of Aggregation of Silicon During Siliconization, and the Nature of the Silicon Phase in Siliconized Graphite," in *Silicon Carbide*, I. N. Frantsevich, ed., Consultants Bureau, New York, 1970, pp. 61-67.

63.   T. I. Kucher, "The Problem of Diffusion in an Evaporating Solid Medium," *Soviet Phys. - Solid State*, **3** (1961) 401.

64.   R. N. Ghoshtagore, "Diffusion from a Thin Film into a Dissociating or Evaporating Solid," *phys. stat. sol.*, **19** (1967) 123.

65. J. R. Ockendon and W. R. Hodgkins, eds., *Moving Boundary Problems in Heat Flow and Diffusion*, Clarendon Press, Oxford, 1975.

66. R. W. Balluffi and J. M. Blakely, "Special Aspects of Diffusion in Thin Films," *Thin Solid Films*, 25 (1975) 363.

67. D. Shaw, ed., *Atomic Diffusion in Semiconductors*, Plenum Press, New York, 1973.

68. J. M. Bind, "Contribution of the Ionic Bonding to the Thermal Stability of SiC Polytypes," *Mat. Res. Bull.*, 14 (1979) 1173.

69. W. Schenk and H. Nabielek, "Iodine Retention in Spherical Fuel Elements under HTR MODUL Accident Conditions," submitted to Jahrestagung Kerntechnik, 1990.

70. "Table of Periodic Properties of the Elements," Sargent-Welch Scientific Company, Skokie, Ill., 1980.

71. D. R. Olander, *Fundamental Aspects of Nuclear Reactor Fuel Elements*, National Technical Information Service, Springfield, Va., 1976, p. 176.

72. R. Förthmann, E. Gyarmati, J. Linke, and E. Wallura, "Influence of Material Properties on the Retention of Fission Products by Silicon Carbide Coatings," *High Temp. - High Press.*, 14 (1982) 477.

73. W. Schenk, G. Pott, and H. Nabielek, "Fuel Accident Performance Testing for Small HTRs," *J. Nucl. Mater.*, 171 (1990) 19.

74. A. Naoumidis, R. Benz, and J. Rottmann, "Identification of Silicon in Small Quantities of SiC-Coated and SiC(TRISO)-Coated Nuclear Fuel Particles," *High Temp. - High Press.*, 14 (1982) 53.

75. Yu. A. Vodakov, G. A. Lomakina, and E. N. Mokhov, "Nonstoichiometry and Polytypism of Silicon Carbide," *Sov. Phys. - Solid State*, 24 (1982) 780.

76. K. L. More, J. Ryu, C. H. Carter, Jr., J. Bentley, and R. F. Davis, "Defects in Silicon Carbide: Their Electrical and Physical Consequences," *Cryst. Latt. Def. and Amorph. Mat.*, 12 (1985) 243.

77. P. Krautwasser, G. M. Begun, and P. Angelini, "Raman Spectral Characterization of Silicon Carbide Nuclear Fuel Coatings," *J. Am. Ceram. Soc.*, 66 (1983) 424.

78. M. H. Hon and R. F. Davis, "Self-Diffusion of ^{14}C in Polycrystalline β-SiC," *J. Mater. Sci.*, 14 (1979) 2411.

79. M. H. Hon and R. F. Davis, "Self-Diffusion of ^{30}Si in Polycrystalline β-SiC," *J. Mater. Sci.*, 15 (1980) 2073.

80. Hj. Matzke, "Radiation Enhanced Diffusion in UO_2 and $(U,Pu)O_2$," *Rad. Effects*, 75 (1983) 317.

81. H. J. de Bruin, G. M. Watson, C. M. Blood, and D. Roman, "Cation Self-diffusion in Fast Neutron-irradiated Beryllium Oxide," *Phil. Mag.*, **16** (1967) 427.

82. J. A. Van Vechten, "Simple Theoretical Estimates of the Schottky Constants and Virtual-Enthalpies of Single Vacancy Formation in Zinc-Blende and Wurtzite Type Semiconductors," *J. Electrochem. Soc.*, **122** (1975) 419.

83. G. P. Pells and D. C. Phillips, "Radiation Damage of α-Al$_2$O$_3$ in the HVEM I. Temperature Dependence of the Displacement Threshold," *J. Nucl. Mater.*, **80** (1979) 207.

84. R. A. Youngman, L. W. Hobbs and T. E. Mitchell, "Electron Irradiation Damage in MgO," *J. Phys. (Paris) Coll. C6*, **41** (1980) C6-227.

85. R. J. Price, "Properties of Silicon Carbide for Nuclear Fuel Particle Coatings," *Nucl. Technol.*, **35** (1977) 320.

86. T. Yano, T. Suzuki, T. Maruyama, and T. Iseki, "Microstructure and Annealing Behavior of Heavily Neutron-Irradiated β-SiC," *J. Nucl. Mater.*, **155-157** (1988) 311.

87. J. A. Van Vechten, "Simple Theoretical Estimates of the Enthalpy of Antistructure Pair Formation and Virtual-Enthalpies of Isolated Antisite Defects in Zinc-Blende and Wurtzite Type Semiconductors," *J. Electrochem. Soc.*, **122** (1975) 423.

88. R. W. Balluffi, "Grain Boundary Diffusion Mechanisms in Metals," in *Diffusion in Crystalline Solids*, G. E. Murch and A. S. Nowick, eds., Academic Press, Orlando, Fla., p.343.

89. W. D. Kingery, "Plausible Concepts Necessary and Sufficient for Interpretation of Ceramic Grain-Boundary Phenomena: II, Solute Segregation, Grain-Boundary Diffusion, and General Discussion," *J. Am. Ceram. Soc.*, **57** (1974) 74.

90. W. D. Kingery, "Plausible Concepts Necessary and Sufficient for Interpretation of Ceramic Grain-Boundary Phenomena: I, Grain-Boundary Characteristics, Structure, and Electrostatic Potential," *J. Am. Ceram. Soc.*, **57** (1974) 1.

91. R. J. Price, "Neutron Irradiation-Induced Voids in β-Silicon Carbide," *J. Nucl. Mater.*, **48** (1973) 47.

92. L. E. Rehn, P. R. Okamoto, D. I. Potter, and H. Wiedersich, "Effect of Solute Misfit and Temperature on Irradiation-Induced Segregation in Binary Ni Alloys," *J. Nucl. Mater.*, **74** (1978) 242.

93. W. Primak, L. H. Fuchs, and P. P. Day, "Radiation Damage in Diamond and Silicon Carbide," *Phys. Rev.*, **103** (1956) 1184.

94. R. N. Kyutt, A. A. Lepneva, G. A. Lomakina, E. N. Mokhov, A. S. Tregubova, M. M. Shcheglov, and G. F. Yuldashev, *Fiz. Tverd. Tela (Leningrad)*, **30** (1988) 2606; *Chemical Abstracts*, **110** (1989) 16270p.

95. T. Suzuki, T. Maruyama, T. Iseki, T. Mori, and M. Ito, "Recovery Behavior in Neutron Irradiated β-SiC," *J. Nucl. Mater.*, **149** (1987) 334.

96. S. Kasahara, T. Suzuki, T. Maruyama, T. Iseki, H. Kawazoe, and M. Ito, "ESR Observations in Neutron-Irradiated and Annealed β-SiC," *J. Nucl. Mater.*, **161** (1989) 261.

97. V. Nagesh, J. W. Farmer, R. F. Davis, and H. S. Kong, "Defects in Neutron Irradiated SiC," *Appl. Phys. Lett.*, **50** (1987) 1138.

98. F. L. Vook and H. J. Stein, "Relation of Neutron to Ion Damage Annealing in Si and Ge," *Rad. Effects*, **2** (1969) 23.

99. W. J. Nellis, "The Effect of Self-Radiation on Crystal Volume," *Inorg. Nucl. Chem. Letters*, **13** (1977) 393.

100. W. J. Weber, "Ingrowth of Lattice Defects in Alpha Irradiated UO_2 Single Crystals," *J. Nucl. Mater.*, **98** (1981) 206.

101. R. J. Price, "Effects of Fast-Neutron Irradiation on Pyrolytic Silicon Carbide," *J. Nucl. Mater.*, **33** (1969) 17.

102. Hj. Matzke, "Radiation Damage in Crystalline Insulators, Oxides and Ceramic Nuclear Fuels," *Rad. Effects*, **64** (1982) 3.

103. N. Nakae, A. Harada, and T. Kirihara, "Irradiation Induced Lattice Defects in UO_2," *J. Nucl. Mater.*, **71** (1978) 314.

104. N. Nakae and T. Kirihara, "Irradiation Induced Volume Change in UO_2," *J. Nucl. Mater.*, **74** (1978) 1.

105. N. Nakae, Y. Iwata, and T. Kirihara, "Thermal Recovery of Defects in Neutron Irradiated UO_2," *J. Nucl. Mater.*, **80** (1979) 314.

106. B. S. Hickman and A. W. Pryor, "The Effect of Neutron Irradiation on Beryllium Oxide," *J. Nucl. Mater.*, **14** (1964) 96.

107. R. S. Wilks, "Neutron-Induced Damage in BeO, Al_2O_3, and MgO - A Review," *J. Nucl. Mater.*, **26** (1968) 137.
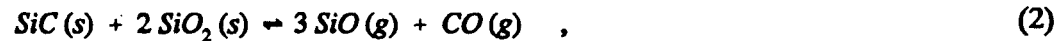
Appendix A. EFFECTS OF OXYGEN ON SILICON CARBIDE STABILITY

Some recent discussions of fuel performance have raised questions about CO pressures for different kernel types. Further investigation suggests the presence of oxygen may have effects on SiC thermal stability which have not been emphasized in recent fuel performance evaluations. This appendix briefly presents information on oxygen-enhanced SiC decomposition mechanisms which may be significant at accident condition temperatures much lower than 2000°C, and which may provide some explanation of an apparent difference in fission product release behavior from $(Th,U)O_2$ and UO_2 fuels in high-temperature FRG sphere ramp tests.

Exposure of SiC to an oxidizing atmosphere has long been know to produce protective surface films of SiO_2. This reaction also occurs in the presence of excess carbon monoxide gas, such as that generated from the fission of oxide fuels, according to the reaction:

$$SiC\,(s)\; +\; 2\,CO\,(g)\; \rightarrow\; SiO_2\,(s)\; +\; 3\,C\,(s)\quad. \tag{1}$$

The rate of this reaction increases rapidly above 1000°C. If the supply of oxidant is limited, corrosion of the SiC can result from formation of gaseous SiO rather than the stable SiO_2 [1]. With sufficient oxidant, formation of the oxide film reduces further reaction of the underlying SiC. However, as temperatures exceed 1500°C the probability increases for the transformation of solid SiO_2 into gaseous SiO by several reactions [2]:

$$SiC\,(s)\; +\; 2\,SiO_2\,(s)\; \rightarrow\; 3\,SiO\,(g)\; +\; CO\,(g)\quad, \tag{2}$$

$$SiC\,(s)\; +\; SiO_2\,(s)\; \rightarrow\; 2\,SiO\,(g)\; +\; C\,(s)\quad, \tag{3}$$

$$2\,SiC\,(s)\; +\; SiO_2\,(s)\; \rightarrow\; 3\,Si\,(s)\; +\; 2\,CO\,(g)\quad. \tag{4}$$

Any free silicon at the surface can also form SiO_2, but its presence will enhance SiO(g) formation at these temperatures. Increasing temperatures above 1500°C increase the volatilization of SiO_2 and ultimately of the SiC itself. Above 1823°C any SiO_2 present will melt.

The predominant decomposition mechanism for SiC at high temperatures has been assumed to be that given by:

$$SiC\,(s)\; \rightarrow\; C\,(s)\; +\; Si\,(g)\quad, \tag{5}$$

i.e., the vaporization of silicon leaving behind a carbon residue [3]. This reaction is the predominant high-temperature decomposition reaction for SiC in a vacuum or an inert atmosphere, but not necessarily in an oxidizing atmosphere. Under the accident condition temperatures normally expected for the MHTGR (1600° to 1700°C) the presence of SiO_2 surface layers could play a role in SiC integrity and fission product retention. SiO_2 can also be an effective diffusion barrier, and layers of SiO_2 have been used in the semiconductor industry to limit diffusion of implanted ions within silicon during annealing. The existence of SiO_2 surface layers and their effect on the retention of FP by SiC should be considered; if relevant, the cracking and resealing of an SiO_2 layer might play a role in nonuniform FP transport through SiC.

The rate of formation and thickness of an SiO_2 layer is strongly dependent on the pressure of the oxidant. The reaction of water vapor with the SiC layer of fuel particles at 1000°C and 1200°C causes continuous weight loss from the SiC layer for H_2O pressures below 10^{-6} atm, but pressures on the order of 10^{-6} atm stabilized the SiC layer. These results may have implications for TRISO particle behavior for different kernels. The oxide fuels generate significant CO pressures, while the carbide and UCO fuels generate much less CO. In traditional fuel performance modeling [4], the oxygen potential is typically used as the unifying thread for explaining the chemical and physical behavior of the fuel and the fission products. Although not pursued in detail in the HTGR program since perhaps the late 1970's [5], such an approach might be useful in correlating the fuel performance behavior of UO_2 vs. $(Th,U)O_2$ vs. UCO vs. UC_2 fuels.

In high-temperature ramp tests on FRG spheres, the krypton release profiles for high-burnup $(Th,U)O_2$ fuel are similar to those for low burnup UO_2 fuel, while high burnup UO_2 fuel exhibits faster Kr release. These results are shown in Figures A.1 and A.2, taken from Ref. [3]. Reference [3] concludes that the faster release from high burnup UO_2 fuel "indicates the operation of a failure mechanism in addition to SiC decomposition" and discusses the large CO gas pressure buildup in high burnup fuels and the maximum temperatures in the AVR reactor as contributing to early pressure-induced failure.

In light of the information on oxygen-enhanced corrosion of the SiC, calculations were performed to approximate the oxygen content in the mixed oxide vs. UO_2 fuels. Design equations exist to calculate the number of oxygen atoms per fission (OPF) for both fuels. These OPF values are used as a measure of the CO generation within the particle during burnup. By using these equations as a measure of the oxygen content within the particles, we can see if some trend is apparent which correlates with the above observations.

The equations used to calculate OPF during the heating ramps are taken from a draft report of the PANAMA code [6]. For $(Th,U)O_2$ fuel the dominant variables are the burnup and the heating temperature:

$$\log OPF = 0.96 - \frac{4420}{T} + 0.4 \times \log N + 0.3 \times \log F_b \quad , \tag{6}$$

with T the heating temperature (K), N = 5 for AVR spheres, and F_b the fractional burnup (FIMA). For UO_2 the burnup is not included as a variable, but the irradiation temperature and time are:

$$\log OPF = -10.08 - \frac{8500}{T_{irr}} + 2 \times \log t_{irr} - 0.404 \times \left(\frac{10^4}{T} - \frac{10^4}{T_{irr} + 75} \right) \quad , \tag{7}$$

with T_{irr} and t_{irr} the irradiation temperature (K) and time (s), respectively. The maximum value of OPF is set at 0.625. For UCO fuels, the OPF value is assumed to be negligble relative to UO_2 and $(Th,U)O_2$ fuels. These equations are used to calculate the OPF during the ramp tests for the spheres portrayed in Figures A.1 and A.2, and the results shown in Fig. A.3. An irradiation temperature of 1000°C was assumed for all spheres. Comparison of the figures shows those spheres which achieve the maximum OPF early in the ramp test are the highest-burnup UO_2 spheres ($\geq$ 6.9% FIMA), followed by AVR 74/6 (5.6% FIMA), AVR 74/8 (2.9%), AVR 70/19 (2.2%), and finally the high-burnup mixed oxide spheres AVR 74/17 and 70/18. This trend correlates with the sequence of ^{85}Kr release in Figures A.1 and A.2. Although the pressure-vessel failure mechanism postulated in Ref. [3] provides the same trend, this result suggests alternative hypotheses of fission gas release

66

mechanisms from SiC are feasible, based on oxygen-enhanced corrosion of the SiC.

Equations (6) and (7) introduce the variables of temperature of irradiation and heating, time of irradiation, and burnup in a consistent and physical manner. Combining the variables of oxygen potential and fast fluence into a hypothesis for accident condition fuel performance may permit a numerical treatment of FRG sphere release data similar to that employed in the US/FRG model, but based more fundamentally on physical mechanisms relevant to SiC and fuel behavior. Pursuit of such an approach may be promising.

REFERENCES

1.   J. E. Antill and J. B. Warburton, "Active to Passive Transition in the Oxidation of SiC," *Corrosion Sci.*, 11 (1971) 337.

2.   E. A. Gulbransen and S. A. Jansson, "The High-Temperature Oxidation, Reduction, and Volatilization Reactions of Silicon and Silicon Carbide," *Oxid. Metals*, 4 (1972) 181.

3.   H. Nabielek, W. Schenk, W. Heit, A-W. Mehner, and D. T. Goodin, "The Performance of High-Temperature Reactor Fuel Particles at Extreme Temperatures," *Nucl. Technol.*, 84 (1989) 62.

4.   D. R. Olander, *Fundamental Aspects of Nuclear Reactor Fuel Elements*, National Technical Information Service, Springfield, Va., 1976.

5.   F. J. Homan, T. B. Lindemer, E. L. Long, Jr., T. N. Tiegs, and R. L. Beatty, "Stoichiometric Effects on Performance of High-Temperature Gas-Cooled Reactor Fuels from the U-C-O System," *Nucl. Technol.*, 35 (1977) 428.

6.   "PANAMA: A Computer Code to Predict TRISO Particle Failure under Accident Conditions," draft report provided by H. Nabielek.
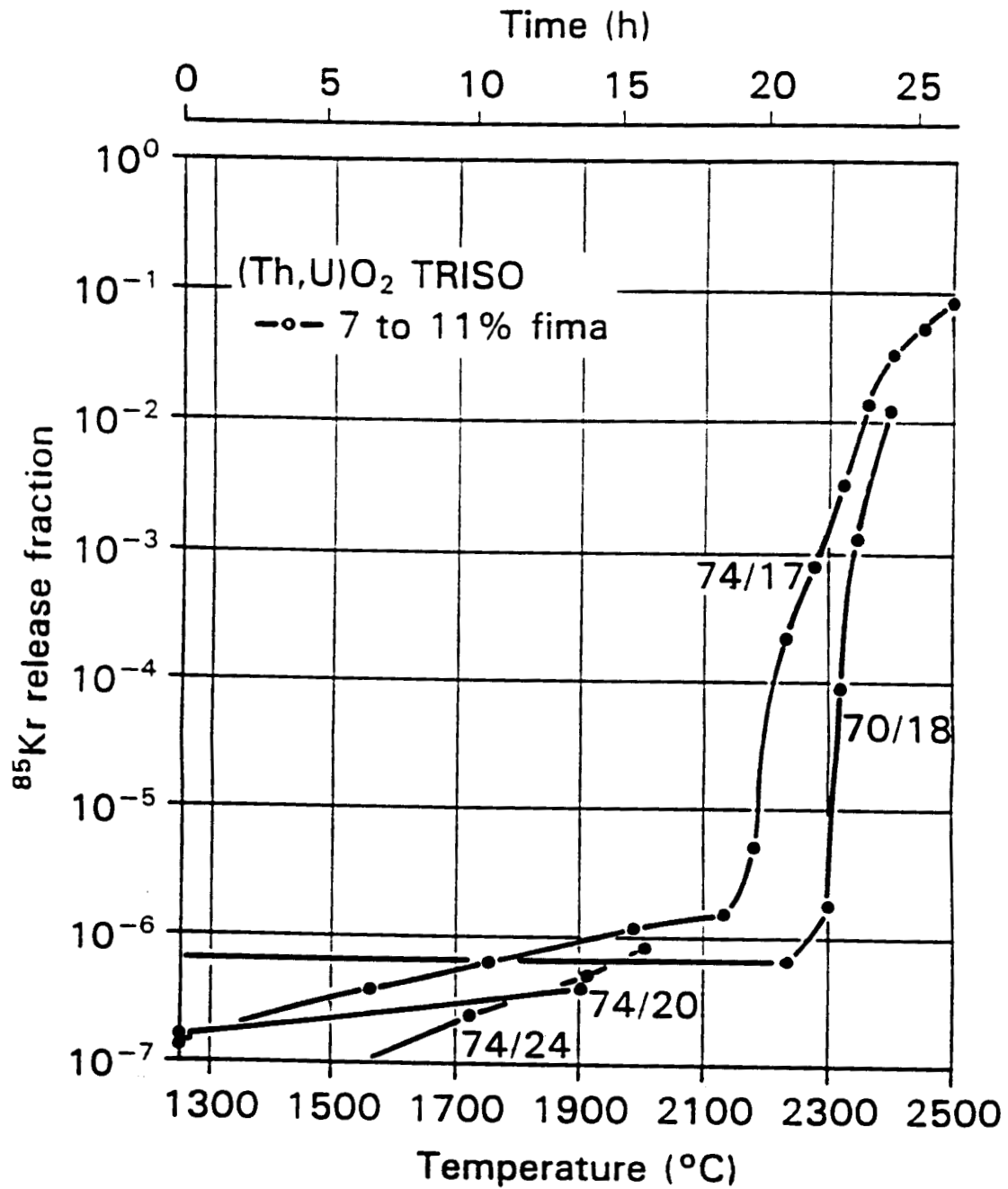
Fig. A.1.   Krypton-85 release as a function of heating temperature during linear ramp tests with spherical AVR fuel elements containing (Th,U)O$_2$ TRISO particles of 7 to 11% FIMA burnup. (from [3])
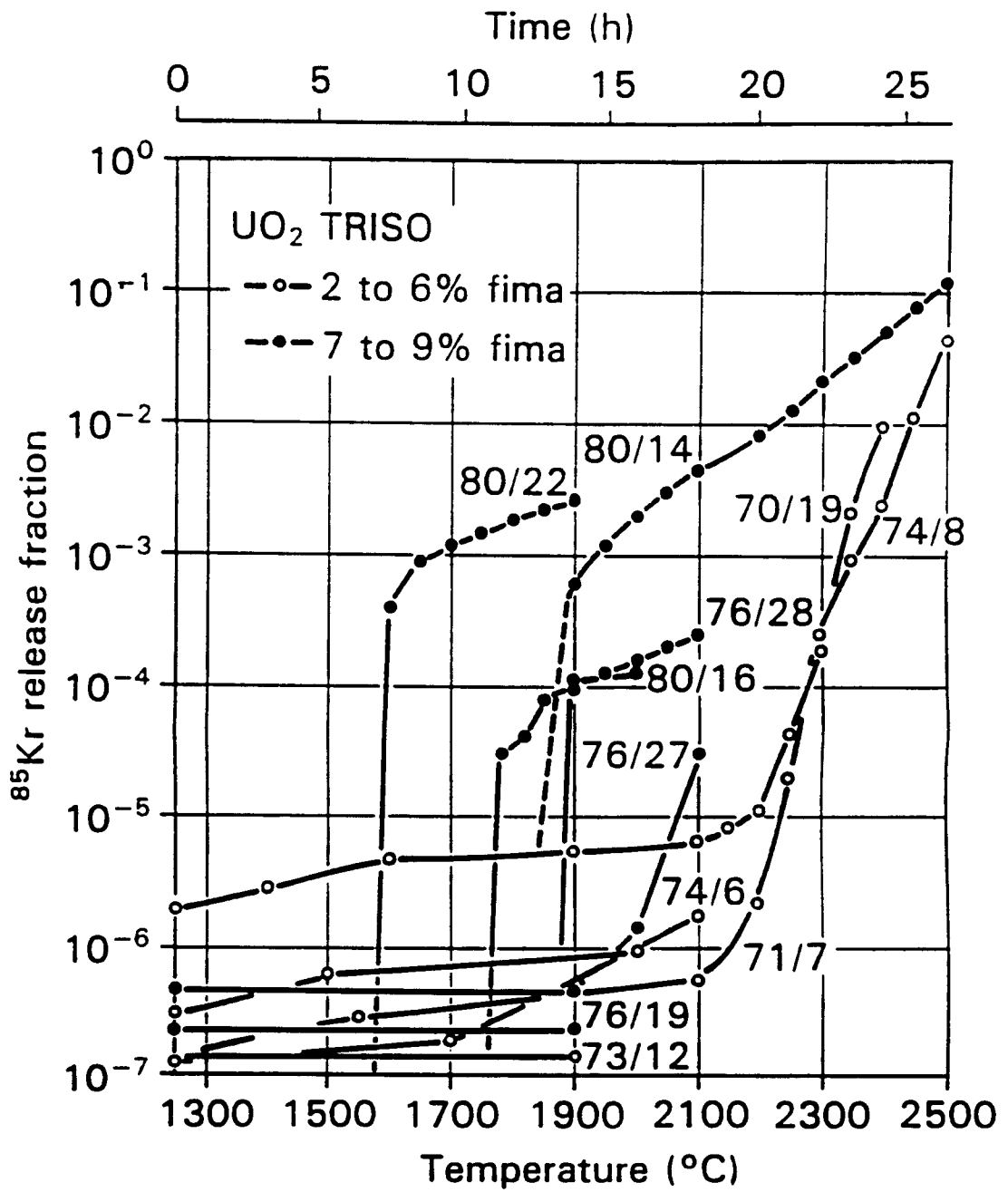
Fig. A.2.   Krypton-85 release as a function of heating temperature during linear ramp tests with spherical AVR fuel elements containing UO$_2$ TRISO particles of 2 to 6 and 7 to 9% FIMA burnup. (from [3])
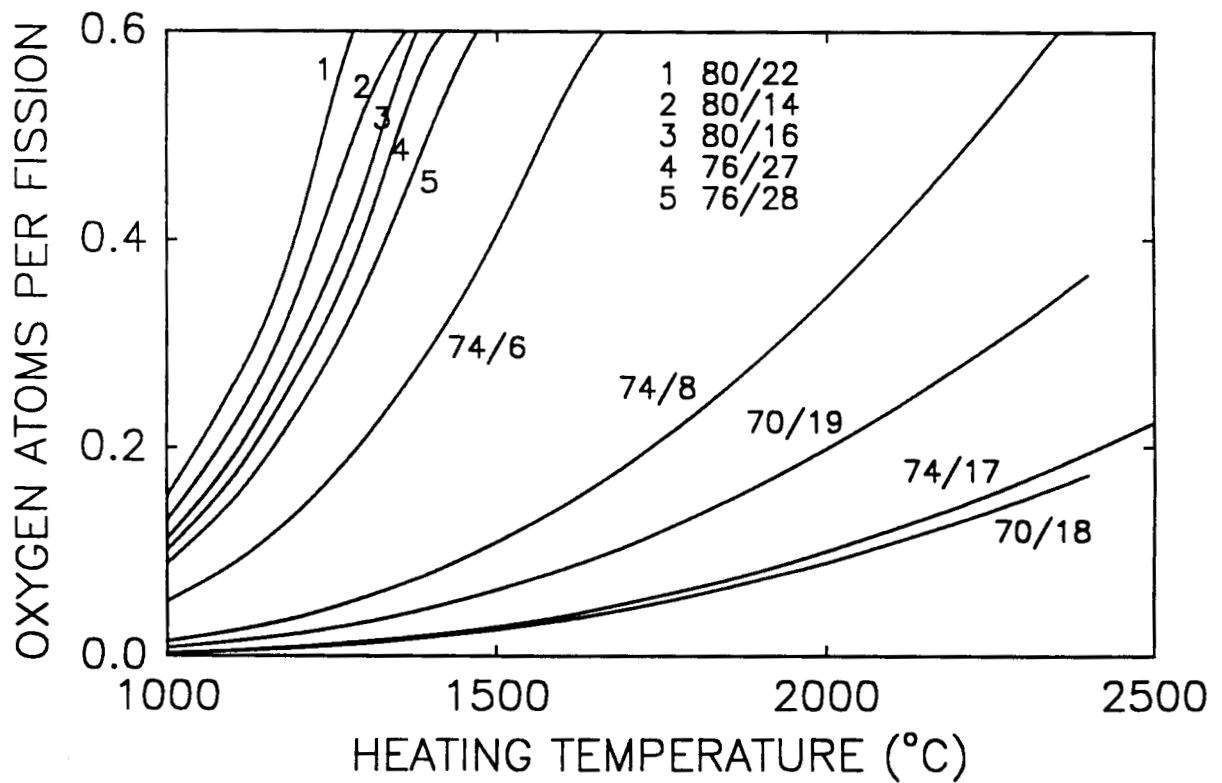
Fig. A.3.   Oxygen atom per fission ratio as a function of heating temperature during linear ramp tests with spherical AVR fuel elements containing UO_2 and $(Th,U)O_2$ particles.